DIELECTRIC AND RELATED PHENOMENA

DRP '94

Abstracts

Zakopane, Poland
12 - 16 September 1994

CRACOW INSTITUTE OF TECHNOLOGY

REPORT DOCUMENTATION PAGE

Form Approved OMB No. 0704-0188

1. AGENCY USE ONLY (Leave blank)	2. REPORT DATE 1994	3. REPORT TYPE AND DATES COVERED Conference Proceedings

4. TITLE AND SUBTITLE

Dielectric and Related Phenomena (DRP '94)

5. FUNDING NUMBERS

F6170894W0908

6. AUTHOR(S)

Conference Committee

7. PERFORMING ORGANIZATION NAME(S) AND ADDRESS(ES)

Royal Holloway and Bedford New College
Egham Hill
Egham, Surrey TW20 0EX
United Kingdom

8. PERFORMING ORGANIZATION REPORT NUMBER

N/A

9. SPONSORING/MONITORING AGENCY NAME(S) AND ADDRESS(ES)

EOARD
PSC 802 BOX 14
FPO 09499-0200

10. SPONSORING/MONITORING AGENCY REPORT NUMBER

CSP 94-1046

11. SUPPLEMENTARY NOTES

12a. DISTRIBUTION/AVAILABILITY STATEMENT

Approved for public release; distribution is unlimited.

12b. DISTRIBUTION CODE

A

13. ABSTRACT (Maximum 200 words)

The Final Proceedings for Dielectric and Related Phenomena, 12 September 1994 - 16 September 1994

14. SUBJECT TERMS

dielectric and related phenomena and their applications

15. NUMBER OF PAGES

162

16. PRICE CODE

N/A

17. SECURITY CLASSIFICATION OF REPORT	18. SECURITY CLASSIFICATION OF THIS PAGE	19. SECURITY CLASSIFICATION OF ABSTRACT	20. LIMITATION OF ABSTRACT
UNCLASSIFIED	UNCLASSIFIED	UNCLASSIFIED	UL

NSN 7540-01-280-5500

Standard Form 298 (Rev. 2-89)
Prescribed by ANSI Std. 239-18
298-102

DIELECTRIC AND RELATED PHENOMENA

DRP '94

Abstracts

Zakopane, Poland
12 ÷ 16 September 1994

CRACOW INSTITUTE OF TECHNOLOGY

DIELECTRIC AND RELATED PHENOMENA

DRP'94

Abstracts

Zakopane, Poland
12 – 16 September 1994

All contributions are printed without any changes on the full responsability
of the authors.

ORGANIZED BY

Cracow Institute of Technology
Textile Institute Technical University of Łódź,
Division Bielsko - Biała and
Chair of Physics of Technical University of Rzeszów,
POLAND

SPONSORS

Polish Ministry of National Education,
International Science Foundation,
American Air Forces,
Asea Brown Boveri.

STEERING COMMITTEE

A.K. Jonscher (Egham) - Chairman,
H. Block (Cranfield),
D.K. Das - Gupta (Bangor),
B. Hilczer (Poznań),
R.M. Hill (London),
F. Kremer (Mainz),
M. Kryszewski (Łódź),
J. Małecki (Poznań),
G. Niklasson (Goeteborg),
Y.O. Roizin (Odessa),
G.M. Sessler (Darmstadt),
A.B. Szymański (Rzeszów),
R.S. Wallin (Pueblo),
C. Wesołowska (Wrocław),
A. Włochowicz (Bielsko - Biała),
L. Wojtczak (Łódź).

ORGANIZING COMMITTEE

Prof. A.B. Szymański
Cracow Institute of Technology
ul. Makowa 16
30 - 650 Kraków, Poland
Telex: 325237 TXCA PL
Fax: (048) (12) 217577, 223606, 555051
E-MAIL: PRZYBYLO@CIT.KRAKOW.PL
or KATFIZ@PLUMCS11.UMCS.LUBLIN.PL

CONTENTS

Plenary lectures

Conference contributing papers

SPONSORS

CHARGE TRANSPORT IN RANDOM ORGANIC PHOTOCONDUCTORS

H. Baessler

Fachbereich Physikalische Chemie und Zentrum fuer Materialwissenschaften der Philipps Universitaet, Marburg, Germany

A conceptual framework will be laid out to describe charge transport in random organic photoconductors such as molecularly doped polymers, glasses prepared by vapor deposition, or conjugated polymers. It rests on the idea that energetic and positional disorder controlls the stochastic hopping motion of charge carriers. The energetic disorder usually arises from random electric fields caused by both static and induced dipole moments. In conjugated polymers it results from the variation of the electrive conjugation lenght. The concept is able to explain the dependence of the charge carrier mobility on temperature, electric field and polarity of the matrix as well as the various temporal features of the time-of-flight signal.

ANOMALOUS TRANSPORT IN GLASSES

A. Bunde
Universitat Hamburg, Hamburg, Germany

Abstract not available.

Recent Advances in Electrical Degradation and Breakdown in Polymers

Dr John C Fothergill
Department of Engineering, University of Leicester, Leicester, LE1 7RH, UK

The talk will centre around the considerable recent advances that have been made in water treeing and electrical treeing. Some of these have been due to a better understanding of aspects of electrical breakdown which will also be presented.

Many theories of water treeing have been proposed and virtually all of them can be shown to be untrue or, at least, not the whole truth. It seems that , in order to explain the phenomenon completely, It is necessary to consider water treeing as synergistic electrical/chemical/physical effect which takes places in several stages [1]. Some new [2] results indicate how difficult water treeing is to accelerate in a way useful for predicting an insulating system's resistance to it. Some unpublished results on a new water tree retarding material will also be given.

Electrical treeing has been studied carefully since Mason's seminal work in the 1950s [3]. However most of the work has been on the nature of the partial discharge within the tree. Recently work has progressed to relate the fractal nature of the tree shape to the time to breakdown and to the way the discharge in a branch produces a new branch [4]. A particularly encouraging feature of this model is the prediction of the rather peculiar non-monotonic relationship between the length of an electrical tree after a given ageing time and the ageing voltage. The fractal shape predictions are also very realistic. Not all aspects of tree growth have been explained however and it seems likely that it is necessary to invoke an electromechanical cracking mechanism. This has been suggested before by Arbab, Auckland and Varlow [5]. Such a mechanism may be filamentary electromechanical breakdown [6].

1. Dissado, L.A. and Fothergill, J.C.: *Electrical Degradation and Breakdown in Polymers*, Peter Peregrinus, 1992

2. Houlgreave, J.A. and Fothergill, J.C.: *The effect of Power Supply Frequency on the Initiation and Growth of Water Trees*, 4th. Int. Conf. on Properties and Applications of Dielectric Materials, Brisbane, July 1994

3. for example: Mason, J.H. in *Progress in dielectrics* eds. Birks, J.B. & Schulman, J.H. (Heywood, London, 1959), 1, pp 1-58

4. Fothergill, J.C., Dissado, L.A. & Sweeney, P.J.J.: *A "discharge-avalanche" theory of the propagation of electrical trees - a physical basis for their voltage dependence*, accepted for publication in IEEE Trans. Dielectrics and Electrical Insulation.

5. Arbab, M.N., Auckland, D.W. & Varlow, B.R.: Conf. Elec. Insul. & Diel. Phenom., 1987, 425-431

6. Fothergill, J.C.: *Filamentary Electromechanical Breakdown*, IEEE Trans Electr. Insul. 26(6), 1991, 1124-1129

DIELECTRIC METHODS IN INTERFACE STUDIES

M.Kryszewski [*] and G.W.Bąk [+]
   [*] Center of Molecular and Macromolecular Studies, Polish Academy of
      Sciences, ul.Sienkiewicza 112, 90-363 Łódź, Poland
   [+] Institute of Physics, Technical Univ. of Łódź, ul.Wólczańska 219,
      93-005 Łódź, Poland

The importance of multiphase and heterogeneous systems has increased significantly in the last decades. In this situation the interest in all kinds of boundary phenomena has increased too. All the phenomena taking place at the phase boundary may be divided into two groups. The phenomena occurring in the substance being between the two basic phases of two-phase system belong to the first group and may be called the interphase phenomena. Discussing the interphase phenomena we should distinguish a few various cases, i.e.:

1. The inter-grain regions in polycrystalline structures. Such regions are usually more disordered then the substance inside the crystallites.
2. Substance adsorbed on surfaces of a multiphase system. The properties of thin films of materials adsorbed on surfaces usually differs from the properties of bulk material. There are some differences between adsorption of non-polar and polar molecules on solid surfaces [1], so the two cases of adsorption should be discussed separately.
3. If we take into account that there exists some interphase substance in a two-phase system, the system becomes actually a three-phase one. There are many models describing macroscopic properties of such systems .

Maxwell-Wagner interfacial polarization, leaching of surface fragments of composite compounds, transport and polarization in interfacial electrolytes and related osmotic pressure may be numbered among the interfacial phenomena which belong to the second group of the boundary effects. All these phenomena are of particular importance for water ageing of composite materials which is discussed in the next part of the paper. The division of the boundary phenomena into interphase phenomena and interfacial phenomena is not perfectly precise, as the two groups are not quite separable. The interfacial phenomena can have influence on properties of the interphase substance and the properties of the interphase substance can influence the interfacial phenomena too.

There are several methods to study the interphase and interfacial phenomena, but the dielectric methods seem to be a particulary useful way to get comparatively simple and straightforward understanding of the two phenomena in heterogeneous systems.

POWDERS

In case of polycrystalline structures we have to do with more disordered material at the grain boundaries. In polar substances such disordered regions

just result in a broader dielectric loss peak connected with orientational dipolar polarization. More interesting situation occurs when the dielectric response is controlled by semi-free movement of charge carriers (hopping, multiple trapping). Applying sufficiently low frequency of measuring electric field we can detect dissipation of charge carriers at inter-grain regions. The dielectric response of polycrystalline aromatic hydrocarbons may be an example of such a phenomenon [2]. At about 10 Hz the slope of $\chi''(\omega)$ curve changes distinctly. The value of the activation energy varies considerably as well and the low-frequency value is equal to about 0.2 eV. The low-frequency value of the activation energy is by one order of magnitude greater than the high-frequency one which characterize the charge transport inside the grains of polycrystalline structure.

ADSORBED SURFACE PHASES

Solid surfaces almost always adsorb a layer of molecules of gases or liquids they are exposed to. In case of adsorption of polar molecules at a surface of a polar solid the thickness of the adsorbed layer may be quite considerable and be greater than 10 monomolecular layers. The dielectric and conducting properties of such adsorbed layer may change with changing layer thickness. Dielectric measurements make it possible to estimate the influence of adsorbed layer thickness on the properties of adsorbed substance because in case of dielectric additivity we get [1]:

$$\varepsilon'_{measured} = \varepsilon'_1 + (\varepsilon_2 - \varepsilon'_1)v_2$$

where ε'_1 is the permittivity of adsorbent, ε'_2 is the permittivity of adsorbed layer and v_2 is the volume fraction of the adsorbed substance. The measured dielectric permittivity is a linear function of the volume fraction with the slope dependent on the dielectric permittivity of the adsorbed substance. The change of the slope means that the dielectric properties of adsorbed sub-stance change with its increasing volume fraction as it will be shown later on.

Adsorption of non-polar molecules on chemically inert surface

Adsorption of butane on silica gel, titanium oxide or porous glass is an example of adsorption of this kind [3]. Two linear regions of the dependence of dielectric permittivity on volume fraction of adsorbed butane on silica gel have been found. The permittivities for butane on silica gel proved to be 1.84 for the layers first adsorbed and 1.57 for the further region. The lower value of permittivity is probably related to the later adsorption on sites adjacent to residual hydroxyl groups on silica surface. The permittivity for liquid butane is equal to 1.9. But in case of adsorption of butane on non-porous titanium oxide only a single linear relation between the measured permittivity and the volume fraction of adsorbed substance is detected and the value of dielectric permittivity agrees with that for the liquid phase within the experimental error. In general the non-polar substances may sometimes change their dielectric properties with increasing thickness of adsorbed layer but the phenomenon is rather not as common as in case of polar molecules.

Adsorption of polar molecules on chemically inert surfaces.

In case of adsorption of polar molecules two different regions of dependence of the permittivity on the volume fraction of adsorbed substance is nearly

6

always registered. Adsorption of ethyl chloride and sulphur dioxide on titanium oxide and silicon gel are examples of two different linear regions with different slopes of effective permittivity vs. volume fraction curve [3]. It turns out that the intersection of the two linear regions takes place where the surface acquires a unimolecular layer. The value of unilayer permittivity is usually considerably lower than that of liquid phase and relatively weakly dependent on temperature. This means that the molecular reorientation of adsorbed substance differs significantly from the liquid or gaseous state.

Hydroxyl groups on silica and silicate system surfaces have been found to have influence on reorientation of polar molecules adsorbed close to the groups. It has been shown that if the hydroxyl groups are removed by strong heating (1200 K) the region of reduced permittivity is not detected [3]. It suggests that the molecular reorientation in the presence of hydroxyl groups is more limited.

Adsorption of water is a very important process from both theoretical and practical point of view. Much attention has been paid to adsorption of water on surfaces of oxides (silicon and titanium oxides and γ-alumina) and silica gel where water molecules are held strongly. Some relaxation processes were detected at comparatively low frequencies (about 1kHz) and temperatures (100K-300K). The relaxation processes have nothing to do with free rotation of molecules and must be connected with strong interaction of water molecules and adsorbent surface. An interesting phenomenon relating to adsorption of water on γ-alumina surfaces has been reported. Over frequency range 100 kHz -10 MHz three absorption peaks have been detected, at least one of them turned out to be sharper in contour then a Debye process [4]. It suggests there should exist some resonance dielectric absorption probably resulting from oscillations of water molecular layers.

INTERPHASE PHENOMENA IN HETEROGENEOUS MATERIALS

In the last decades a great interest has been paid to heterogeneous materials consisting of at least two phases. If two-phase material is exposed to water or air humidity an interlayer of some electrolyte originates between the two basic phases and such a composite becomes actually a three-phase system. One of the important models to describe physical properties of such three-phase systems is Maurer's model though other methods to describe such systems are also used. Maurer's model may be used to describe the shear modulus, bulk modulus, thermal expansitivity and dielectric properties of composites with interfacial conducting layers [5]. Most of composites exposed to humidity fulfills the following assumptions:1)The volume of interlayer is much smaller than the volume of other components 2)Electrical conductivity of the interlayer is finite and greater than zero. As a result of the above assumptions we get the following conclusions:1)The relaxation of such a system is Debye-like 2)Low-frequency limit of dielectric permittivity depends on the permittivity of matrix substance and the volume fraction of the filler and is independent of the permittivity of the filler 3)The relaxation time is inversely proportional to the volume fraction of the interlayer and its electrical conductivity. Maurer's model

has been tested for many polymer composites exposed to humidity. An experiment carried out very carefully by Steeman, Maurer and van Es [6] is a good example of such a test. Dielectric monitoring of water absorption in glass-bead-filled high-density polyethylene is described in their paper and their results are in good agreement with the model.

WATER AGEING OF COMPOSITES

Among the interfacial phenomena the formation of electrolyte in the interface volume and the osmotic pressure resulting from the former are comparatively weakly known. The formation of electrolye results from leaching of surface elements of composite components during exposition to water. The osmotic pressure results from differences of ion concentration in the interlayer and the surrounding water. The glass fiber treated with silane epoxy/ polyethylene terephtalate (PET) and the untreated glass fiber/PET composites aged in water may be a good example of the influence of osmotic pressure on stability of composites [7] In case of the treated glass fiber/PET composite the leaching of ions from glass surface rather does not occur. As a result the dielectric properties of the composite does not change essentially during water ageing whereas the dielectric response of the untreated glass fiber/PET composite change distinctly with time during exposition to water. The influence of water ageing on coherence of the untreated fiber/PET composite was confirmed by electron micrographs. The results may be interpreted by means of the osmotic pressure giving rise to the increase of the distance between the glass fibres and PET matrix.

The dielectric measurements on heterogeneous and multiphase systems may be a source of essential information about physical properties of the systems. The measurements of mechanical properies (shear modulus, bulk modulus) may give much additional information about the systems. In case of water ageing of polymer composites the dielectric properties of the composites give information about modification of surface of composite components, while the mechanical measurements give information about plasticization of polymer matrix first of all.

REFERENCES

1. N.E.Hill et.al., Dielectric Properties and Molecular Behaviour, Nostrand Reinhold, London 1969
2. G.W.Bąk, J.Phys.C:Solid State Phys vol 21, pp.3447-3465,1988
3. R.McIntosh, Dielectric Behaviour of Phys cally Adsorbed Gases, Arnhold, London 1966
4. G.Eber, Angew.Chem. vol.70, p.385, 1960
5. F.H.J.Maurer, Proc.3-rd Int.Conf. Composite Interfaces, Cleveland, USA, May 21-24 1990, p.491
6. P.A.M.Steeman, F.H.Maurer, M.A. van Es, Polymer vol.32, 1991, p.523
7. C.Bastioli et. al., Proc. 2-nd Int.Conf. Composite Interfaces, Cleveland, USA, June 13-17 1988, p.189

MOLECULAR REORIENTATION IN LIQUID CRYSTALS VIA NEUTRON SCATTERING, DIELECTRIC RELAXATION AND RELATED METHODS

J. A. Janik
Institute of Nuclear Physics, Kraków, Poland

Abstract not available.

ADVANTAGES AND PROBLEMS OF THE USE OF POLYMERS IN HIGH VOLTAGE APPLICATIONS

R. Patsch

*Institute for Materials of Electrical Engineering
University of Siegen, Germany*

During the last decades polymer materials have been increasingly used in commercial high voltage equipment. The specific properties of the polymers led to advantages in different fields, in some cases the production techniques are easier in some cases there is less need for maintenance during service. Some new solutions have become possible only due to the specific properties of polymers, but in some cases there have drawbacks too, because unexpected problems occurred.

Taking the example of high voltage cables the advantages and the specific requirements in regard to the technological processes during manufacture of the solid insulation will be discussed. Additionally the influence of the service conditions on the useful life time will be discussed.

The relevant degradation mechanisms will be discussed especially in regard to the influence if changes in the procedures during the manufacturing process and specific service conditions. The mainly non-electrical phenomena that influence the so-called 'water treeing' process will be discussed.

Finally typical diagnostic tools that monitor changes in the dielectric properties will be presented and discussed from the physical point of view in regard to their ability to monitor the actual state of deterioration of polymer insulated medium voltage cables.

INTERCONNECTION BETWEEN THE EMPIRICAL AND THE THEORETICAL "FIRST PASSAGE" RELAXATION FUNCTIONS

Karina Weron

Instytute of Physics, Technical University of Wroclaw,
Wroclaw, Poland

We present the probabilistic representation [1-4] of the cluster model [5] for dielectric relaxation in dipolar systems yielding a broad class of observed dielectric responses (D, KWW, BD, CC, CD, HN) [6]. The analysis is based on a new definition of the so-called "first passage" relaxation function which is the mathematically correct representation of the statistical meaning of the relaxation function of a system of dipoles and contains the traditional definition expressed as a weighted average of exponential relaxations as a special case. However, we show that in contrast to the traditional definition the new one explains the universality of the dielectric relaxation law. Moreover, via a tool of order statistics, we prove that the "first passage" relaxation function expresses the proportion of dipoles which did not change their imposed aligned orientation up to the time t and hence that it is, essentially, identical with the experimental meaning of a relaxation function [7].

We provide also a graphical illustration of possible dielectric responses from the derived "first passage" relaxation function and show the interconnection with the widely used empirical responses (KWW, HN) [8].

REFERENCES

1. K. Weron, A probabilistic mechanism hidden behind the universal power law for dielectric relaxation: General relaxation equation, J. Phys. Condens. Matter, vol.3, p.9151-9162, 1991.

2. K. Weron, Reply to the comment by A. Hunt, J. Phys. Condens. Matter, vol.4, p.10507-10512, 1992.

3. K. Weron and A. Jurlewicz, Two forms of self-similarity as a fundamental feature of the power-law dielectric response, J. Phys. A: Math. Gen., vol.26, p.395-410, 1993.

4. A. Jurlewicz and K. Weron, A relationship between asymmetric Lévy-stable distributions and the dielectric susceptibility, J. Stat. Phys., vol.73, p.69-81, 1993.

5. L.A. Dissado and R.M. Hill, A cluster approach to the structure of imperfect materials and their relaxation spectroscopy, Proc. Roy. Soc. A, vol.390, p.131-180, 1983.

6. A.K. Jonscher, *Dielectric Relaxation in Solids*, Chelsea Dielectrics, London, 1983.

7. A. Weron, K. Weron and W.A. Woyczynski, Relaxation functions in dipolar materials, J. Stat. Phys., 1994, *submitted*.

8. A. Jurlewicz, K. Kosmulski and K. Weron, in preparation.

MOLECULAR DYNAMICS AND ALIGNMENT BEHAVIOUR OF LIQUID CRYSTAL POLYMERS AS STUDIED BY DIELECTRIC RELAXATION SPECTROSCOPY

Graham Williams
Department of Chemistry, University of Wales, Swansea,
Singleton Park, Swansea SA2 8PP,
United Kingdom.

Low molar mass liquid crystals in their nematic, smectic and ferroelectric states, find increasing applications in optical displays and storage devices. Polymeric analogues, as side chain liquid crystal polymers (SCLC polymers), while not sufficiently fast for optical displays, find potential applications as optical storage media using thermal or photophysical processes to generate optical contrast. While LC materials are ordered in the structural sense they are also dynamically disordered. The LC-forming (mesogenic) groups undergo anisotropic reorientational motions that may be monitored using broad-band dielectric relaxation spectroscopy (DRS).

The macroscopic alignment of LCSC polymers in directing ac or dc electric fields is a dielectric process involving the frequency-dependent anisotropy of the dielectric permittivity $\Delta\varepsilon'(\omega) = \varepsilon'_{\parallel}(\omega) - \varepsilon_{\perp}(\omega)$, where $\omega = 2\pi f/\text{Hz}$. It will be shown how homeotropically-aligned (H) and planarly-aligned (P) samples of siloxane-chain and carbon-chain polymers may be obtained using the two-frequency addressing principle together with carefully-chosen thermal treatments of samples.

The alignment behaviour of siloxane-chain and carbon-chain LCSC polymers in directing E-fields is described and is rationalized in terms of continuum electrohydrodynamics. The DRS behaviour of H, P and intermediately-aligned films thus prepared are described and the systematic changes in the multiple dielectric relaxation processes that are observed are interpreted in terms of a molecular theory for the dielectric properties of a LC phase in which the dipolar mesogenic head groups undergo anisotropic motions in the local LC-potential.

DIELECTRIC RELAXATION AND COMPLEX FORMATION IN SOME MALEIMIDES – STYRENE SYSTEMS

K.N. ABD – EL NOUR, S.L ABD – EL – MESSIEH and M.Z. ELSABEE[*]

Microwave Physics Department

National Research centre. Dokki, Cairo. Egypt.

[*] Faculty of Science, Kuwait University, Kuwait

Dielectric relaxation behaviour of polar molecules in non polar solvents using microwave absorption methods have been frequently studied. Such studies using binary mixtures, however, are limited. The work reported here is an investigation of the molecular interaction which is expectedly, takes place between some substituted maleimides namely N– phenyl maleimides (NPMI) and o– m– and P– nitro N. phenyl maleimides with styrene which was chosen to act as a non – polar donor. Different mole fractions 0.25, 0.50 and 0.75 from the binary mixtures in dilute solutions of carbon tetrachloride and benzene were prepared.

The dielectric loss ϵ''/x data which were obtoined at frequency range 0.2–18 GHz using a sweep frequency generator, HP were analysed by the sum of two Debye (1) terms (or even one term). An example of the analysis, Fig (1) shows the variation of ϵ''/x versus the applied frequency for o– nitro NPMI, mixed with styrene with the different mole fractions in corbon tetrachloride and benzene. The values of the relaxation times obtained for the investigated maleimide – styrene systems with the different mole fractions are found to be higher than the maleimide itself. This could be attributed to some sort of molecular interaction which is expected to be formed via the pi–delocalized electron cloud of the phenyl ring. This may lead to the increase in the molecular volume and consequently the relaxation time.

As styrene is considered to be a non–polar, another approach was tried to study the molecular interaction which is expected to takes place between the investigated maleimides and styrene through the solvent mixtures of either styrene – CCl4 or styrene – benzene. The values of

ϵ''/x for such systems were analysed in the same way as mentioned before and the relaxation times obtained are illustrated graphically in Fig (2). The experimental values of τ which are found to be higher than those calculated from the individual τ_i's when the mole fraction is taken into account could be attributed to the molecular interaction between the different maleimides and styrene.

To find an expression describing these interactions, the ratio between the measured values of τ and those calculated from the individual τ_i's are considered. It is interesting to notice that these ratios incrase in the order p_nitro NPMI, m_nitro NPMI, o_nitro NPMI and NPMI. The existence of two carbonyl groups in the maleimide ring attract electrons away from the double bond, thus imparting a partial positive charge upon it. The presence of nitro group attached to the maleimide ring could increase the electron withdrawing ability of the phenyl ring which is considered to be a maximum in the p_position.

Also, it is interesting to notice that the molecular interaction formed in CCl4 solutions is higher than that formed in benzene solutions. Benzene is considered to be an aromatic donor which could compete with styrene and thus decreasing its available concentration required to form the complex between the substituted maleimides and styrene.

The interaction between the maleimides and styrene is also studied quantitavely by means of dielectric polarization measurements using the method of Few and Smith (2). The equilibrium constant K was abtained and it is interesting to find that its values follow the trend given by the dielectric relaxation measurements.

REFERENCES

1.   C.P. Smyth, "Dielectric behaviour and structure" McGraw Hill In. New york, 1955

2.   M.G. Mikhael, S.M. Mokhtar, G.R. Saad and M.M. Naoum, J. polym Sci. vol.27, P.185, 1989
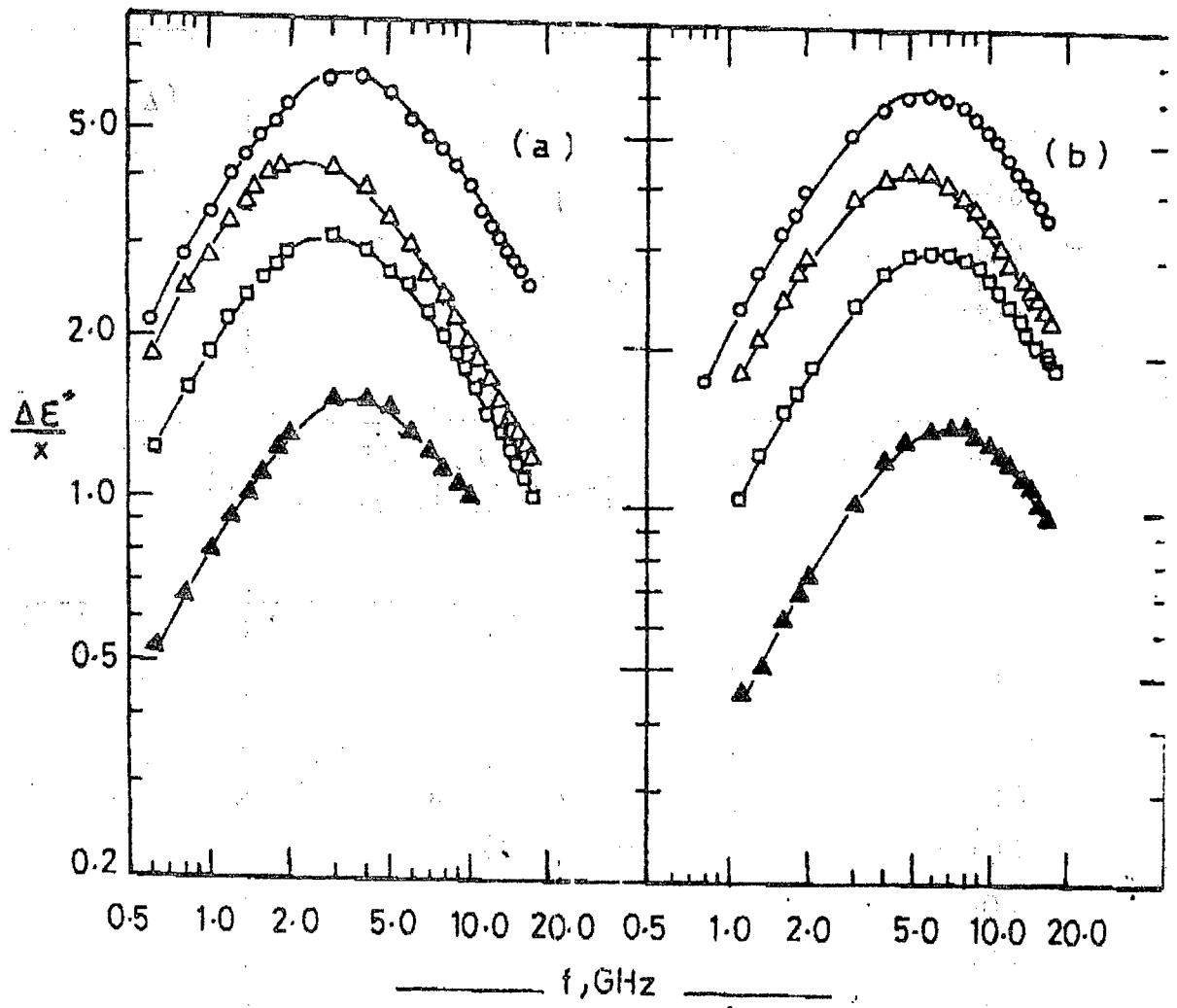
Fig (1) Frequency dependence of dielectric loss $\frac{\Delta \epsilon'}{x}$ of O o-nitro
NPMI and its mixtures with styrene with mole
fraction ▲ o.25 □ o.5o △ o.75 at 2o°C in C Cl$_4$ (a)
Benzene (b)·
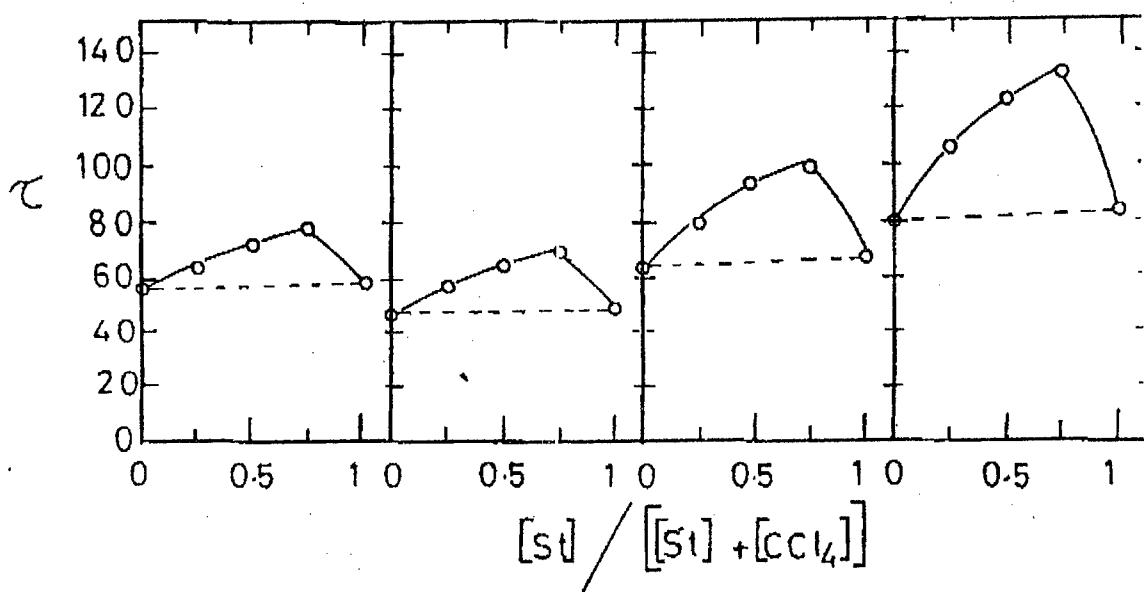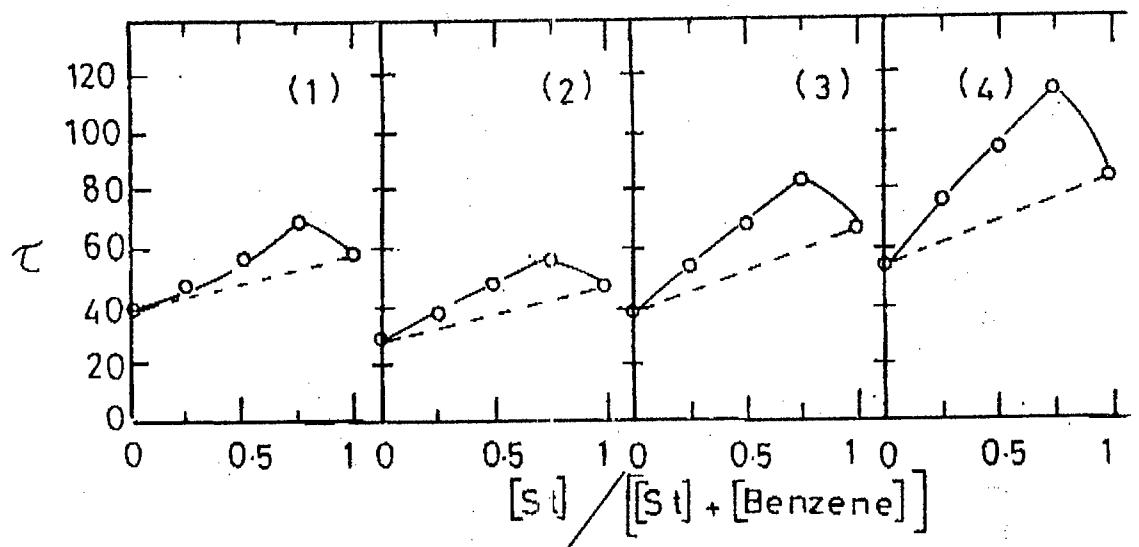
Fig (2) Relation between the relaxation time τ of (1) NPMI
(2) o-nitro NPMI (3) m-nitro NPMI (4) p-nitro NPMI
and the mole fraction of styrene in solvent mixtures.
Maleimide concentration = o.5 mol%

DIELECTRIC PERMITIVITY AND DIELECTRIC SUSCEPTIBILITY OF LIQUID CRYSTALS

P.Adamski
Institute of Physics Technical University of Łódź   93 005 Łódź
Wólczańska str. 219 Poland

The dielectric properties of a matter are characterized by its dielectric permittivity ε , refractive index n and dielectric susceptibility X. Electric properties of molecules are described their polarizability α and a mean square dipole moment μ .As we know a liquid crystals belong to the substances having an axially symmetric arrangement of molecules. This system is characterized by an optical axis and two components of refractive indices $n_{//}$ and $n_{\perp}$ or dielectric permittivities $\varepsilon_{//}$ and $\varepsilon_{\perp}$ as functions of temperature. For each temperature of a mesophase these two values must fulfill a mathematic base :$(\varepsilon_{//} - \varepsilon)/(\varepsilon_{\perp} -\varepsilon)= - 2$. Where $\varepsilon = (\varepsilon_{//} + 2 \varepsilon_{\perp})/3$. It means that all equations for ε and X based on the local electric field theory must fulfill a mentioned above a mathematic base.Having calculated the values ε and ε from Mossottie's Equation we obtain a Equation ($\varepsilon_{//} -\varepsilon)/(\varepsilon_{\perp} - \varepsilon) =[(1+2X_{//})/(1-X_{//}) - \varepsilon]/[(1+2X_{\perp})/ (1-X_{\perp}) - \varepsilon]$. In the last Equation the right side is not equal - 2. The same results are obtained using the other equations [1-6] based on the Lorentz local electric field theory. This is a reason that we determine to find a new relation between dielectric permittivity and dielectric susceptibility of liquid crystals.New equations must be motivated on the base of Maxwell electrodynamics. We assume that the information about local electric field exists at the values of dielectric susceptibility tensor components.This tensor characterizes a dielectric properties of substances investigated.If we want to obtain a good results at the dielectric investigations we must find a new formula combining a dielectric permittivity with a dielectric susceptibility.Here it is an aim of this work

THEORETICAL

The two refractive indices $n_{//}$ and $n_{\perp}$ have been obtained by the use of refractometer and two one of dielectric permitivity $\varepsilon_{//}$ and $\varepsilon_{\perp}$ .The values of refractive indices are connected with the magnitude of deformation polarization phenomenon.The dielectric properties of substances are characterized by two polarization phenomenons.One of them is a mentioned above deformation phenomenon. The second one is the orientation polarization of substance which molecule have a finite dipole moment μ.

Now we want to give a motivation of a new relation between dielectric permittivity and components of dielectric susceptibility of second row tensor.The dielectric susceptibility tensor X_{ij} is a sum of two one because two dielectric phenomenons exist at the process of polarization of dielectric substance.All of these tensors are described at the main coordinate system therefore their components are laying on the diagonal line of tensor.

According to the transformation law of second row tensor the components of X_{ij} tensor may be written at a new coordinate system.

$$X_{ij} = X \delta_{ij} + (X_{//} - X_{\perp})(z_i z_j - 1/3 \, \delta_{ij}) \qquad (1)$$

where δ_{ij} – is the Kroneker symbol. z_i and z'_j – are a projections of singular vectors on the optical axis and, $X = (X_{\parallel}^d + 2 X_{\perp}^d)/3 + (X_{\parallel}^o + 2 X_{\perp}^o)/3 = X^d + X^o$.

Having the dielectric susceptibility tensor in a new coordinate system we can write the components of polarization vector P of the substance investigated.

$$P_i = X E_i + (X_{\parallel} - X_{\perp})(E_z z_i - 1/3 E_i) \qquad (2)$$

Now according to the electrodynamics theory, the induction vector D_i may be written in the two way. The first is

$$D_i = \varepsilon_0 \varepsilon_{ij} E (r,t) \qquad (3)$$

and the second one may be written as

$$D_i = \varepsilon_0 E_i (r,t) + \varepsilon_0 P_i (r,t) \qquad (4)$$

where ε_{ij} is the dielectric permittivity tensor of the matter investigated.

Combining Equations (3) and (4) you can write:

$$(\varepsilon_{ij} - \delta_{ij}) E_j (r,t) = P_i (r,t) \qquad (5)$$

The two components of dielectric permittivity ε and ε are obtained for axially symmetric materials from Equations (5) and (2).

$$\varepsilon_{\parallel} - 1 = X^d + X^o + 2/3 [(X_{\parallel}^d - X_{\perp}^d)+(X_{\parallel}^o - X_{\perp}^o)] \qquad (6)$$

$$\varepsilon_{\perp} - 1 = X^d + X^o - 1/3 [(X_{\parallel}^d - X_{\perp}^d)+(X_{\parallel}^o - X_{\perp}^o)]$$

The Equations (6) are combining a dielectric permittivity components ε and ε with a dielectric susceptibility components $X_{\parallel}$ and $X_{\perp}$. Now we can check if the mathematic base of two numbers is fulfilled by the quantities of Equations (6). According to this mathematic base the relation $(\varepsilon_{\parallel} - \varepsilon)/(\varepsilon_{\perp} - \varepsilon)$ must be equal – 2. We remember that ε is equal $(\varepsilon_{\parallel} + 2 \varepsilon_{\perp})/3$. From the Equations (6) it can be obtained $\varepsilon = 1 + (X^d + X^o)$. Combining mentioned relation for ε with the Equations (6) you can write a new one.

$$\varepsilon_{\parallel} - \varepsilon = 2/3 [(X_{\parallel}^d - X_{\perp}^d) + (X_{\parallel}^o - X_{\perp}^o)] \qquad (7)$$

$$\varepsilon_{\perp} - \varepsilon = -1/3 [(X_{\parallel}^d - X_{\perp}^d) + (X_{\parallel}^o - X_{\perp}^o)]$$

From the Equations (7) it is very easily to ascertain that the dielectric permitivity components ε and ε fulfill the mathematic base of two any numbers. We remember that all equations basing on the local electric field theory of Lorentz do not make it. It is a additional proof that equations founded on the base of local electric field theory are wrong. In work [7] we motivated the new mathematic formulas for the relation between refractive indices $n_{\parallel}$ and $n_{\perp}$, and the components of dielectric susceptibilities of deformation polarization.

$$n_{\parallel}^2 - 1 = X^d + 2/3(X_{\parallel}^d - X_{\perp}^d) \qquad (8)$$

$$n_{\perp}^2 - 1 = X^d - 1/3(X_{\parallel}^d - X_{\perp}^d)$$

where $X^d = (X_\|^d + 2 X_\perp^d)/3$.

Putting the Equations (8) to the one (6) you can obtain a new Equations.:

$$\varepsilon_\| - n_\|^2 = X^0 + 2/3 (X_|^0 - X_\perp^0) \qquad (9)$$

$$\varepsilon_\perp - n_\perp^2 = X^0 - 1/3 (X_|^c - X_\perp^0)$$

Equations (9) are very important one for the investigation of dielectric properties of liquid crystals and low molecular weight liquid.We must say that Equations (9) were obtained without any assumption of a local electric field model.We can test the Equations (9) assuming that the $X_\|$ is equal $X_\perp$ for a case of isotropic liquid.It is easily to calculate a mean dielectric permittivity $\varepsilon = (\varepsilon + 2 \varepsilon)/ 3$ and mean square refractive index $n^2 = (n^2 + 2 n^2)/ 3$ in order to obtain the new equation for a isotropic liquid .This Equation has a simple mathematic form:

$$\varepsilon - n^2 = X^0 \qquad (10)$$

If we want to use of Equation (10) to a study of dielectric properties of liquid we must have a evident formula of dielectric susceptibility in this case.In the literature [8] you can fined the motivation of relation between the dielectric susceptibility X and mean square dipole moment of molecule of medium investigated.Now we will describe a manner of obtaining of temperature dependence of dielectric susceptibility and mean square dipole moment of molecule.

Each dipole moment of molecule ,belonged to the collection of molecules , has a potential energy at a electric field E.The value of this energy is equal.: $U = - \mu E \cos \gamma = -(\mu . E)$.In order to obtain a value of polarization vector P of the polar dielecric we must calculate a sum of dipole moment projections on the direction of electric field E.To this end we take a sphere having singular radius and calculate a number of molecules which directions of dipole moments are contained between angles γ and $\gamma + \Delta \gamma$ .As we know the thermodynamic theory gives the formula on base which the value of polarization vector may be calculated.

$$P = \frac{N\mu \int_0^\pi e^{\frac{\mu E \cos\gamma}{k T}} \sin \gamma \cos \gamma \, d\gamma}{\int_0^\pi e^{\frac{\mu E \cos\gamma}{k T}} \sin \gamma \, d\gamma}$$

Assuming $\mu E/kT$ is equal a and $\cos \gamma$ is equal x we can calculate the value of polarization vector P in the direction of electric field E.

$$P = N \mu [\operatorname{ctg} h \, a - 1/a].$$

This is a Langevin's formula from work [8].Taking a principle a<1 , what is correct because a dipole moment is very small quantity , the ctg h a may be factorized on the sequence.: $\operatorname{ctg} h \, a = 1/a + a/3 - a^2/45$ ...Taking only two

first sequences for the count we obtain the values of polarization vector P

$$P = (N \mu^2 E)/ 3 k T = X^0 \varepsilon_0 E$$

hence $\qquad X^0 = (N \mu^2)/ 3 k T \varepsilon_0$

where N is number of molecule per the unit volume of dielectric. ε_0 - is dielectric constant of vacuum . k - is Boltzmann's constant.Having a evident formula for a dielectric susceptibility you can calculate a value of mean square dipole moments of molecules of different substances.In this work we calculated a mean square dipole moments for a four chemical substances. Below these results are illustrated:

Acetone	25 $^\circ$C	ε = 20.5	n^2 = 2.11	d (kg/m^2) = 785	μ^2= 4.677 D^2
Nitromethane	20	35.87	1.9	1124	5.541
Nitrobenzene	25	35.25	2.43	1198	7.430
Etheretylene	20	4.33	1.97	713	1.987

CONCLUSION

The new important Equations were leaded out for the study of dielectric properties of a axially symmetric and having optical axis materials from the laws of Maxwell's electrodynamics.
Obtained Equations may replace a hitherto existing Equations of Mossottie,Debye and an others.
The new Equation may be use to the study of mean square dipole moments of low molecular weight liquid as well of liquid crystal molecules.

REFERENCE

1.P.Debye, "Polar Molecules " Chemical Catalog Co (1929).
2.L.Onsager, J.Am.Chem.Soc.59, 1486 (1936).
3.C.P.Smuth, " Dielectric Behavior and Structure" N.Y. (1955)
4.H.Frohlich, "Theory of Dielectrics " Oxford Univ. Press (1959).
5.W.I.Minkin,O.A.Osipow, I.A.Zdanow," Momenty Dipolowe w Chemii Organicznej PWN .Warszawa (1970).
6.E.M.Averyanov and M.A.Osipov, Soviet Physics Uspekhi,33, 365 (1990).
7.P.Adamski, Molecular Materials 3, (1993).
8.P.Langevin, Journal de Phys. 4, 678 (1905).

SURFACE LUMINESCENCE OF $YBA_2CU_3O_{7-\delta}$

A. A. Avdeenko, V. V. Eremenko, P. V. Zinoviev,
N. B. Silaeva, T. V. Sukhareva, Yu. A. Tiunov, V. I. Fomin

B. I. Verkin Institute for Low Temperature Physics &
Engineering of Ukrainian Academy of Sciences
310164, Kharkov, Ukraine

Spectroscopy of different high-T_c superconductors (HTSC) in a wide spectral region was carried out immediately after discovery of the phenomenon of high-T_c superconductivity. However the number of reports on the HTSC luminescence is relatively small. The obtained results and especially their interpretations are fairly inconsistent (e.g. [1-3]). Such situation with the luminescence studies of HTSC is induced by different facts, in particular, the extremely low luminescence quantum yield in the visible spectrum, radiation instability of HTSC crystal lattices under intensive light exposure and difficult interpretation of the spectra due to the influence of processes induced by the interaction of HTSC surface and environment.

The present work is concerned with comparison of the luminescence spectra of single crystals and polycrystals (ceramics) of HTSC $YBa_2Cu_3O_{7-\delta}$ under the excitation in a wide spectral region. The spectra excitation sources were a mercury-discharge lamp (λ_{exc}= 366, 436 and 549 nm) and the fourth harmonic of a YAG laser with Nd (λ_{exc} = 265 nm). The photoluminescence was detected using a cooled photoelectronic multiplier FEU-79 in the photon counting or dc current regime with a scanning monochromator MDR-3. Photoluminescence spectra were not corrected for the spectral sensitivity of a photomultiplier. The HTSC samples were specified by the X-ray diffraction analysis, Raman spectra and noncontact measurement of T_c. The studied samples were, in fact, uniphase (in ceramics the share of accompanying phase of $BaCuO_2$ did not exceed 1-2%, the oxygen index $7 - \delta$ was equal to about 6.95 and $T_c \cong 92$ K).

Figure 1 shows the luminescence spectra of HTSC ceramics $YBa_2Cu_3O_{7-\delta}$. The unpolished surface spectrum (curve 1) exhibit a continuum with two maxima at about 440 and 530 nm. After mechanical polishing of the surface by fine-grained diamond abrasive the luminescence spectrum transforms (curve 2), the band at $\lambda_{max} \cong 440$ nm, in fact, disappears and that at $\lambda_{max} \cong 530$ nm becomes dominant and the spectral integral intensity appreciably increases. It should be noted that similar evolution of the luminescence spectrum of HTSC ceramics $YBa_2Cu_3O_{7-\delta}$ is also observed due to irradiation of

the surface by powerful laser pulses [4,5].
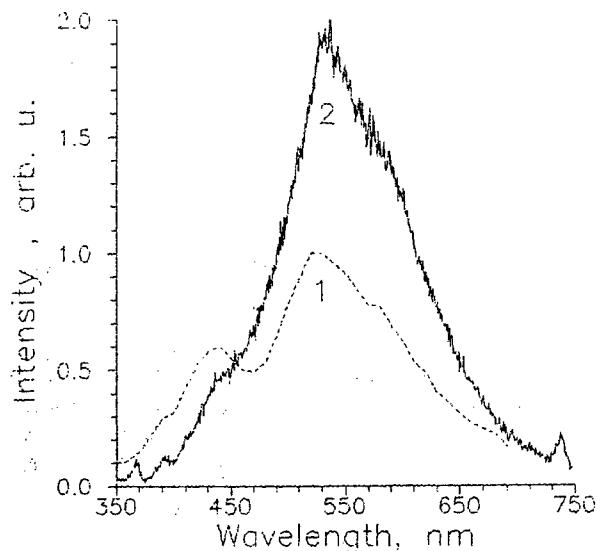
Fig. 1. Luminescence spectra of ceramic HTSC $YBa_2Cu_3O_{7-\delta}$ at room temperature:
(1) - unpolished surface;
(2) - surface after mechanical polishing.
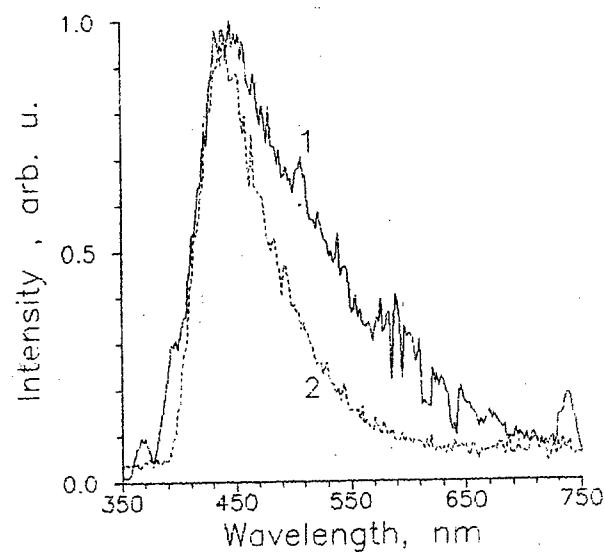
Fig. 2. Luminescence spectra of $YBa_2Cu_3O_{7-\delta}$ single crystal at room temperature before (1) and after (2) additional annealing.

The luminescence spectra of $YBa_2Cu_3O_{7-\delta}$ single crystals qualitatively differ from those of ceramics and excibit upon excitation by a mercury-discharging lamp with λ_{exc} = 366 nm only one band with $\lambda_{max} \cong$ 440 nm (Fig. 2, curve 1). Moreover, after additional annealing at $450°$ C for 10 hours this band narrows (Fig. 2, curve 2). It is significant that

the luminescence spectrum of a $YBa_2Cu_3O_{7-\delta}$ single crystal freshly out in high vacuum exhibits only the band at $\lambda_{max} \cong$ 440 nm [6].

Comparison of the luminescence spectra of ceramic and single crystal HTSC samples of $YBa_2Cu_3O_{7-\delta}$ make it possible to conclude that the intrinsic HTSC emission is responsible only for the band at $\lambda_{max} \cong$ 440 nm. The 530 nm band which is enhances due to both the mechanical and radiation [4,5] effect on the HTSC surface seems to be due to the formation of emission centers induced by either photodefects [5] or new luminescent phases [4].

For dielectric single crystal samples of $YBa_2Cu_3O_{7-\delta}$ with the low oxygen concentration $(\delta > 0.6)$ the intrinsic exciton emission band was searched which would correspond to the exciton absorption band (at 2.5 - 1.9 eV) [7]. However one failed to observe such a band at the experimental conditions.

Of special interest is the luminescence of HTSC samples where one of the copper sites is substituted by the elements of transition metals. Observation of fine luminescence spectra of dopants (luminescence marks) could give very important information about the electron excitation energy and charge transfer at the transition and HTSC material to the superconducting state.

Our studies showed that even in the case when, according to the X-ray diffraction analysis, doped elements (Mn, Cr) substituted copper, separate dopant luminescence spectra were not observed. We assume that this can be accounted for by the fact that in the place of copper substitution local charge transfer complexes were formed [8]. Such complexes should have extremely broad luminescence bands. We plan to study their luminescence.

REFERENCES

1. Lushchik I. B., Kuusman I. L. et al.//Pis'ma v Zh. Eksp. Teor. Fiz. - 1987 - 46, N 3 - P. 122-124.
2. Eremenko V. V., Fugol I. Ya., Samovarov V. N. et al.// Pis'ma v Zh. Eksp. Teor. Fiz. - 1987 - 47, N 10 - P. 529-533.
3. Stankevich V. G., Svechnikov N. Yu. et al.// J.Luminescence. - 1991. - 48-49. - P. 845-848.
4. Remon A., Garcia J. A., Gomez P. et al.// Phys. Status Solidi. - 1993. - A136. - P. K127-K130.
5. Avdeenko A. A., Zinoviev P. V., Sukhareva T. V. et al.// Zh. Prikl. Spektrosk. - 1993. - 58, N 3-4. - P. 404-406.
6. Stankevich V. G., Svechnikov N. Yu., Kaznacheev V. V. et al.// Phys. Rev. - 1993. - B47, N 2. - P. 1024-1028.
7. Fugol I. Ya., Samovarov V. N. et al.// Fiz. Nizk. Temp. - 1992. - 18, N 3. - P. 296-301.
8. Aksenov I., Yasuda T., Segava Y., Sato S.// J. Appl. Phys. - 1993. - 74, N. 3. - P. 403-406.

THE DIELECTRIC PROPERTIES OF HUMID DIATOMITES

A. BĄK, K. CHŁĘDOWSKA
Physics Department, Rzeszów Technical University, W. Pola 2,
35-959 Rzeszów, Poland

We have performed dielectric measurements on natural organic sedimentary rocks, i.e., carpathian diatomites. The diatomites are very light and porous materials. SiO_2 is their main constituent [1]. The measurements are reported for two kinds of diatomites, easily and difficult for mechanical processing. For that reason we called first as "soft" and second as "hard" diatomite.

Dielectric measurements are reported in the frequency range 10^{-3} - 10^4 Hz and time range 10^{-3} - 10^4 s for different values of the applied step voltage. Frequency - domain measurements were made using a Solartron Frequency Response Analyzer (FRA) in Royal Holloway (Egham). Time - domain measurements were made in our laboratory.
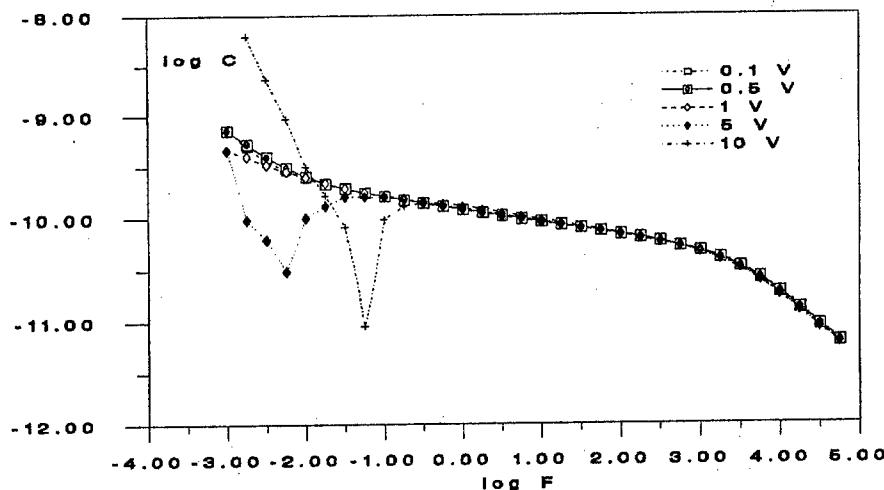
Fig.1. The frequency dependence of the real part of the complex capacitance at 50% rh for different values of the step voltage for "soft" diatomite. A negative capacitance for 5 and 10 V is observed.

Figs. 1 and 2 shown the frequency dependence real $C'(\omega)$ and imaginary $C''(\omega)$ components of the complex capacitance for "soft" material at constant humidity rh = 50%.
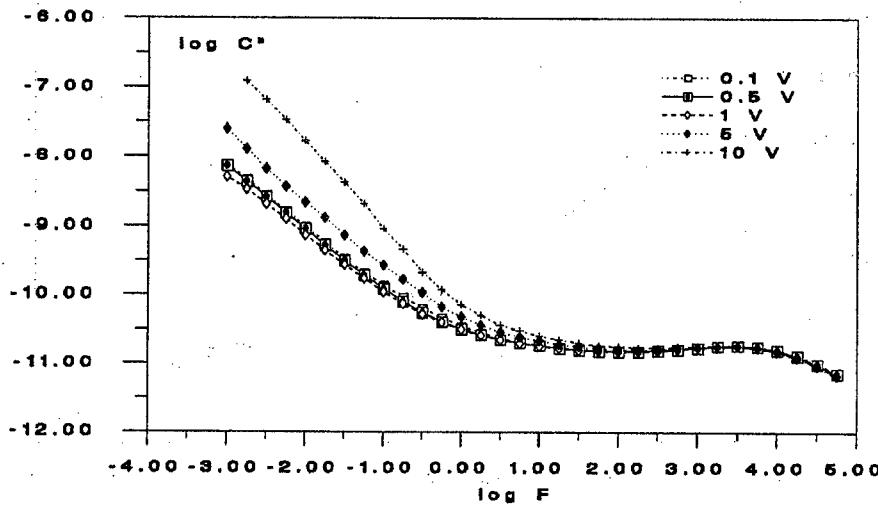
Fig. 2. The frequency dependence of the imaginary part of the complex capacitance at 50% rh for different values of the step voltage for "soft" diatomite.

Figs. 3 and 4 shown the corresponding data for "hard" diatomite, for rh = 76%. The data in these figures show a strong dispersion of the real and imaginary parts of the capacitance at low frequencies. The frequency dependences of the both, real and imaginary components we may describe by means the power - law [2] $C''(\omega) \sim \omega^{n_1-1}$; $C'(\omega) \sim \omega^{n_2-1}$
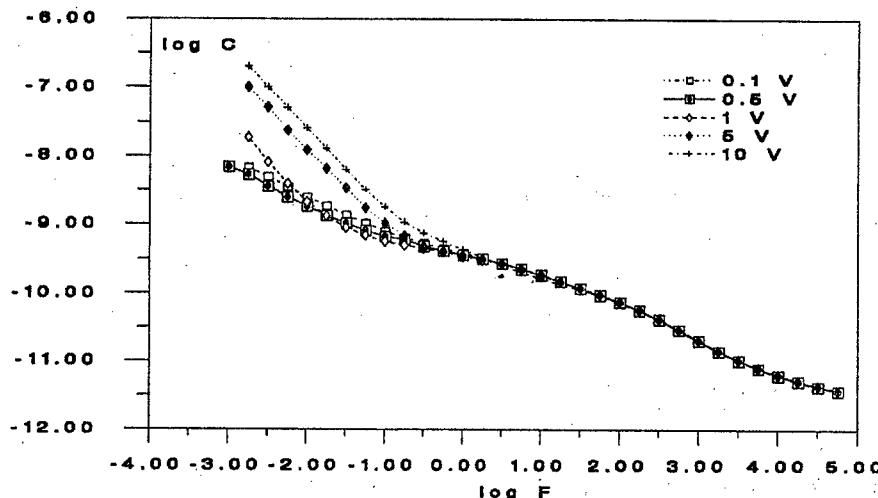
Fig. 3. The frequency dependence of the real part of the complex capacitance at 76% rh for different values of the step voltage for "hard" diatomite.
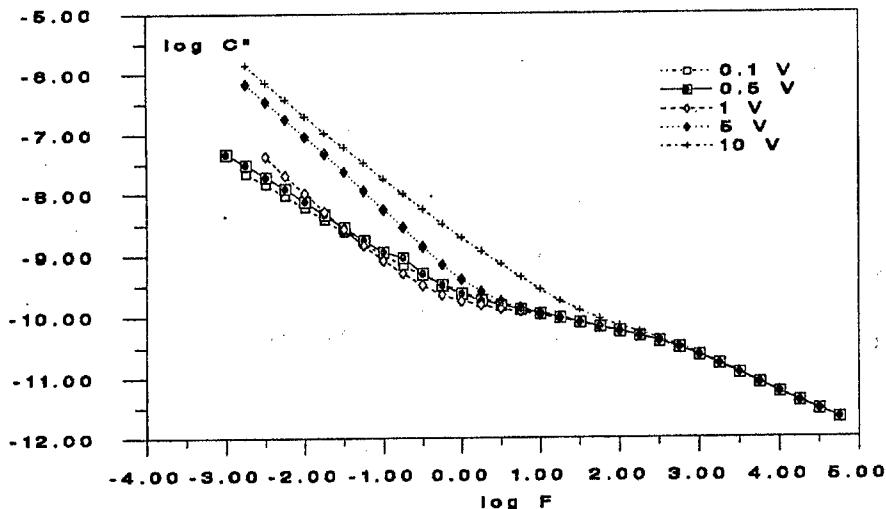
Fig. 4. The frequency dependence of the imaginary part of the complex capacitance at 76% rh for different values of the step voltage for "hard" diatomite.

But $n_1 \neq n_2$ and the slope these curves varied between -0,2 to -1,18. The ratio of the two components is not consistent with the Kramers - Kronig relation. That means strongly non-linear behaviour in the response with respect to the amplitude of the applied electric field.
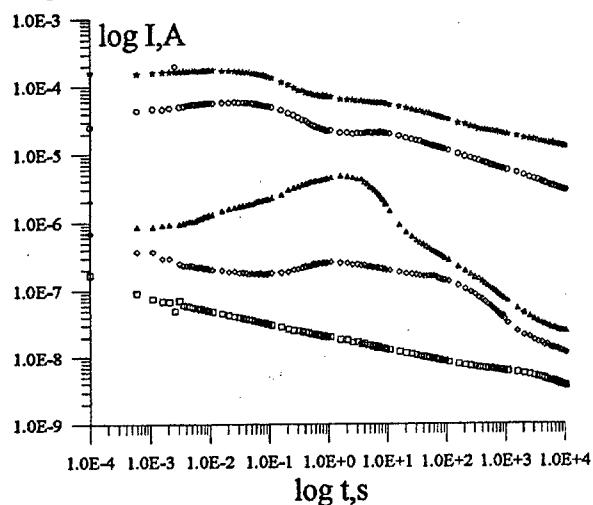
Fig.5.The charging current for the same sample as in Fig.1. rh = 80%

In Fig. 1 we can see additional effect, namely negative values of capacitance $C'(\omega)$ at low frequencies for 5 and 10 rms amplitude. This effect has been observed in the past [3,4,5,6]. As it was pointed [7], the negative capacitance may be associated with time - domain response where it corresponds to a slowly rising current in the time domain under a voltage step excitation.

Fig.5 shows the results of time - domain response:

charging currents for values of amplitudes V of the charging voltage step corresponding to values as in Fig.1. We observed a large peak of current for V = 0,5V, and there for over range negative capacitance. The peak of current also appear for "hard" material. The negative capacitance is absent for "hard" material. It seems, must be other reasons for appearence these peaks. Measurements were made with painted silver paste contacts. We believe the silver electrodes are ion-injecting (but the reasons of this are unknown for us). The confirmation of the concept of ion-injecting electrodes requires of the next experimental studies.

1. J. Kotlarczyk, T. Leśniak, Dolna część formacji menilitowej z poziomem diatomitów z Futomy w jednostce skolskiej polskich Karpat, Wydawnictwo Akademii Górniczo-Hutniczej, Kraków 1990.
2. A.K. Jonscher, Dielectric Relaxation in Solids, Chelsea Dielectric Press, London 1983.
3. E.F. Owede, A.K. Jonscher, J Electrochemical Society, 135, 7, 1757, 1988
4. A.K. Jonscher, J. Mat. Sci, 26, 1618, 1991.
5. R.D. Armstrong, R.E. Firman, H.R. Thirsk, Disc. Faraday Soc., 36, 244, 1973.
6. D.R. Francescetti, J.R. Mcdonald, Electroanal. Chem, 82, 271, 1977.
7. A.K. Jonscher, J. Chem. Soc. Faraday Trans, 2, 82, 75, 1986.

BIOACTIVE GLASS-CERAMICS

L. Bērzina

Technical University, Riga, Latvia

Formation of phases during glass synthesis in the system $CaO-Nb_2O_5-P_2O_5$ at the temperature 1400° C was determined. In the glass forming region the relationships between the physical properties and chemical composition and structure of glasses were investigated. Conditions of crystallisation and products of crystallisation of glasses were established.

Glass ceramics (GC) were obtained by powder technology, and extensive investigations were carried out to evaluate their properties. The complex evaluation of both the mechanical properties and the results of *in vivo* tests allowed to reveal the optimal glass compositions for obtaining GC. *In vivo* studies of GC with the Ca/P ratio 0.9-1.1 and 10-15 mol% Nb_2O_5 confirmed their biocompatibility with soft tissues in white rats. The study of response reactions in the implants vicinity were carried out after 1, 2, 4, 6 and 7 months of implantation.

To promote ions exchange between the living body and bioceramics (BC) implants the optimal composition of glass was modified with Na_2O (up to 10 mol%). The highest bending strength (130 MPa by 4-point test) has the BC with 8 mol% Na_2O (designated as 4N). A detailed study of the relationships between the structure and mechanical strength in dependence upon the conditions of synthesis of the BC "4N" at the temperature range from 600° to 1200° C was made.

To evaluate the bioactivity of BC "4N" a cylindrical specimens (diam. 5 mm, length 5 mm) were manufactured and implanted into the tibia of 12 rabbits. After 7 months of implantation the implants were removed and subjected to micro X-ray analysis to detect the distribution of chemical elements in the interfacial zones: glass ceramic-bone, glass ceramic-bone callus and bone-bone callus.

LOW FREQUENCY ELECTRICAL PROPERTIES OF CHITOSAN.

St. Boryniec, H. Struszczyk, Institute of Chemical Fibers, Lodz,Poland
M. Olejnik, Chair of Physics, Technical University of Rzeszów, Poland
A.B. Szymański, Technical University of Rzeszow and Cracow Institute of Technology.

Abstract.

Chitosan /poly/ 2-amino-2-deoxy-b, D-glucose/ is a polymer obtained by deacetylation of chitin, one of the most widespread in nature organic polymer.High water retention value observed for chitosan would suggest considerable ionic conductivity of this material.

The present experiments have been undertaken to egzamine this assumption. The sandwich type polymer samples were investigated by time-domain set up. The applied apparatus was capable of recording current transient fortimes ranging from 1ms up to 10 s, for broad range of sample impedances and temperatures. The polimer has been investigated for different humidity content,as well as with the use of electrodes of different properties.

The results of measurement will be demonstrated.

ELECTROMAGNETIC METHOD FOR QUALITY ESTIMATION OF DIALECTRIC COATING IN UNDERGROUND PIPELINES.

A.M.Briskin. V.N.Uchanin.
Institute of Automatic Control Devices.
5a, Naukova st., Lviv, 290601,Ukraine.

Underground metallic structures, such as pipelines are exploited in conditions of immersion into electrolytic medium. For corrosion protection metallic parts of pipelines are insulated by dialectric coating. For this purpose organic dialectric materials such as polyethylene are usually used. The damages of insulating coating and coating quality reduction lead to corrosion fracture of damaged zone with great pecuniary and ecological losses [1].

That is why the cathodic protection was suggested as the complimentary means avoid the corrosion damages. The uncovered metal play a part of cathode relatively to surrounding electrolyte. The protection is realized by external current application. The surface of uncovered metal becomes equipotential and dangerous corrosion current does not take place.

The effectiveness of cathode protection is in great dependence of dialectric coating quality that is changed during the pipeline exploiting due to the influence of mechanical and chemical factors. For coating quality restoration it is nesessary to have the information about insulating coating conditions along the pipeline track: the sections with damaged coating that have insufficiently high dialectric properties.

The existed methods of dialectric coating testing are based on the protection current, the protection potential or the insulator resistance measurements and others. The majority of this methods are labour-consuming and not efficient because the pipeline opening is needed for direct contact with pipe. But last years the uncontact and high

productive methods were developed. This methods were based on the measurement of magnetic field strength excited by the current that flow along the pipe.It is possible to use the current of protection station or to excite the current from separate generator that is connected with pipe. The cathodic protection stations are carried as biphaze rectifier feeded by installed along pipeline special line ofindustrial frequency tension. In dependence of humidity and acidity of soil this stations are disposed at a distance from 2 to 50 kilometres.

For obstacle avoidence connected with the influence of magnetic field of Earth and other hindrances the uncontact methods are based on alternating magnetic field measurement. For cathodic protection current measurement the second harmonic of industrial frequency (100-120 Hz) may be used. And when the separate generator as current sourse is used the work frequency 1 KHz not indided with the harmonics of industrial tension usually is selected [2]. Uncontact methods provide the pipeline current measurement, the leakage current and dialectric coating spesific electric conductivity estimation.

For uncontact current measurement method analysis the electrodynamic model of pipeline as a long and thin conductor with current J is used. The magnetic field strength H at the distance h from conductor (the axis of pipeline) is determined by known correlation:

$$H = J/2\pi h$$

and the measured current is

$$J = 2\pi H h . \tag{1}$$

But in most cases we do not have the information about the burial depth of pipeline. In this case it is sufficiently to measure the magnetic field strength in another point at the distance L from first point. Second measurement point must lie on the straight line connected the first measurement point with the pipeline axis. The magnetic field components in first (H_1) and second (H_2) points

were determined according the correlation

$$H_1 = \frac{J}{2\pi h} \; ; \; H_2 = \frac{J}{2\pi(h+L)} \; ;$$

where:
h – the distance " first point – pipeline axis ",
$h+L$ – the distance " second point – pipeline axis ".
   From common decision of this equation it not difficult to determine the pipeline current as

$$J = 2\pi h \frac{H_1 H_2}{H_2 - H_1} .$$

(2)

   The specific current leakage by the unit of pipeline length (current gradient) is determined by the current measurement along pipeline. This characteristic is in direct correlation with dialectric coating quality. Insulating pipe is one of the casing (electrode) of condenser. The second casing of condenser is the conductive medium. When there is the potential difference we have only the condensive current for good insulated pipeline. This current do not correlate with insulating coating quality. But there is current leakage in the case of damaged coating and this component of pipeline current is connected with insulating coating quality. This statement is correct only for alternative component of pipeline current.
   The measurement of current gradient along pipeline gives the integral characteristic of insulating coating conductivity on rather lengthy parts of pipe. The dimention of this parts depends of the insulating coating damages degree. The detection of local insulating coating damages is difficult due to the small resolution of this method. This limitations were connected with apparatus and methodical errors.The leakage current measurement on the limited part of pipeline provide the possibility to decrease the influence of this errors. The essence of this method consist in the measurement of magnetic field component created by pipeline current in two sections along pipeline situated from each other at some distance (usually 10-15 m). In each section electromagnetic field is measured in two

points at different from pipe axis.

The value of relative current leakage is determined in accordance with the next correlation [3]:

$$\delta J = 1 - \frac{H_2 - H_1}{H_2' - H_1'} \cdot \frac{H_1' \cdot H_2'}{H_1 \cdot H_2}$$

where H_1' and H_2' are the magnetic field component in the second section.

The current leakage measurement combined with the measurement of pipeline potencial given the possibility to determine the spesific resistance of dialectric coating. The limit value of the pipeline coating spesific resistance is normalized. When measured value of spesific resistance is less than permissible value the remount works are required.

The new portable device for estimation the quality of dialectric coating in underground pipeline is designed.The special algorithm and scheme of signal processing were offered for sensitivity increasing due the industrial errors repression [4].

References:
1. P. Davies, M. Richert, Pipeline coating defect survey techniques and cathodic protection assesment, Internal and external protection of pipes. 7-th Int.conference, London, 1987,pp. 21-25.
2. Howell M.I., A Means of Evalueting the Integrity of the Insulating Coating of Long Buried Conductors , Industrial Corrosion, November, 1986, pp. 22-26.
3. Briskin A.M., Dikmarova L.P., Mizjuk L.Ya.,The method and apparatus for uncontact detection of relative current leakage on part of underground pipeline, Patient certificate N 1777103 , Bulletin of inventions, Moskow,1982, N 43 (In Russian).
4. Briskin A.M., Kazakovtzeva M.A., Uchanin V.N.,The device for uncontact measurement of current in underground pipeline, Patient certificate N 1795384 , Bulletin of Inventions, Moskow, 1993, N6 (In Russian).

Cyclohexane in cylindrical silica cavity. Molecular dynamics simulation

A. Bródka

Institute of Physics, University of Silesia,

Uniwersytecka 4, 40-007 Katowice, Poland

Molecular dynamics of cyclohexane in cylindrical pore of 25 Å diameter in amorphous silica is studied by computer simulation. The solid is represented by an atomic model that takes into account microscopic structure of the surface. A cyclohexane molecule is approximated by a rigid set of six Lennard-Jones interaction centres. The calculations are carried out in the isothermal ensemble for $T=293.3$ K. A series of computer simulations is performed and number of the molecules is increasing from 2 to 60 in the consecutive simulations. This procedure mimics filling the pore with cyclohexane and allows one to study adsorption process. The maximum number of cyclohexanes correspond to about 50% of liquid density. Initially, molecules are adsorbed on the silica surface and for higher densities cyclohexane forms second layer. Translational and rotational correlation functions are calculated and discussed in terms of number of the cyclohexane molecules in the system. The mean square displacement of the molecules from the contact layer is analysed using solution of the diffusion equation.

GLASS-CERAMICS GRADIENT COATINGS FOR BIOMEDICAL APPLICATIONS

R. Cimdins

Technical University, Riga, Latvia

The main requirements to implant materials are the biocompatibility and long-term stability in the physiological environment of living body. Metal implants partially comply with these requirements, however their surface is not bioactive and it is an obstacle of bonding with living tissues. Therefore there is a significant interest in the use of hydroxyapatite (HAp) coated metal implants which accelerate the rate of bonding with bone tissues and act as a barrier between the body and metal implants.

To ensure sufficient bonding strength and long term stability of a plasma-sprayed HAp-coating on metal implant the two layers coating method is proposed. At the first stage the metal implant is coated with dense 20-30 μm thick phosphate glass layer. After this either all or particular areas of the surface are coated with HAp by plasma spraying.

Testing of the bond strength between the coatings and implants were performed on experimental specimens according to standard DIN 50160. The bonding strength between the HAp coating and the intermediate glass coating is 35-45 MPa which exceeds the bond strength between HAp coating and titanium about 10 times. The bond strength between titanium and glass coating is 50-60 MPa.

To evaluate the biocompatibility and bioactivity of coatings obtained the titanium specimens as cylinders (5 mm length, 5 mm diameter) were prepared. 6 specimens were coated with two-layers coating, other 6 were coated only with glass. All specimens were implanted for 3 months into the rabbits tibia. Testing of the bonding strength between the bone tissues and implants was performed by push-out method.

Electric Properties of Water Tree –
3-D Computer Model

Tadeusz Czaszejko
Department of Electrical and Computer Systems Engineering
Monash University, Caulfield Campus
PO Box 197, Caulfield East, Melbourne
Victoria 3145, Australia.

ABSTRACT

*A computer model simulating electric proper-
ties of water trees in 3-d has been developed.
Tree-like patterns of various sizes, grown from
a needle electrode, were generated by a random
walk process. The simulation was performed on
3-d regular grid of electric impedances. The rate
of change of current to the ground versus the
size of the tree pattern was examined. This was
compared with the experimental results of J.D.
Cross and J.Y. Koo [2]. The computer model
shows that if water has sufficient conductivity,
water in a water tree cluster is contained in a
dispersed form. Water tree channels may be in-
terconnected only if conductivity of water in wa-
ter tree is not greater than that of distilled water
$(10^{-4}\ S/m)$.*

INTRODUCTION

There are computer stochastic models that sim-
ulate tree-like, branched, fractal patterns, such
as those often seen in a breakdown of solid,
liquid or gaseous dielectrics, developed several
years ago [7, 8, 6, 9]. Fractal properties of elec-
tric tree patterns in polymeric materials were
also studied [1, 4, 5] and compared with com-
puter generated models [1, 5]. These studies
concluded that there is generally a good agree-
ment between the fractal properties of experi-
mentaly generated electric trees and their com-
puter generated counterparts.

Successful reproduction of electric tree pat-
terns in computer simulations has not led, so
far, to modelling of electric properties of insula-
tion affected by treeing. The presence of electric
discharges in the tree channels makes the task
of modeling of electrical treeing in a dielectric
material rather difficult.

Water treeing does not present this difficulty.
An insulation area affected by water treeing
may be seen as a mixture of three components:
(1) dielectric material, (2) water and (3) un-
filled voids. Water and unfilled voids are con-
tained in interconnected water tree channels or,
as argued in [2], they may be seen as a clus-
ter of dispersed micro-voids filled with water.
By assigning appropriate dielectric properties
(conductivity and dielectric constant) to all re-
gions of dielectric, it may be possible to re-
produce the electric properties of such an ob-
ject. The behaviour of such a model could then
be compared with electrical measurements re-
ported in [2]. The results of this approach in
a two-dimensional model may be found in [3].
This work presents a three-dimensional model
of water tree.

COMPUTER MODEL

The Dielectric Breakdown Model introduced
by Niemeyer, Pietronero and Wiesman [7, 8] re-
lates the probability of growth of the discharge
pattern to a local electric potential satisfying
Laplace's equation $\nabla^2\phi = 0$. The model is
formulated on a 2-dimensional square lattice,
and the Laplacian operator, ∇^2, is discretized.
Then, the discrete Laplace equation is solved
repeatedly for every step of growth. Therefore,
a large system of linear algebraic equations have
to be solved many times over which results with
excessive computation time. Even more so if the
model is 3-dimensional.

Alternatively, a Diffusion Limited Aggrega-
tion (DLA) model may be used to generate pat-
terns which are statistically identical to those
generated by the Dielectric Breakdown Model
[8, 6, 5, 10]. The DLA patterns are generated

through a random walk process, and therefore, require very little computation.

In the proposed model, the water tree pattern is generated through a random walk on a 3-dimensional, cubic lattice of points. The top surface of the lattice, together with a pyramid depression (a needle electrode), represents the high potential electrode. The tip of the needle electrode is placed at the centre of the cube. The angle at the tip is 30°. The bottom surface of the cube represents the ground electrode. Random seeds are placed around the tip of the needle electrode on a length equal to 10% of the total length of the needle.

A random walking particle is released from a random location on a sphere centered at the tip of the needle electrode. The particle undergoes a random walk, jumping one lattice unit, choosing direction randomly, until at least one of the neighbour sites represents a seed point placed on the electrode, or already belongs to the aggregate. Then, the link is made between the random walker and such a neighbour to extend a branch of the tree. This procedure is repeated until the tree reaches the desired size.

The links between the grid points, established by random walker, form a lattice of cellular admittances. Each admittance represents a parallel combination of a local, cellular conductance and susceptance. The value of the cellular conductance and susceptance depends on the local conductivity and permittivity. The conductivity of cells representing polyethylene and empty voids was set to zero. The conductivity in a cell representing a section of a branch of water tree was set between that of pure water (10^{-6} S/m) and sea water (4 S/m). The relative permittivity was set at 2.2, 80.0 and 1.0 for polyethylene, water and empty voids respectively.

The development of water trees in such a network is represented by a change of admittance at the location of water tree branches. The admittance of a section of a branch may take the value of the admittance of a water cell, if the section is filled with water, or the value of admittance of an empty void cell for an unfilled section. The percentage of unfilled sections could be varied and their location was chosen randomly. If water tree channels are interconnected the percentage of unfilled sections is zero. The larger the number of unfilled voids, the more dispersed is water contained within the tree.
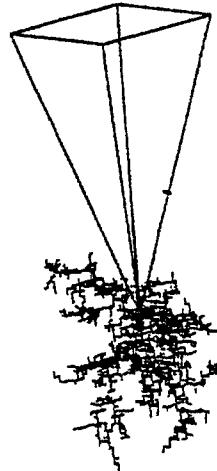
Figure 1: Computer simulated tree containing 1500 branches.

If the growth of water tree produces a change in the electric field within the insulation, the total flux to the ground electrode will change as reported in [2]. In the proposed model, changes in the electric properties of the network resulting from the development of water tree are reflected in the change of the total current to ground electrode.

In order to determine the changes in the current, potentials at all nodes of the network have to be calculated. The iterative (over-relaxation) method was used to solve a system of algebraic equations resulting from Kirchhoff's current low.

$$V_{i,j,k} = \frac{1}{Y_{i,j,k}}(Yl_{i,j,k}V_{i-1,j,k} + Yr_{i,j,k}V_{i+1,j,k} + Yb_{i,j,k}V_{i,j-1,k} + Yf_{i,j,k}V_{i,j+1,k} + Yd_{i,j,k}V_{i,j,k-1} + Yu_{i,j,k}V_{i,j,k+1})$$

(1)

where:

$V_{i,j,k}$ – potential at location (i,j,k);

$Y_{i,j,k} = Yl_{i,j,k} + Yr_{i,j,k} + Yb_{i,j,k} + Yf_{i,j,k} + Yd_{i,j,k} + Yu_{i,j,k}$

– self-admittance of the node (i,j,k);

Yl, Yr, Yb, Yf, Yu, Yd – admittances to the left, right, back, forth, up and down of the node (i,j,k).
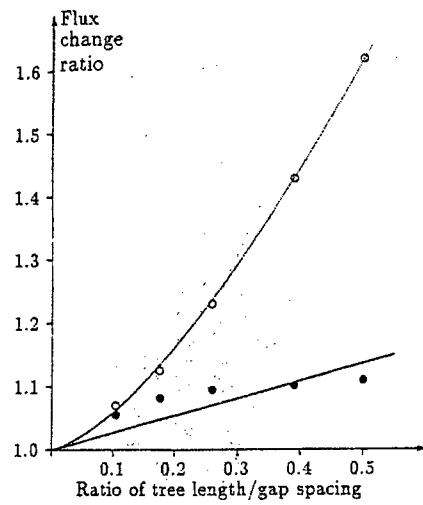
Figure 2: Relative change of ground current as a funtion of water tree length and conductivity of water.

The total current was calculated as a sum of currents entering the ground electrode from the nodes located directly above:

$$I_{tot} = \sum_{i,j} V_{i,j,K-1} Y u_{i,j,K-1} \qquad (2)$$

where:

n – number of nodes to the left and right from i_{tip};

$V_{i,j,K-1}$ – potential at the node (i,j,K-1);

$Y d_{i,j,K-1}$ – admittance linking node (i,j,K-1) and ground electrode;

K – height of the lattice.

RESULTS

Computations were performed on a $100 \times 100 \times 100$ lattice, on which water trees containing up to 1500 branches were grown. This represented the length of up to 50% of the gap between the tip of the needle and ground electrode. An example of such water tree pattern is shown in Fig. 1.
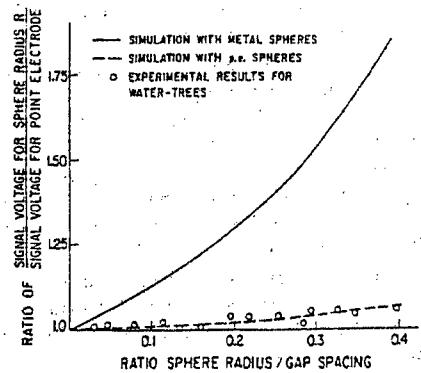
Figure 3: Voltage on measuring electrode as a function of water tree radius.

Computations of the ground electrode current were repeated four times, each time for different set of random numbers, and the average values were calculated. The relative change of the current for various sizes of water trees and for two different values of conductivity of water is shown in Fig. 2.

There was a negligible difference in current if the conductivity of water was increased above 10^{-4} S/m, which corresponds with the range of conductivities from that of water with small ionic content, e.g. tap water, up to that of see water (4 S/m).

Fig. 2 shows that if water tree branches contain water of low conductivity (10^{-6} S/m), the relative change of current caused by water tree growth is similar to that obtained experimentally in [2] and shown in Fig. 3. If water has conductivity of 10^{-4} S/m or higher, the relative change of current is similar to that obtained in [2] in the experiment with a conducting sphere.

DISCUSSION AND CONCLUSION

The results obtained from the computer model show that if water tree is to have interconnected channels, the conductivity of water contained in these channels should not exceed that of distilled water (10^{-6} S/m). It has been known, however, that regions of polyethylene affected by water treeing contain traces of salts. It is most likely, therefore, that these salts dissolved in water increase the conductivity of water above the value of 10^{-6} S/m. This, in turn, should cause larger relative changes of

current than those obtained experimentally in [2]. Consequently, water tree channels cannot be fully filled with water. Water tree branches filled with water have to be separated by hollow channels, if channels are interconnected, or sepaprated from each other by the dielectric. The two-dimensional model in [3] shows that at least 30% of water tree channels must be unfilled if water tree branches are interconnected.

References

[1] Barclay A.L., Swenney P.J., Dissado L.A., Stevens G.C., "Stochastic Modeling of Electrical Treeing: Fractal and Statistical Characteristics", J. Phys. D: Appl. Phys., Vol. 25, 1990, pp. 1526–1545.

[2] Cross J.D., Koo J.Y, "Some Observations on the Structure of Water Trees", IEEE Trans. EI-19, No.4, 1984, pp. 303–306.

[3] Czaszejko T., "A Network Model of Water Tree", IEEE 1993 Annual Report, Conference on Electrical Insulation and Dielectric Phenomena, Oct. 17–20, 1994, Pocono Manor, USA, pp. 726–731.

[4] Fujimori S., "Fractal Analysis of Tree Figures", Proc. of the 3rd Inter. Conf. on Properties and Applications of Dielectric materials, July 8–12, 1991, Tokyo, Japan, pp. 131–134.

[5] Kudo K., Maruyama S., "Studies on the Fractal Properties of Electrical Trees", Proc. of the 3rd Inter. Conf. on Properties and Applications of Dielectric materials, July 8–12, 1991, Tokyo, Japan, pp. 135–138.

[6] Murat M., "2–D Dielectric Breakdown Between Parallel Lines", Fractals in Physics, Elsevier Science Publishers B.V., 1986, pp. 169–171.

[7] Niemeyer L., Pietronero L., Wiesmann H.J., "Fractal Dimension of Dielectric Breakdown", Phys. Rev. Lett. Vol. 52, No. 12, March 1984, pp. 1033–1036.

[8] Pietronero L., Wiesman H.J., "Sochastic Model for Dielectric Breakdown", J. Stat. Phys., Vol. 36, Nos. 5/6, 1984, pp. 909–916.

[9] Satpathy S., "Dielectric Breakdown in Three Dimensions", Fractals in Physics, Elsevier Science Publishers B.V., 1986, pp. 173–176.

[10] Vicsek T., "Fractal Growth Phenomena", World Scientific, 1992.

UNIVERSALITY OF AC CONDUCTION AT LOW TEMPERATURES

J. Dyre

Institute of Math. and Physics, IMUFA University of Roskilde
Roskilde, Denmark

This paper reports the results of extensive computer simulations in two and three dimensions of AC conduction in thermally activated systems at low temperatures. Two models have been studied, the "macroscopic" model "1" and the standard symmetric hopping model "2". For both models it is assumed that the conductivity resp. jump rates are thermally activated with an activation energy that varies randomly according to some probability distribution. For both models it was found that the AC conductivity at low temperatures, except for a trivial scaling, becomes completely independent of the activation energy probability distribution. This phenomenon is referred to as "universality". The universality is predicted from the approximate analytical treatment offered by the effective medium approximation (EMA), and the EMA prediction is also quantitatively very good.

References
[1]. J. C. Dyre, Phys. Rev. B 48, 12511 (1993).
[2.]. J. C. Dyre, Phys. Rev. B 49, 11709 (1994).

THE USE OF TDDS FOR STRUCTURAL AND DYNAMIC INVESTIGATIONS OF PROTEIN MOLECULES IN SOLUTIONS.

I.V.Ermolina, I.N.Ivoylov, A.G.Krushelnitsky, V.D.Fedotov

Kazan Institute of Biology Russian Academy of Sciences.

The results of polarization and relaxation investigations of aqueous protein solutions by the time domain dielectric spectroscopy (TDDS) are presented. The dipole correlation function (DCF) of myoglobin solutions in the wide range of concentrations from 0.2% to 64% have been obtained. The analysis of FDC has shown that within the experimental frequency range 500 KHz - 1 GHz the samples has a few relaxation processes. The total polarization amplitude reflects the behaviour of only protein molecules and doesn't carry any information about solvent. This polarization is created by the orientation tumbling of protein molecules possessing the large dipole moment and by the internal motions of various protein part - polar and charged aminoacid residues. Thus, the mechanizm of polarization is diffusional tumbling of fluctuated protein dipole and is well described by the Onsager-Oncley model. In the common case DCF may be decomposed to three components "1" with different correlation times. Their relative amplitudes depend on protein concentration in solution. Particulary, at concentration < 6% the amplitude of the slowest process become so small that we can't registrate this prosess and DCF become two-components. Two shortest components are conventionally attributed to the internal motion and Brownian tumbling as a whole. The third component has the correlation time depending on concentration and approximately 5-10 times longer than that of the Brownian tumbling. The analogious results were obtained when analising the correlation function obtained by the nonselective proton NMR-relaxation method "2". Thus, a complex shape of DCF unambiguously indicates that the Brownian tumbling of a protein in solution is anisotropic. Otherwise, for a separate molecule it is difficult to suggest any relaxation mechanism with time less than the Brownian tumbling. Our experiments have shown that the correlation time and relative amplitude of the longest component are different for different proteins and sensitive to pH of a protein solution. To explain the origin of this component we have advanced the model of the protein motion in solution that takes into account interprotein electrostatic interactions. Each dipole moment of the protein molecule in solution experiences electrostatic torques from the electric charges and dipoles of neghboring proteins. This gives rise to the anisotropy of the protein Brownian rotation and residual correlation which is dependent on the strength of interprotein electrostatic interactions. But as it follows from the experiment the DCF decays to zero. The time of this slow process is equal to the life time of the Brownian tumbling anisotropy and probably is defined by the protein translational diffusion.

To analyse the microdynamical parameters behaviour according with the presented model we have calculated the Brownian dynamics for a single dipole in

the constant lectric field and for a set of dipoles placed as a cubic lattice. Furthermore the results of the viscosity measurements in wide concentration range were used. Ourestimations do not contradict to the presented model which takes into account the electrostatic interactions of macromolecules. Thus, on the basis of the investigations described above one may conclude that for the protein solutions with concentration about a few percentage (particularly, for myoglobin < 6%) the interprotein interactions may be neglected. As for the TDDS method such solutions are diluted. DCF has the simplest shape, that is why its analysis becames more easier. Therefore the use of the small protein concentration solutions is optimal just for the investigation of protein molecules under various conditions. As an example, the results of temperature denaturation investigation of 2% solution ofbovine pancreatic ribonuclease A (RNase A) at pH 2.7 in range 10-95 degree C are presented here. Several temperature intervals characterizing the native state, compact-denaturated state and denaturated state of RNase A have been observed. .hese results agree well well with the data obtained by nonselective proton NMR relaxation in our laboratory and by other methods presented in literature.

[1] I.V.Ermolina, A.G.Krushelnitsky, I.V.Ivoylov, Yu.D.Feldman, V.D.Fedotov
Appl.Magn.Res., 5, 265--283,1993
[2] A.G.Krushelnitsky, V.D.Fedotov, J. Biomol. Struc. & Dynam., 11, 121-141, 1993.

ON THE POSSIBILITIES OF THE THERMAL-NOISE STATISTICAL ANALYSIS IN EXPERIMENTAL STUDIES OF DIELECTRICS AND OTHER DYNAMICAL SYSTEMS

V.A.Goncharov

Zavoisky Institute of Physics and Technology,
Sibirsky trakt 10/7, Kazan 420029, Tatarstan, Russia.

As distinct from well-known "active" (frequency- and time-domain) methods of dielectric measurements, the fluctuation ones, based on the statistical analysis of the own electrical thermal noise of a sample under test, do not imply any probing signal to be used. A fundamental peculiarity of the fluctuation measurements is that, in practice, they produce no disturbance of studied system's thermal eqilibrium. So, the fluctuation methods turn out to be irreplaceable when studiyng media with strong non-linearity with respect to the electric field, for instance, ferroelectrics (including ferroelectric liquid crystals), electrolytes (particularly, biopolymer solutions), or substances in the vicinity of phase transitions [1 and refs therein]. These methods were for a long time considered just as complementary techniques, for the thermal noise two-sided spectral density is a real function containing no phase information. However, it has been shown in [1,2] that, potentially, the fluctuation measurements allow one to obtain complele information on the dynamical properties of studied dielectrics, being no less informative than the "active" methods. Actually, the Nyquist formula [3],

$$S_x(\omega) = 2\ kT \cdot Re Z(\omega) \tag{1}$$

$(S_x(\omega) = \int_{-\infty}^{\infty} K_x(t)\exp(-i\omega t)dt = 2\int_0^{\infty} K_x(t)\cos(\omega t)dt$ is the spectral density of the fluctuation EMF $X(t)$ existing across the terminals of a two-pole device with the complex impedance $Z(\omega)$, $K_x(t) = \lim_{\Delta\to\infty}(1/\Delta)\int_0^{\Delta} X(t')\cdot X(t+t')dt'$ the autocorrelation function of $X(t)$, k the Boltzmann constant,

T the temperature), which is the expression of the fluctuation- dissipation theorem (at $\hbar\omega \ll kT$) [2] for electrical circuits and is usually used for the thermal noise analysis, can be written in the generalized form

$$L[K_x(t)] = kT \cdot Z(\omega) \qquad (2)$$

($L[K_x(t)] = \int_0^\infty K_x(t)\exp(-pt)dt$ is the Laplace transform of $K_x(t)$, $p = \alpha + i\omega$, $\alpha \to 0$). Formula (2) is the direct expression for the complex impedance of a two-pole device via its fluctuation EMF autocorrelation function; it can be derived from (1) either with the help of Kramers-Kronig relations, or by a simpler way used in [1,2].

Let us consider the simplest measuring system realizing the fluctuation dielectric measurements [1,2]. The system consists of: the input circuit comprising the measuring cell with the studied sample, the reference condenser, and the short circuit, which can in turn be connected to the input of the fast low-noise amplifier; the correlator of the amplifier's output signal; and the computer executing all further calculations. Let C_0 be the measuring cell working capacitance, C_1 the capacitance comprising the leads' and the amplifier's input capacitances and that caused by the cell fringing fields, C_2 a reference capacitance also comprising the leads' and amplifier's input components, and R_1 the measuring circuit's external shunt resistance. Let us introduce an effective permittivity

$$\varepsilon_{ef}(\omega) = \varepsilon(\omega) + C_1/C_0 + 1/(i\omega R_2 C_0) \qquad (3),$$

where $\varepsilon(\omega) = \varepsilon'(\omega) - i\varepsilon''(\omega) = L[\dot\varphi(t)] = L\{(d/dt)[\varepsilon_\infty + \phi(t)]\}$ is the complex permittivity of the sample, $\varphi(t)$ its response function, $\phi(t)$ the "dipole" component of $\varphi(t)$, $\varepsilon_\infty = \varepsilon(\infty)$, $R_2^{-1} = C_0\sigma/\varepsilon_0 + R_1^{-1} = \sigma_{ef}/\varepsilon_0$ is the total ohmic conductance of the measuring circuit, ε_0 the permittivity of the vacuum, σ the sample's low-frequency conductivity, and σ_{ef} a certain effective conductivity. Then, for the cell with the sample, eq.(2) takes the form

$$L[K_x^{samp}(t)] = kT/[i\omega \, C_0 \varepsilon_{ef}(\omega)] \qquad (4),$$

and, for the reference condenser,

$$L[K_x^{ref}(t)] = kT/(i\omega\, C_2 + R_1^{-1}) \tag{5},$$

whence $K_x^{ref}(t)=(kT/C_2)\exp[-t/(R_1 C_2)]$ and $K_x^{ref}(0)=kT/C_2$ (6).

In practice it is convenient to operate with functions $f_1(t)= K_Y^{ref}(t) - K_Y^{short}(t)$, $f_2(t)= K_Y^{samp}(t) - K_Y^{short}(t)$ (7), where $K_Y^{ref}(t)$ and $K_Y^{short}(t)$ are the autocorrelation functions of the amplifier output signal for the cases when the reference condenser is connected to the amplifier input, and when the input is short-circuited. $K_Y^{samp}(t)$ is that for the input terminated in the sample-filled cell. Subtracting $K_Y^{short}(t)$ accounts for the amplifier's own noise. In case of an ideal amplifier with the frequency-independent real gain factor H,

$$f_1(t)= H^2 K_x^{ref}(t) \quad \text{and} \quad f_2(t)= H^2 K_x^{samp}(t) \tag{8}.$$

Eqs (4,6,8) then give: $\varepsilon_{ef}(\omega)= 1/\{i\omega\, L[f(t)]\}$ (9), $f(t)= (C_0/C_2)\{\exp[-t/(R_1 C_2)] - [f_1(t) - f_2(t)]/f_1(0)\}$ (10).

Laplace inversion of eqs (9,5) yields a set of relations for direct time-domain treatment of observables:

$$\int_0^t \dot{\phi}_{ef}(t')f(t-t')dt' = g(t) \tag{11},$$

where $g(t) = 1 - f(t)/f(0)$, $\phi_{ef}(t) = \varphi_{ef}(t) - \varphi_{ef}(0)$, $\varphi_{ef}(t)$ is the response function corresponding to $\varepsilon_{ef}(\omega)$ ($\varepsilon_{ef}(t)=L[\dot{\varphi}_{ef}(t)]$), $\dot{\phi}_{ef}(t)= \dot{\phi}(t) + \sigma_{ef}/\varepsilon_0 = \dot{\phi}(t) + 1/(R_2 C_0)$,

$$\varepsilon_\infty + C_1/C_0 = \varphi_{ef}(0) = 1/f(0) \tag{12}.$$

Since $\dot{\phi}(\infty) = 0$, one has : $\dot{\phi}(t) = \dot{\phi}_{ef}(t) - \dot{\phi}_{ef}(\infty)$ (13).

Solving eq (11) numerically with respect to $\dot{\phi}_{ef}(t)$, taking the shunt conductance (eq.(13)) into account, integrating $\dot{\phi}(t)$ between 0 and t, and adding ε_∞ found from (12), one obtains the sample's response function $\varphi(t)$. As for the complex permittivity of the sample, it can either be computed from obtained $\varphi(t)$, $\varepsilon(\omega)= L[\dot{\varphi}(t)]$, or be found directly with the help of eqs (9,3), R_2 in (3) being determined as [1,2] $R_2 = R_1 \int_0^\infty f_2(t)dt / \int_0^\infty f_1(t)dt$.

The function f(t) might be called an "inverse dielectric response function". In fact, one has from (9) at $R_2 \to \infty$ and $C_1=0$: $1/\varepsilon(\omega)= L[\dot{f}(t)]$, whereas $\varepsilon(\omega)= L[\dot{\varphi}(t)]$. So, the basic relation between the electric field **E** and the displacement **D** in the dielectric, $\mathbf{D}(t) = \varepsilon_0 \int_{-\infty}^t \mathbf{E}(t')\dot{\varphi}(t - t')dt'$, can be

rewritten in the form $E(t) = (1/\varepsilon_0)\int_{-\infty}^{t} D(t')\dot{\varphi}(t - t')dt'$ where $f(t)$ describes the time course of the electric field after the displacement has been instantaneously switched.

It should be noted that, for "large R_2", eq.(4) gives $K_x^{samp}(t) = (kT/C_0)f(t)$, i.e., in this case (provided $C_1=0$) the autocorrelation function of the sample- filled cell's fluctuation EMF differs from the "inverse dielectric response function" of the sample only by a constant factor. In more general case of $C_1 \neq 0$ and finite R_2, $f(t)$ can be said to be an effective inverse response function.

Thus, the treatment of the fluctuation dielectric measurements data gives one the customary quantities (dielectric response function and complex permittivity); these quantities correspond to the equilibrium state of the dielectric, which is of importance when studying non-linear media.

As far as eq.(2) holds independent on the nature of the complex impedance $Z(\omega)$ (similarly to eq.(1), see [3]), one can as well use eq.(2) to develop many other experimental methods for the investigation of different relaxation and resonance phenomena (EPR, NMR, acoustic relaxation, etc.).

A series of results obtained by here described method for non-conducting liquids, liquid crystals and electrolytes are represented in the report. Some results of thermal-noise studies of ferromagnetic resonance are also reported.

REFERENCES

1. V.A.Goncharov and I.V.Ovchinnikov. On the study of the dynamical behaviour of dielectrics by thermal-noise correlation analysis. Chem.Phys.Letters 111 (1984) 521.

2. V.A.Goncharov. Pulsed and fluctuation dielectric spectroscopy and molecular motion in liquid crystals. Candidate's thesis. Kazan, 1986.

3. E.M.Lifshitz and L.P.Pitaevski. Stat.fizika 2. Nauka, Moskow, 1978.

4. L.D.Landau and E.M.Lifshitz. Stat.fizika 1. Nauka, Moscow, 1976.

DYNAMICS OF WEAKLY BONDED IONS
IN CUBIC OXIDE PYROCHLORE $Cd_2Nb_2O_7$

B.Hilczer[*], N.N.Kolpakova[**], J.Wolak[*], M.Wiesner[***]

[*] Institute of Molecular Physics, Polish Academy of Sciences,

Smoluchowskiego 17, PL 60-179 Poznań, Poland

[**] Ioffe Physico-Technical Institute RAN, Politechnicheskaya 26, 194021

St. Petersburg, Russia

[***] Institute of Physics, Adam Mickiewicz University, Grunwaldzka 6,

PL 60-780 Poznań, Poland

Among $A_2B_2O_7$ oxides of the pyrochlore family, only $Cd_2Nb_2O_7$ and $Cd_2Nb_2O_6S$ exhibit ferroelectric properties as well as undergo a sequence of phase transitions [1]. The cubic oxide pyrochlore $Cd_2Nb_2O_7$ attracts attention due to a large variety of phase transitions between 4 and 500 K. Its phase diagram includes ferroelastic and ferroelectric states, which exist down to 4 K, with the glassy state appearing on their background below 18 K:

VII	VI	V	IV	III	II	I
Monoclinic	?	Orthorhombic	Orthorhombic		Cubic	Cubic
C	INC	mm2	mmm		m3m	m3m
18	45	86	196	205	312	T (K)

Ferroelectric | Paraelectric

Ferroelastic | Paraelastic
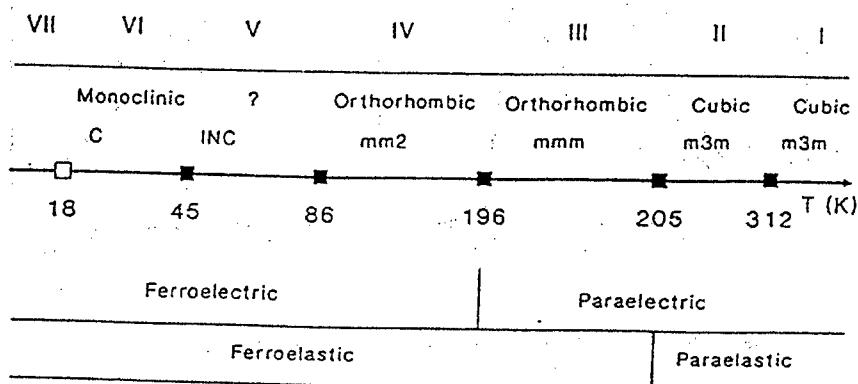
In ferroelectric phase of this pyrochlore, there is a maximum in $\epsilon'(T)$ at $T < T_c = 196$ K which arises at frequencies lower than 1 MHz and does not correspond to phase transition. This maximum is originated from domain motions and reorientations

47

of ferroelectrically non-active dipoles Cd-O(7th) [2,3]. Nevertheless, mechanisms of low-frequency dielectric relaxation in $Cd_2Nb_2O_7$ are not clear [2-5]. The aim of this study is to elucidate the nature of the dielectric relaxation between 100 and 300 K and to get more evidences for contribution of relaxation of ferroelastic-ferroelectric domains as well as of Cd-O(7th) dipoles in the pyrochlore crystal lattice. For this reason, $\epsilon'(T)$, $\epsilon''(T)$ and tgδ of single crystals of different stoichiometry were studied over a wide frequency range of 25 Hz to 1 MHz and a wide range of measuring ac field strengths of 1 V/cm to 110 V/cm for uniaxial pressure of $0 \leq X < 4$ MPa. An analysis of the experimental data reveals that we are dealing with two Debye-type relaxation processes in the ferroelectric phase (Figs. 1 and 2).
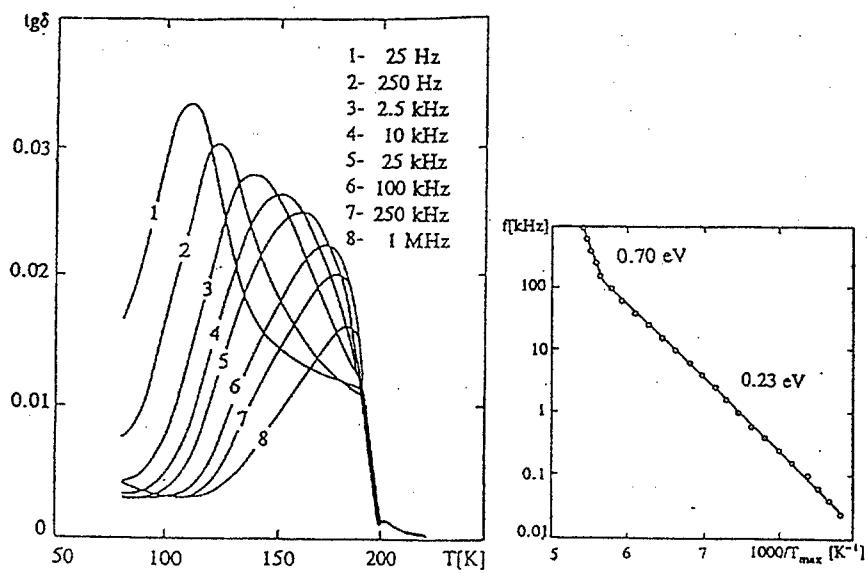
Figure 1. tgδ vs. T and Arrhenius plot for stoichiometric $Cd_2Nb_2O_7$ single crystal for X=O.

For stoichiometric crystals (Cd:Nb ratio equals to 1:1) the relaxation of Cd-O(7) dipoles is characterized by activation energy of 0.23 eV and domain wall relaxation is characterized by activation energy of 0.70 eV. Uniaxial pressure applied to the crystal increases the activation energy of domain relaxation process. The energy also increases when ac field strength increases or when stoichiometry of single crystal is distorted and
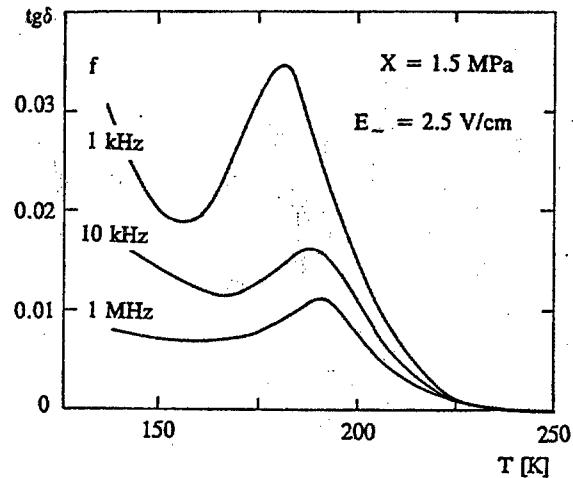
Figure 2. Pressure-induced change in tgδ vs. T.

the role of lattice defects becomes meaningful: activation energy of domain wall relaxation of crystals with distorted stoichiometry (yellow) was found to increase to ~ 1.46 eV. As to the system of Cd-O(7th) dipoles, its activation energy is unaffected neither by ac field strength and uniaxial pressure nor by change in stoichiometry of crystal and defects in the crystal. The system of these disordered dipoles in the pyrochlore network is formed in paraelectric phase due to weak bonds of Cd ions and of the "seventh" oxygens to the $(NbO_6)^{n-}$-octahedra-formed network (Fig.3). These dipoles are originated from displacements of O_2-(7th) ions relative to Cd^{2+} ions along the $[111]_{cub}$ axis in spacious lattice of the pyrochlore. These dipoles are supposed to be also a precursor of glassy state in $Cd_2Nb_2O_7$ below 18 K [6].

The cubic oxide pyrochlore $Cd_2Nb_2O_7$ is the first example of ferroelectrics in which ferroelectric and ferroelastic domains and a disordered dipole system exist simultaneously, with both of relaxation mechanisms observed down to 4 K.
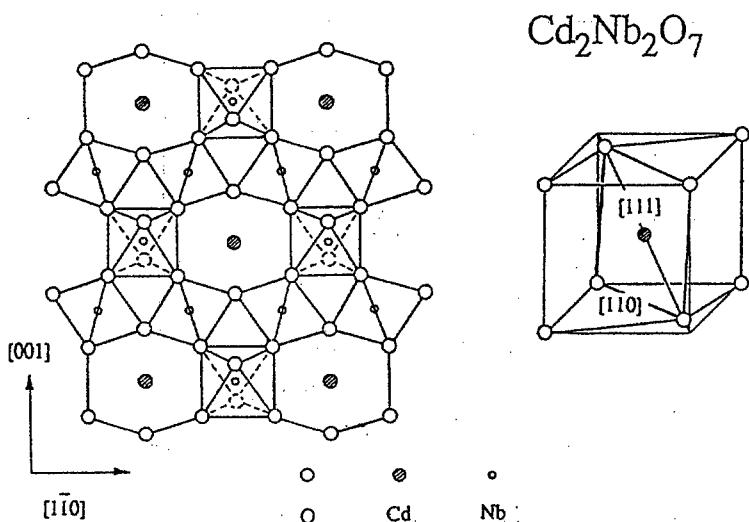
$$Cd_2Nb_2O_7$$

Distances at 297 K	[Å]
Cd-O	2.628(1)
Cd-O(7)	2.246(1)
Nb-O	1.967(1)

Figure 3. Projection of polyhedra configuration in Cd_2Nb_2O pyrochlore on the (110) plane at room temperature. Insert: Coordination scalenohedron $(CdO_8)^{n-}$ with symmetry of D_{3d}-3m depressed along the [111] axis.

References

1. Landolt-Börnstein (1981) Ferroelectrics and Related Substances, Gr. III, vol. 16a (N.Y. Springer-Verlag).

2. Kolpakova N.N., Margraf R., Połomska M., J. Phys.: Condensed Matter (1994) 6, 2787.

3. Kolpakova N.N., Połomska M., Margraf R., Soviet Fizika Tverd. Tela (1990) 32, 1893.

4. Swartz S.L., Randall C.A., Bhalla A.S., J. Amer. Ceram. Soc. (1989) 72, 637.

5. Kolpakova N.N., Margraf R., Pietraszko A., Soviet Fizika Tverd. Tela (1987) 29, 2638.

6. Kolpakova N.N., Hilczer B., Wolak J., Wiesner M., Phase Transitions (1993).

MOTHER NATURE RELAXES IN FRACTAL TIMES

A. K. Jonscher
Royal Holloway New College, Egham, United Kingdom

Abstract not available

INFLUENCE OF AGEING PHENOMENA ON CHARGE TRANSPORT IN P-QUATERPHENYL POLYCRYSTALLINE THIN FILMS .

S.Kania , J.Kondrasiuk , A.Lipiński

*Technical University of Łódź , Institute of Physics ,
ul. Wólczańska 219 , 93 - 005 Łódź , Poland*

The drift mobility , the most important parameter describing the transport mechanism in organic solids , is the subject of extensive studies in many laboratories . The drift mobility in organic layers , is usually determined using the well-known time-of-flight method .

The films of p-quaterphenyl were prepared by thermal vacuum evaporation at a pressure of the order 10^{-5} Torr on the glass substrates . For investigation of electrical and photoelectrical properties, the samples were sandwiched between gold (bottom) and semitransparent aluminium (top) electrodes . The thickness of the p-quaterphenyl layers were 18 - 22 μm and were determined using the MII - 4 interferometer microscope or by capacitance measurements .

From optical investigations results , that the thermal vacuum evaporated p-quaterphenyl samples had polycristalline structures and the mean size of the crystallites was about 2-3 μm .

The surface roughness of those layers estimated by the optical reflectometric method using the He-Ne laser ($\lambda < 0,6328$ μm) was small ($\hbar < 0,2$ μm) [1] .

Above mentioned p-quaterphenyl layers were aged in about $4 \cdot 10^{4}$ hours time at a room temperature , at an atmospheric pressure and at relative humidity order 70 % . The layers were influenced by molecules of the atmospheric oxygen (O_2) and by high polarity molecules of water (H_2O) .

For those samples comparative investigations were made . The structure of those layers remains polycrystalline , and the size of the crystallites have not been changed too much . If the partly recrystallisation occurs , then it is under measurable level . The surface roughness has not been changed either . For these p-quaterphenyl layers the investigations of the transient currents were carried out . Free carriers were generated by a short duration light pulse of a speedlamp (duration about 3 μs) .

The layers were so photosensitive , that the current impulses on the oscilloscope , OS - 102 type , screen were observed without demanding to employ operational preamplifier .

Current - time impulses both for holes as for electrons possessed characteristic kink point , so , it was possible to do direct determing time of flight of the carriers by examining the layer. Typical current impulse for holes is presented in a Fig.1 , so typical impulses for electrons is presented in a Fig.2 . Determined mobility of holes field intensity dependent (from $1,1 \cdot 10^{4}$ V/cm to from $4 \cdot 10^{5}$ V/cm) is constant in magnitude ($0,9 \pm 0,2$) $\cdot 10^{-4}$ cm^2/Vs .

Similarly it is for mobility of electrons , however , it has got a little great value ($1,7 \pm 0,2$) • 10^{-4} cm^2/Vs .
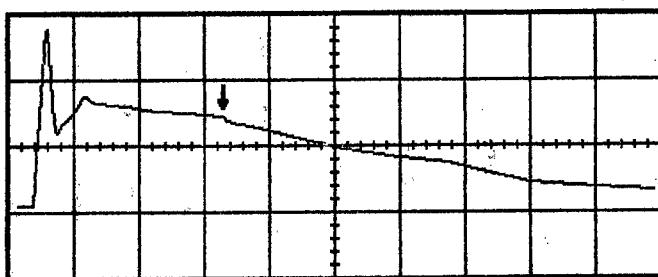
Fig.1. Typical impulse current-time for holes in aged polycrystalline layers of p-quaterphenyl . Vertical axis 2• 10^{-7} A/div . Horizontal axis 100 µs/div . Thicknes of the layer $D = 18$ µm . Voltage $U = 128$ V .
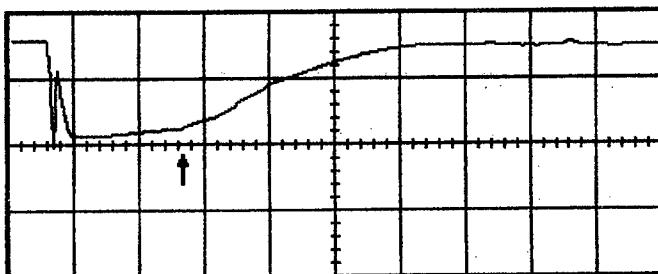
Fig.2. Typical impulse current-time for electrons in aged polycrystalline layers of p-quaterphenyl . Vertical axis 2• 10^{-7} A/div . Horizontal axis 100 µs/div . Thicknes of the layer $D = 18$ µm . Voltage $U = 128$ V .

Values of carrier mobilities depend on field intensity for p-quaterphenyl layers examined at atmospheric pressure in several hours since the thermal vacuum evaporation [2] and for aged layers , in comparison is shown in Fig.3 .

Hole's mobility values differ a little . Whereas it was able to evaluate electron's mobility after the ageing period , because the examined layers had gone to "electric stable" state and they were without tendency in switching from low conductivity state to high conductivity state , and without reversal .

It seems that interactions of the molecules of oxygen O_2 and steam H_2O with the p-quaterphenyl layers are so fast , so longer ageing does not influence on carrier mobility .

Then the chemisorption occurs , and then in-diffusion to interlayer space occurs , with that , that the process is quasi - inverse [4 , 5] . It seems to be indicated by the fact that the drift mobility measurements made in vacuum in order 10^{-5} Torr , for the p-quaterphenyl layers , which were in presence of molecules O_2 and H_2O for
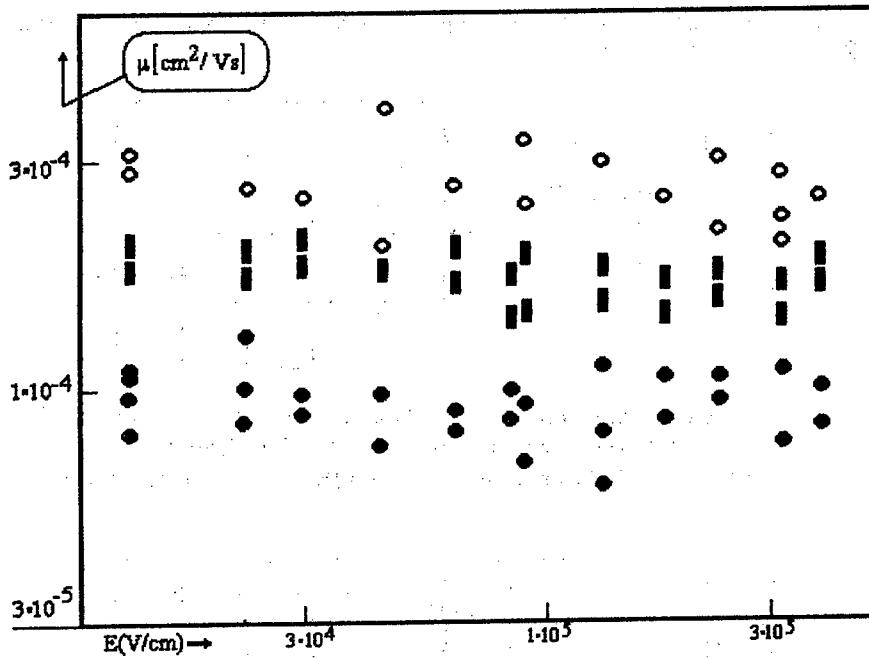
Fig. 3. Dependence of the charge mobility in the p-quaterphenyl layers on
the electric field .

○ - holes [2]
● - holes for aged layers
▮ - electrons for aged layers .

several houres since evaporation (in standard coditions) gives values less over an order
of magnitude (about $1 \cdot 10^{-5}$ cm^2/Vs) [3] .

Whereas stabilization qantity of conductivity is more probably associated with
displacement of "misfit " dislocations and intergranular stress and stress among
crystallite and substrate .

Authors wish to thank Dr.W.Mycielski for his support .

REFERENCES
[1] S.Kania et all. , Proc. Conference on Surface Physics , Łódź (Poland) ,16-17 Dec.
1986 , vol. 1 , p. 255 , 1986 .
[2] S.Kania , J.Kondrasiuk and A.Lipiński , Proc. of National Conf. Molecular
Crystals 1989 , Częstochowa - Kokotek (Poland) , 25-26 Sept .1989 , p.26 ,1989.
[3] S.Kania and W.Mycielski , ibid. , p.27 .
[4] A.Proń , D.Billaud , S.Lefrant , Wiss. Berichte Ak. der Wiss. der DDR , vol. 29,
p. 27 ,1984 .
[5] G.Wegner et all. , Mol. Cryst. Liq. Cryst. , vol. 118 , p. 85 , 1985 .

BARRIERS TO CARRIER TRANSPORT IN DISORDERED AND HIGHLY NON-UNIFORMED MATERIALS

S.D. Khanin

GIRICOND Scientific & Research Institute, 194223, St.Petersburg, Russia

Barriers to carrier transport determine conductivity and nonlinear properties of disordered and highly non-uniformed electronic materials. Carrier transport mechanisms in amorphous dielectric tantalum, niobium and aluminium oxides and in ZnO- based polycrystalline semiconductors are studied. Combination of the researches of materials with different structure in the framework of one investigation is due to deep analogy in kinetic properties of these systems. It lies in exponential dependence of electron transition probabilities on barriers parameters both in amorphous and polycrystalline systems.

Barriers nature and their parameters are defined in non-crystalline metal oxides with hopping conduction by the analysis of current-voltage characteristics, temperature-DC conductivity dependencies, optical absorption and low-frequency dielectric spectroscopy data. The original experimental techniques, based on nonlinear and non-equilibrium effects, are used. Nature of intercrystalline potential barriers and mechanisms of their deformation in DC regime in polycrystalline semiconductors are studied by means of thermally stimulated current spectroscopy.

The hypothesis about barriers formation in amorphous metal oxides due to supersmall polarons is verified.

Influence of electrically active impurity defects on barriers parameters and nonlinear properties of studied materials are researched especially. There is hydrogen dopant content in amorphous metal oxide make possible to reveal barriers parameters dependencies on filling degree and energetic distribution of localized electronic states.

Theory of hopping conduction in disordered systems with potential barriers between localized states is developed in the works of Mott, Firsov, Efros, Bryksin, Bottger, Zvyagin, Emin and others. Kinetic properties of different materials including amorphous metal oxides [1- 7] are interpreted in the terms of this theory. But barriers nature is not yet clarified. Formation of small polarons was one of barriers nature hypotheses. But no reliable experimental substation was gained yet. Besides, in the case of d-metal
(tantalum, niobium) oxides possibility of supersmall polaron formation, was not taken into account. We intend to fill this gap and to reveal reversible and irreversible barrier deformation in high electric fields, showing in specific current-voltage characteristics and oxide dielectric breakdown.

The formulated problems are solved by means of complex of electrophysical and optical methods on the model samples with controlled composition and structure. They are: current-voltage and conductivity-temperature curves analysis in DC regime, low-

frequency dielectric spectroscopy, optical absorption analysis and thermally stimulated current spectroscopy.

Current-voltage and conductivity-temperature curves analysis serves as necessary control mean of studied materials properties and as research method of barriers and of connected with them charge transport mechanisms. So, the hopping conductivity calculation on the basis of small polaron model accounting atoms thermal oscillations influence on resonance integral (supersmall polarons) predicts the existence of amendment in temperature conductivity dependence. It's exponent has a second item, equal to kT/E, where $E=M\omega^2 / 4\alpha^2$ (M - ion mass, ω - characteristic phonon frequency, k - Boltsman constant).

In order to test the supersmall polaron existence hypothesis in amorphous dielectric metal oxides we carried out detailed analysis of σ (T) . Our analysis shows that at high temperatures the transport of charge in amorphous tantalum oxide may be vie supersmall polarons [4].

Barriers parameters dependence on filling degree of localized states and their energetic distribution is revealed by analyzing doping impurity effect on kinetic properties. Hydrogen is the impurity, determining the filling degree of localized states in tantalum and niobium oxides. Proton injection and transport in anodic dielectric films leads to partial oxide reduction and therefore to localized states filling degree increase [8-9]. Oxide doping is made by electrochemical method in cathode polarization regime of anodic film \in contact with water solution electrolyte. Amount of hydrogen is varied by change in this regime. Distribution and concentration of hydrogen nuclei in the film are controlled experimentally by nuclear methods.

The effect of filling localized states degree on energetic barriers parameters is traced by current-voltage and temperature-conductivity curves analysis on the samples with various hydrogen content. It is shown that the electron conductivity decreases with doping impurity concentration while density of states maximum is crossed by Fermi level. So, knowing the impurity concentrations we determined the energetic localized states distribution from experimental data.

Barriers caused by small polaron formation and localized states energy discrepancy are studied by independent on electrical measurement optical absorption method too [10]. This technique consists in measurement of repeatedly reflected irradiation from metal oxides samples. The idea of the experiments is to test the existence of interband optical absorption maximum. The theory predicts it's energy to be equal to $4E_a+E_F$ where E_a - polaron jumps activation energy, E_F - difference between energy of Fermi level and localized states density maximum. Comparative analysis of absorption peak energy and shape for undoped and doped samples enabled us to trace change of localized states filling degree (energy of Fermi level) with doping impurity concentration. Parameters E_a and E_F were evaluated on the basis of experimental data complex of

σ(T) and optical absorption measurements.

Low-frequency dielectric spectroscopy combines several techniques. The first consists in the isothermal relaxation current-time curves analysis in strong electric field. For experimental data interpretation we used the non-stationary hopping conduction

theory. It is based on the supposition the jumps with decreasing probability begin to participate in current transport. The theory predicts the dependence of $\sigma(t)$ on critical jump probability W_c determining the moment of infinite cluster origin. We studied the $\sigma(t)$ dependence for amorphous metal oxides at different temperatures and different values of electric field strength and reconstructed the function of W_c (E,T) from experimental data.

The second technique consists in the analysis of hopping A.C. conductivity frequency dependence with and without D.C. bias in the voltage range where non-ohmic conductivity decreases with increasing field. This effect is due to change in charge carriers path and to electronic density redistribution. It may be substantial only upon condition that the cluster of involved in transport localized states is sufficiently large, i.e. at sufficiently low frequencies. There must exist certain boundary frequency ω_0 such that upon reaching it cluster of states size becomes so small field strength to be able to effect non-stationary conductivity. As it seen from theoretical model dependence $W_c(E,T)$ can be reconstructed from experimental data on $\omega_0(E,T)$. In case of strong electron -phonon interaction ω_0 increases with temperature. Otherwise , it decreases with temperature. So, presence of strong electron-phonon interaction is judged by direction of boundary frequency shift while varying temperature .

Experimentally determined character of $W_c(E,T)$ enabled us to make conclusion about polarons formation and the mechanisms of D.C. field barriers deformation in amorphous metal oxide films.

The third technique is directed for determining charge carries low mobility. It is based on photo-memory effect experimentally discovered in amorphous tantalum oxide: optical excitation of dielectric gives rise to maximum in loss tangent frequency dependence in infrasonic range, which increases in magnitude and shifts toward lower frequencies with time. Model, which takes into account optical excitation non-uniformity, i.e. generation of non-equilibrium charge carriers in surface layer has been developed to explain this effect. It was shown that $(tg\delta_{max})^2$ is proportional to the width of surface layer enriched by non-equilibrium charge carriers. So, it is possible to determine charge carries mobility from the slope of linear section of the curve representing $(tg\delta_{max})^2$ as function of time elapsed after injection of an electronic packet. $\mu(T,E)$ dependence restructed from experimental data gives the direct information about barriers parameters and their field deformation in studied materials.

Nonisothermal currents spectroscopy method is used for nature and parameters determination of electrically active defects which form barriers and show there the properties of elementary relaxators. Thermally stimulated short-circuit currents (TSSCC) analysis on the samples polarized in electric field is the main method here. Qualitative spectrum analysis enables us to establish defects nature and quantitative analysis - to determine energetical relaxators parameters. Experimental procedure consists in analysis of maxima parameters dependence on polarization conditions. The results obtained indicate dipole type of investigating relaxators [11] and agree with above mentioned results of hopping transport investigation in studied materials.

REFERENCES

1. S.D.Khanin, Problems of the electrophysics of metal oxide capacitor dielectrics, Reviews of electronic technology (Moscow), ser.5, issue 1(1524), 1990.

2. V.V.Bryksin, A.V.Goltsev, and S.D.Khanin, Relation between the tangent of the angle of dielectric losses and low drift mobility, Phil. Mag. (b), vol.64, pp.91-100, 1991.

3. V.V.Bryksin, L.G.Karpukhina, and S.D.Khanin , Frequency dependence of the conductivity of D.C. biased amorphous tantalum oxides, Phys.Solid State, vol.32, pp.3564-3571, 1990.

4. V.V.Bryksin, S.D.Khanin, Ultrasmall polarons in amorphous tantalum oxide, Phys. Solid State, vol.35, pp.1126-1128, 1993.

5. S.D.Khanin, Hopping conduction in metal oxide films and their insulating properties, Proc. of the 4-th International Conference on Conduction and Breakdown in Solid Dielectrics, Italy, 1992, pp.57-62.

6. S.D.Khanin, Strong field effects in disordered dielectrics with hopping conduction, IEEE, Sixth International Conference on Dielectric Materials, Measurements and Applications, UK, 1992, pp.454-459.

7. S.D.Khanin, Low frequency dielectric spectroscopy as a technique for determination of a low mobility and a tight electron-phonon coupling in disordered materials exemplified by tantalum oxide dielectric films, Proc.of the 1st Symposium on Low Frequency Dielectric Spectroscopy and Related Problems, pt.2, Zeszyty Naukowe Politechniki Rzeszowkiej, vol.13, pp.73-79, 1991.

8. S.D.Khanin, The Proton transport and properties of dielectric films of transition metal oxides, ibid, Abstracts of the Conference "Dielectric and Related Phenomena" (DRP'92), pp.53-55, 1992.

9. G.M.Gusinsky, L.G.Karpukhina, V.M.Muzhdaba, V.O.Naidenov, G.F.Tomilenko, and S.D.Khanin, Proton-injection stimulated phenomena in amorphous tantalum oxide, Phys. Solid State, vol.29, pp.3253-3257, 1987.

10. G.M.Gusinsky, L.G.Karpukhina, and S.D.Khanin, Connection between electronic and ionic processes in capacitor systems with oxide dielectric, Proc. of the International Conference "Dielectrics-93", Russia, pt.2, pp.86-87, 1993.

11. Yu.A.Gorokhovatsky, L.A.Kiseleva, and S.D.Khanin, Polarization phenomena in amorphous oxides of transition metals, Proc. of the International Conference "Dielectrics-93", Russia, pt.1, pp.29-30, 1993.

ELECTRON-LATTICE RELAXATION IN RADIATIONAL PHYSICS

A.E.Kiv, E.P.Britavskaya, G.D.Urum

Pedagogical Institute after K.D.Ushinski, Odessa
270020 Ukraine

The radiational effects in solids appear as a result of the elastic particle collisions (in this case an atom receives an energy that larger then some critical value E_d - displacement energy) or as a result of the electron subsystem excitation and the electron-lattice relaxation. In the last case we have subthreshold mechanisms of defect creation (transfered energy $E > E_d$) [1].

The task comes to the theoretical investigation of the influence of various types of localized electron excitations upon the potential relief of the atom displacement and the consideration of radiationless transitions of the electron excitation energy to the lattice. There are two variants of this radiationless transitions. Firstly, the relaxation of the electron subsystem excitation results in thermal effects, which determine the ordinary thermal activation of atom displacement. Secondly, the electron excitation leads directly to the reconstruction of varios configurations in the crystal lattice.

We are considered the mechanisms belong chiefly to last variant. The quantum-chemical modelling method was used in our investigations. This method was developed on the basis of the traditional molecular dynamics method (MDM) [2].

In all cases of MDM application we in fact suggested that the adiabatic approximation is satisfied. In traditional calculations we are using the adiabatic potentials. But we cannot receive them by ab initio method and we are obliged to use the different empirical data for interatomic potentials constructing. Therefore it is impossible to take into account electronic excitations in the processes of atom displacement simulation. In order to solve this problem we developed a modification of MDM which was called quantum – chemical modelling of atoms configurations change. The algorithm of quantum-chemical modelling is

$$x_i(0), \ v_i(0), \ F_i(0) \ \Rightarrow \ x_i(\tau), \ v_i(\tau)$$

$$x_i(\tau) \ \Rightarrow \ \text{New CH}$$

$$\text{New CH} \ \Rightarrow \ \text{New } \phi(\tau)$$

$$\text{New } \phi(\tau) \ \Rightarrow \ \Delta U_i$$

$$U(0) + \Delta U_i \ \Rightarrow \ F_i(\tau)$$

$$x_i(\tau), \ v_i(\tau), \ F_i(\tau) \ \Rightarrow \ x_i(2\tau), \ v_i(2\tau) \ \text{etc.}$$

where: $x_i(0)$, $v_i(0)$ and $F_i(0)$ are the coordinates, velocities and forces at initial moment, τ is the time step, CH are coefficients of the atom orbitals hybridization, ΔU_i is the first correction to potential. As one can see this method includes the calculation of potential correction at the each step of atoms displacement. The algorithm described here enables one to investigate the displacement of atoms constantly taking into account the interaction of the electron and lattice subsystems. This method makes it possible to exceed the limits of the adiabatic approximation and regard the energy transition from electron to the lattice subsystem and vice versa. There are serious difficulties in this algorithm realization connected with including in standard MDM the quantum-mechanical calculations. But for small clusters and small impurity-defect complexes in nonmetallic solids many problems were solved.

In order to investigate the non-impact atom displacement process in silicon we constructed the potential relief for the atomic displacement in the small silicon cluster in given direction. A composite (quantum – classical) model of the diamond lattice cluster was used. Two inner coordination spheres (17 atoms) were described quantum – mechanically in two-centre approximation. Two external spheres (31 atoms in the cluster altogether) were described by means of classical potentials of the Morse type. The volumetric size of the classical part of the cluster could be enlarged if required. The configurations investigated were to be found in the "quantum nucleus" of the cluster. Boundary conditions are provided by the dissipative forces acting on boundary atoms of external spheres. The calculation of the potential relief was carried out in the following way. The central atom of the cluster was displaced some distance in the <111> direction. For this position of the displaced atom the relaxated coordinates are calculated by means of the gradient method (the method of fastest down grade). The relaxation was effected sequentially for all groups of equivalent bonds with iterative cycles: each group of equivalent bonds has its particular step in the method of fastest down grade. According to quantum-chemical modelling scheme the hybrid coefficients in the angular part of wave functions are calculated before each subsequent relaxation step, and the forces determining at the given relaxation step are calculated with regard to the modified state of the electron subsystem related to the cluster configuration of the preceding step. After finishing of iterative cycles for the first displaced position of central atom this atom displaced to another position. Two conclusions are

arised from these calculations: the existence of two coupled semi-vacancies in silicon and the possibility of their dissociation to separated Frenkel pairs under the small thermal fluctuations. Therefore it was established that the new types of defect configurations exist in diamond-like crystals. Above described semi-vacancies represent so called orientional defects. The bonds around the orientational defects are in strained state. In fact these bonds can be considered as excited. This is a reason for a particular states of crystals characterized by long time relaxation to equilibrium parameters. These crystal states play an essential role in the natural deterioration of electronic devises [3]. There are some other metastable defect configurations which appear as a result of subthreshold shock mechanism of radiation defect creation.

References

[1] V.S.Vavilov, A.E.Kiv, O.R.Niyasova, Defect Creation and Migration Mechanisms in Semiconductor, Nauka, Moscow, 1981.
[2] V.V.Kirsanov, A.N.Orlov//UFN,1984,T.142, P. 219-264.
[3] V.S.Vavilov, A.E.Kiv et al., Radiation Effects in Solid Electronics, Radio i svyaz, Moscow, 1990.

DIELECTRIC AND OPTICAL SPECTROSCOPY STUDIES OF THE FERROELECTRIC LC MIXTURES

A. Kocot

Institute of Physics, University of Silesia,
Uniwersytecka 4, 40-007 Katowice, Poland

The dielectric, electro-optical, tilt angle and spontaneous polarisation measurements are reported for BDH ferroelectric mixtures SCE13, SCE8 and ZLI 3654. Analysis of the data has been carried out in the framework of the generalised Landau model [1]. Temperature variations of the tilt angle and the polarisation are fitted with the power low and power coefficients are found to be consistent with the Landau model. Dielectric measurements have been done in the frequency range 5 Hz - 13 MHz in SmC* and SmA phases. Two collective director relaxation modes have been observed. By superimposing dc bias, soft mode contribution can be separated in SmC* phase. Both frequency and reciprocal dielectric strength of the soft mode show critical slowing down behaviour in the vicinity of the SmA -SmC* transition. Using dynamic equations of the Landau model, rotational viscosities of the Goldstone mode, soft mode and the elastic modulus have been found. From relations governing the behaviour of the tilt, spontaneous polarisation and the helical pitch, almost all important material parameters have been estimated. A simple model of the ferroelectric switching has been used [2] to analyse the dielectric and the optical response. Different director profiles have been considered for explaining the experimental spectra.

[1] T.Carlsson, B.Zcks, C.Filipic and A.Levstic, Phys. Rev. A. 42, 877 (1990)
[2] A.Kocot, R.Wrzalik, J.K.Vij and R.Zentel, J.Appl.Phys.,75,728 (1994).

SUPERCAPACITORS WITH POLYANILINE ELECTRODES.

I.L.Kogan, G.V.Gedrovich, M.I.Rudacova, L.S.Fokeeva

Institute of Chemical Physics, Chernogolovka, Moscow Region,
142432, Russian Federation.

The possibility of using double layer capacity in the field of electrode ideal polarization for the supercapacitors design is well known, devices with carbon black electrodes being studied most extensively [1]. Besides several publications [2-6] devoted to elucidation of the conducting polymer polyaniline - electrolyte capacity were published. So it became interesting to imply polyaniline instead of or together with carbon black in double layer capacitor. This problem looks very attractive also owing to high corrosion stability, low temperature coefficient of resistivity and variety of technological approaches to electrode formation characteristic of this polymer. This work presents main properties of laboratory samples of supercapacitor composed from pressed or paste polyaniline electrodes.

The battery of the consequently connected 10 elements (fig.1) each of them composed from two polyaniline electrodes, polypropylene separator wetted with 38% sulfuric acid was used due to low voltage ~0.5V of individual component, with current collectors being made from glasscarbon or graphite.
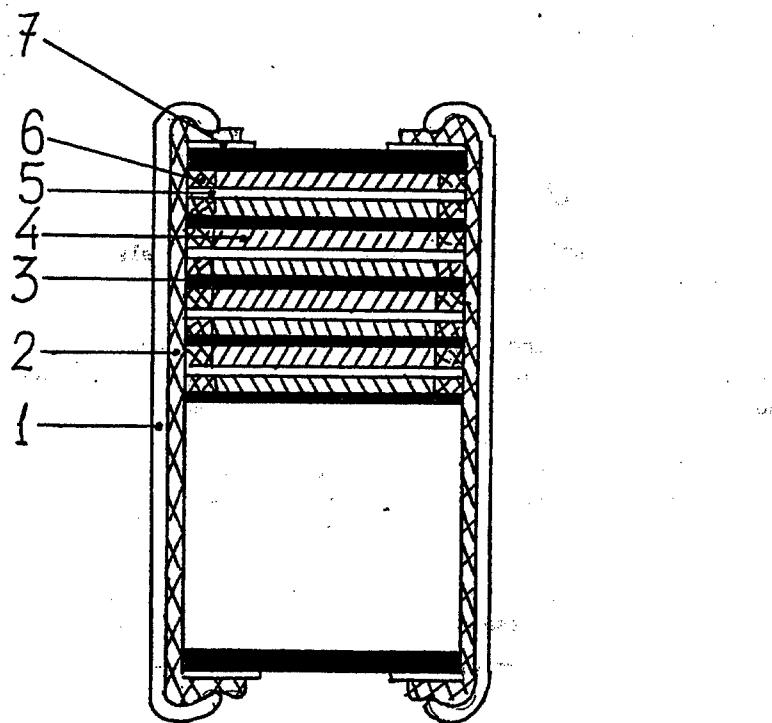
Fig.1.Construction of the supercapacitor. 1-body, 2-insulator, 3 -current collector, 4-polyaniline, 5-separator, 6-plastic ring, 7-rubber ring.

For the capacity to increase composite electrode from polyaniline
and carbon black were used. Capacity - carbon black content relations
defined per complete mass of electrode and polyaniline introduced in the
individual element (fig.2) surprisingly have two maxima at 20% and 50%.
Simple calculations based on the assumption that repeating unit consist
from the two rings and hydrosulfate counterion lead to conclusion that
in course of charge of the paste electrode (50% carbon black content) 1
electron is accumulated per 5 repeating unit.
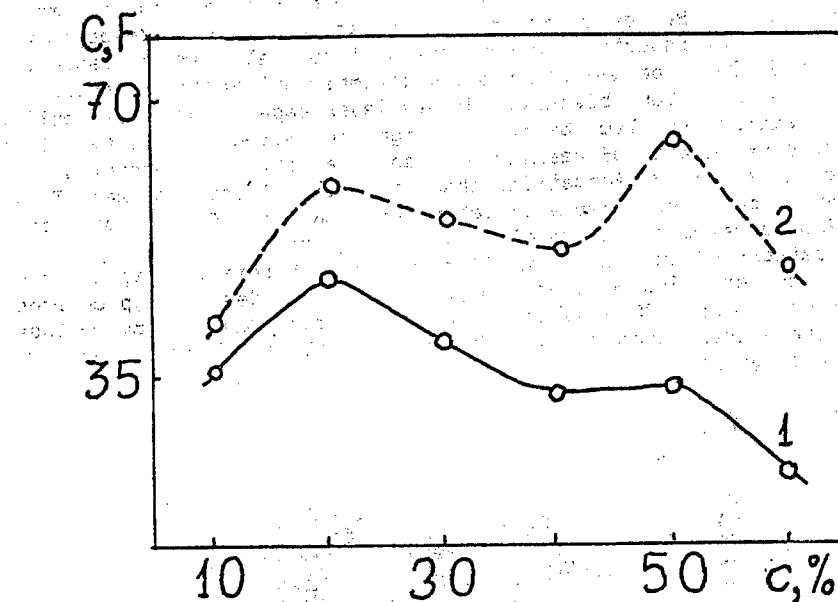
Fig.2. Capacity vs carbon black content in electrode. 1-Calculated
per full mass of electrodes, 2-per polyaniline

Charge-discharge characteristic of the supercapacitor (with 20%
carbon black content electrodes) is depicted on the fig.3. Some
deviation from the linearity probably caused by the side ox-red
reactions of the polyaniline.

Table 1 contains main characteristics of the two supercapacitors
with pressed and paste electrodes of the same composition.

TABLE 1.

Characteristic	Battery from the pressed electrodes	Battery from the paste electrodes
Diameter (cm)	2.5	2 5
Volume (cm²)	20.1	20.1
Voltage (V)	4.5	5.0
Capacity (F)	2.5	3.1
Resistivity (50Гц)	2.7	3.4
Specific capacity (Fcm⁻³)	0.13	0.15
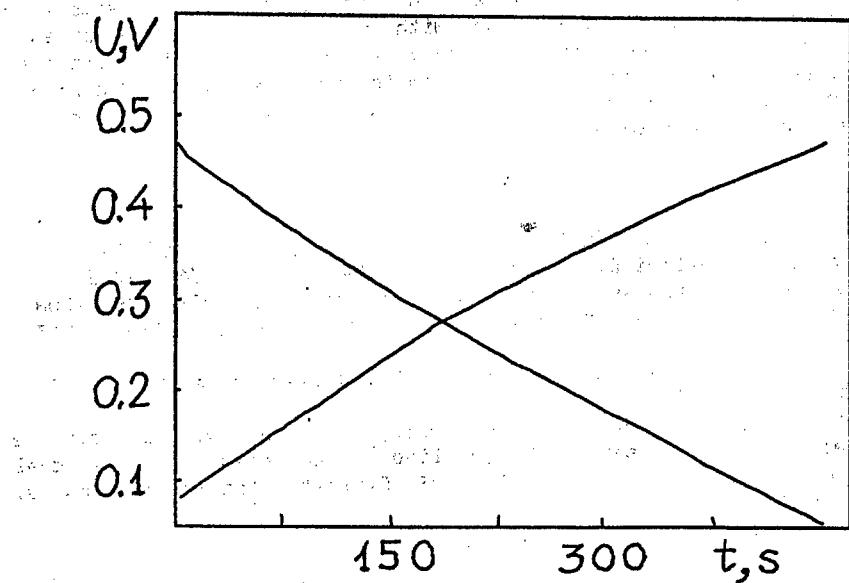
Fig.3 Charge — discharge characteristics at constant current 40mA of the capacitive element with identical electrodes of composition 80% polyaniline : 20% carbon black.
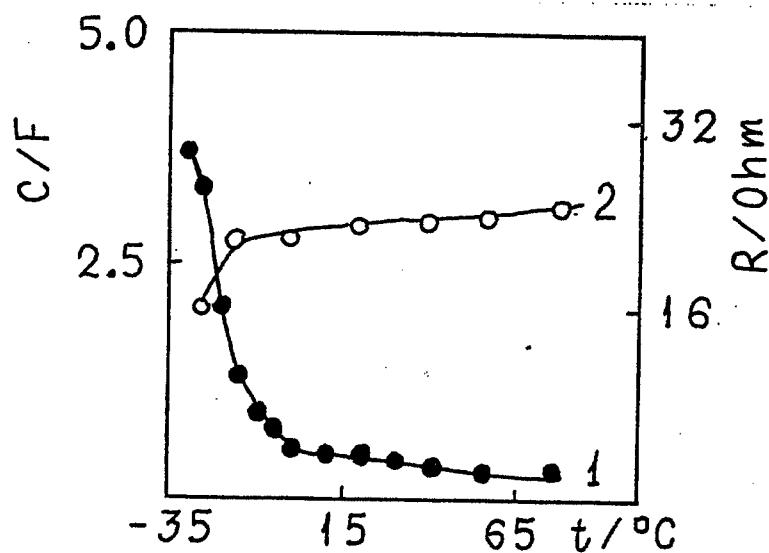
Fig.4. Temperature dependencies of the resistivity (1) and capacity (2) of the battery of supercapacitors with paste electrodes of composition 80% polyaniline : 20% carbon black

These results show that device with paste electrodes has some more preferable properties in comparison with one composed from pressed plates. Temperature behavior of the capacity and resistivity defined at 50 Hz is presented on the fig.4. It remains to note that 1000 charge - discharge cycles led not to essential increase of the resistivity of the capacitor under investigation.

Literature

1.Sanada K., Hosokawa M. NEC Research & Development 1979. N55. P21.
2.Rubinstein I. Sabatani E. J. Electrochem. Soc. 1987. V134. P3078.
3.Lacroix J.C. K.K.Kanazava, A.Diaz J.Electrochem.Soc. 1989.V136.P1308.
4.J.Tanguy, N.Mermilliod, M.Hoclet J. Electrochem. Soc. 1987. V134. P.795.
5.Genies E.M., Penneau J.F., Vieil E. J.Electroanal.Chem. 1990. V.283.P205.
6.Kogan Y.L, Gedrovich G.V, Rudakova M.I., Savchenko V.I. Capacitance properties of the massive polyaniline electrodes International Conference on Science and Technology of Synthetic Metals. Abstracts. Geteborg 1992.

THERMALLY STIMULATED DEPOLARISATION CURRENTS IN POLY (EPOXYPROPYLCARBAZOLE) LAYERS

F. Kuliesius, P. K. Mackus
Faculty of Physics, Vilnius University, Vilnius, Lithuania

Thermaly Stimulated Depolarisation Currents (TSDC) in poly (epoxypropylcarbazole) (PEPCa) layers has been performed as complementary investigation beside dielectrical spectroscopy (0.00001 - 100 000 Hz). Conventional TSDC as well as thermal sampling of PEPCa have been investigated in the temperature range 100 - 350 K. Close relationship between TSDC and isothermal depolarisation current has been observed. Linear dependence of released charge upon polarisation time and poling electric field strength as well as insensitivity to polarity of applied electrical field and sample thickness have been established, what testifies that dipole orientational processes occurs in the studied region. The thermal activation energies of relaxations have been measured by means of partial heating. The thermally stimulated depolarisation current spectra have been analysed in terms of a continuous relaxation time spectrum.

NONLINEAR DIELECTRIC STUDIES OF
4-n-HEPTYLOXY-4'-CYANOBIPHENYL – BENZENE
SOLUTIONS

Jerzy Małecki and Jadwiga Nowak

Institute of Molecular Physics, Polish Academy of Sciences, Smoluchowskiego 17

PL 60-179 Poznań, Poland

Nonlinear Dielectric Effect (NDE) is a strong method applied for get an information on intermolecular interactions in liquid solutions [1-9]. The nonlinear dielectric effect refers to a nonlinear dependence of electric polarization on electric field strength [8]. This nonlinearity shows a negative deviation assigned to orientational saturation of polarization (Langevine effect) and a positive deviation occurring only in these systems in which the inter- or intramolecular equilibria take place (chemical effect). Electric field favours, in energy sense, the polar products of reaction that leads to an increase of the total system polarization.

In practice, the NDE studies resolve themselves to measurements of change in electric permittivity ($\Delta\varepsilon$) caused by electric field E. Due to quadratic dependence of $\Delta\varepsilon$ on electric field strength the material coefficient $\Delta\varepsilon/E^2$ is a quantitative measure of the NDE. It should be noted that both Langevine and chemical effects have a specific inertia which makes possible dynamical study of the kinetics of fast chemical reactions [1,2].

The results of measurements of the dielectric permittivity (ε) and its change ($\Delta\varepsilon$) under strong, external electric field (E) has been applied to study of molecular interactions and pretransitional effects in solutions of 4-n-heptyloxy-4'-cyanobiphenyl (7-CB) in benzene. All measurements were performed in the equilibrium state (static measurements). The dependences of material coefficient $\Delta\varepsilon/E^2$ on concentration of 7-CB in benzene are shown in Figure 1. Within the whole range of concentrations we observed the effects strongly depending on concentration. It means that a strong molecular association takes place. A very rapid decrease of $\Delta\varepsilon/E^2$ observed for lower temperatures at certain concentrations suggests formation of long, linear associates with high dipole moments.

The temperature dependences of NDE for pure 7-CB and its highly concentrated solutions in benzene are shown in Figure 2. The critical increase of the effect when ap-

proaching to phase transition temperature between isotropic liquid and nematic phase is undoubtedly seen. In the pretransitional region the effect obeys the critical relation [6,10,11]:

$$\left(\frac{\Delta\varepsilon}{E^2}\right)_c = \frac{1}{(T-T^*)^\psi}$$

where $T^* = T^c - \Delta T$ denotes the temperature of hypothetical continuous phase transition. For pure 7-CB the critical exponent $\psi \approx 1$ and decreases with increasing concentration of benzene while ΔT is of the order of 1°C. These observations are in good agreement with the literature data [6,12,13]. In all theoretical models [13-17] the critical fluctuations are assumed to be responsible for the observed critical behaviour of nonlinear dielectric phenomenon.

This critical behaviour exists only for highly concentrated solutions, i.e. above 0.9 mf. In not so concentrated solutions the nematic phase does not exist. Instead, the isotropic liquid-solid phase transition is observed. In this range of concentrations of 7-CB in benzene the experimental results can be interpreted assuming the strong selfassociation leading eventually to large, highly polar molecular clusters. The interpretation is based on the

Figure 1. The dependence of $\Delta\varepsilon/E^2$ on concentration of 7-CB in benzene. The temperature is expressed in °C.
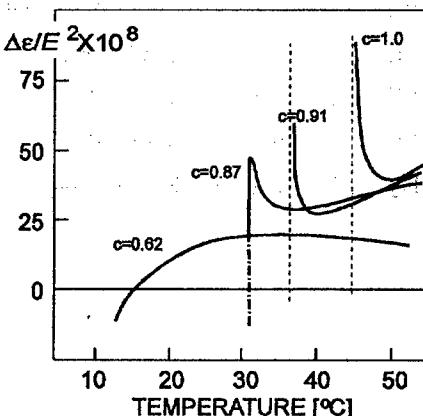
Figure 2. The dependence of $\Delta\varepsilon/E^2$ on temperature for concentrated solutions of 7-CB in benzene. The concentrations are expressed in molar fractions.

theory of chemical NDE effect [4]. The critical behaviour of concentrated solutions and pure 7-CB needs a separate approach.

References

[1] L. Hellemans and L. De Mayer, *J.phys.Chem.* 63, 3490 (1975).

[2] A. Persoons and L. Hellemans, *Biophys.J.* 24, 119 (1978).

[3] A. Piekara, *Proc.Roy.Soc.* 172, 360 (1939); *Acta Phys.Polon.* 10, 37, 107 (1950).

[4] J. Małecki, *J.Chem.Soc. Faraday Trans. II* 72, 104 (1976).

[5] J. Małecki, *J.Chem.Soc. Faraday Trans. II* 72, 1214 (1976).

[6] J. Małecki and J. Zioło, *Chem.Phys.* 35, 187 (1978).

[7] M. Dutkiewicz, *Chem.Phys.* 68, 83 (1982).

[8] C. F. J. Bötcher, *Theory of Electric Polarization*, Elsevier, Amsterdam (1973).

[9] J. Małecki, in *Molecular Interactions* Vol. 3 (Edited by H. Ratajczak and W.J. Orville-Thomas), Wiley, New York, p.183 (1982).

[10] S. J. Rzoska and J. Chrapeć, *Mol.Cryst.Liq.Cryst.* 191, 333 (1990).

[11] S. J. Rzoska, J. Zioło and W. Pyżuk, *Chem.Phys.Letters* 197, 277 (1992).

[12] S. J. Rzoska and J. Zioło, *Liquid Crystals*, 11, 9 (1992).

[13] S. J. Rzoska, J.Zioło and W. Pyżuk, *Acta Phys.Polon.* A78, 915 (1990).

[14] P. G. de Gennes, *Liquid Crystals*, Claredon Press, Oxford, 1974.

[15] J.S . Hoye and G. Stell, *J.Chem.Phys.* 81, 3200 (1984).

[16] J. Goulon, J. L. Greffe and D. W. Oxtoby, *J.Chem.Phys.* 70, 4742 (1979).

[17] A. Onuki and M. Doi, *Europhys.Letters* 17, 63 (1992).

BAND-LIKE R-ℰ-HOPPING TRANSPORT IN THIN LAYERS. THE BOTTGER-BRYKSIN APPROACH.

G. Mancini, J. Rybicki and M. Chybicki
Istituto di Matematica e Fisica, Universita' di Camerino, Camerino (MC), Italia

1. Introduction.

The Bottger-Bryksin model of Marcovian hopping transport (Bottger and Bryksin 1985) applies to the electric fields of arbitrary strength, arbitrary value of the coupling parameter between electrons and phonons, and to any random spatial and energetic distributions of the hopping centres. Thus, it is enough general to cover r- and r-ℰ-hopping cases, both of them in the limits of a strong and a weak electron-phonon coupling (small polaron transport, and band-like transport, respectively). As far as amorphous systems are concerned, the practical application of the model permits, however, only a purely numerical treatment. The calculation of the current-field characteristic for a simulation box containing N random hopping centres requires the solution of the system of N simultaneous non-linear algebraic equations at each value of the field. Despite this difficulty, for a strong electron-phonon interaction in the cases of r- and r-ℰ-hopping, and for r-hopping in the case of a weak electron-phonon interaction, rather reliable current-field, and conductivity-field characteristics can be obtained (Mancini et al. 1993, Rybicki et al. 1994), where a sample of 500 random hopping centres suffices to get the curves not depending qualitatively on the randomness in the centre generation. Particular numerical problems are found only during simulations for r-ℰ-hopping transport in the limit of weak electron-phonon interaction. The characteristics are extremely sensitive to the random distribution of the centres in space, and in energy. For larger numbers of the centres in the simulation box (N of order of 10^3), the problems with the algorithm stability are found, and the precision fails at fairly low fields. Numerically correct curves can be obtained for simulation boxes containing only 100-200 centres. For such a small sample, it is difficult to arrive to any well established results about physical properties of macroscopic samples in a wide range of electric fields, and degrees of macroscopic non-uniformity in spatial centres distribution (a strong dependence of the results on random distribution of centres, and thus a very poor results repeatability for higher fields). However, in a rather limited range of electric fields (up to $E' \approx 0.01$, $E' = eE/2kT\alpha$, where e is the elementary charge, E - the electric field, α - the reciprocal Bohr radius of the centres, k - the Boltzmann constant, T - the temperature; for typical values of parameters $E' = 0.01$ corresponds to $E \approx 10^4$ V/m), and for not too non-uniform macroscopic spatial distributions of the hopping centres, the results are qualitatively independent on the initial random generation of the centres positions and energies, and thus some at least qualitative conclusion can be drawn out.

2. Simulation results.

We have performed our calculations of the current-field characteristics for random systems containing N = 100, and N = 500 hopping centres in a cubic simulation box (for the basic equations and the description of the solution algorithm see Bottger and Bryksin 1985, pp 236-243, and Bottger and Wegener 1984). The centres energies were taken from normal Gaussian distributions of standard deviations $\sigma_\mathcal{E}$ in the range 3kT - 12kT. We used an exponential spatial dependence of the average density $N_h(x)$ of hopping centres, where x is the distance measured from one of the electrodes (0 < x < L, L - the layer thickness). In particular $N_h(x) = N_0 S(x)$, $S(x) = \exp(-x/D)$, where D is a characteristic length of the site concentration decay. The range of the non-uniformity parameter L/D was 0.0 - 2.5 for N = 500, and 0.0 - 1.5 for N = 100. The parameters common to all simulations are: the average electron concentration n = 0.5, and the system dilution $\alpha/\mathcal{N}^{1/3} = 15$ ($\mathcal{N} = N/\Omega$, Ω - the volume of the simulation box). For each set of the input parameters the calculations were repeated for several random initial

generations of the centres within the simulation box. In the figures below we show thus only exemplary, but typical curves.

Fig.1 shows the current - field characteristics for various widths $\sigma_{\mathcal{E}}$ of energetic distribution of the centres (curves a,b,c), and various values of the macroscopic non-uniformity parameter L/D (figures A, B, C). In all the cases the current increases on increasing field. Such a behaviour is quite different from the results obtained for r-hopping. In the latter case the current decreases monotonously with increasing field, reaching a low saturation value at higher fields, much higher than shown in Fig.1 (*cf.* Rybicki *et al*, this conference).

Fig.2 shows the characteristics of Figs 1A, and 1C, normalised to the current values at a very low field, $E' = 0.0001$ (curves a,b,c). The approximately linear increase of the currents in the r-$\mathcal{E}$-hopping regime on increasing field is evident. For comparison, the characteristics obtained for r-hopping transport are added (curves d in Fig. 2). As it is seen, in the considered field range the r-hopping currents remain almost constant, decreasing slightly on increasing field (by few percent). Such a behaviour can be explained by the field dependence of the symmetrized transition probability $W_{mm'}$ between the centres. The latter in the limit weak electron-phonon coupling (band-like transport) reads (Bottger and Bryksin 1985, p. 238):

$$W_{m'm} = W_0' \left[\sinh \left| V_{m'm} \right| \beta / 2 \right]^{-1} \cdot \exp\left(-2\alpha \left| R_{m'm} \right| \right),$$

where $| R_{mm'} |$ is the distance between the m-th and m'-th hopping site, $V_{m'm} = V_{m'} - V_m$, $V_m = \mathcal{E}_m + eu_m$, $\mathcal{E}_m$ - the energy of the m-th site, u_m - potential of the external field E at the point R_m, $\beta = kT$, and the prefactor W_0 depends only weakly on the external electric field E, as well on the site position R_m and energy $\mathcal{E}_m$. Without any energetic disorder of hopping centres (r-hopping), the transition probability decreases simply on increasing field as $1/\sinh[e|u_m-u_{m'}|\beta/2]$, and the numerically calculated currents (curves d in Fig.2) are monotonously decreasing functions of E. In such a case only the nearest-neighbour hops are effective. The presence of the energetic disorder allows for the variable-range hopping, which promotes the carrier transport effectively.
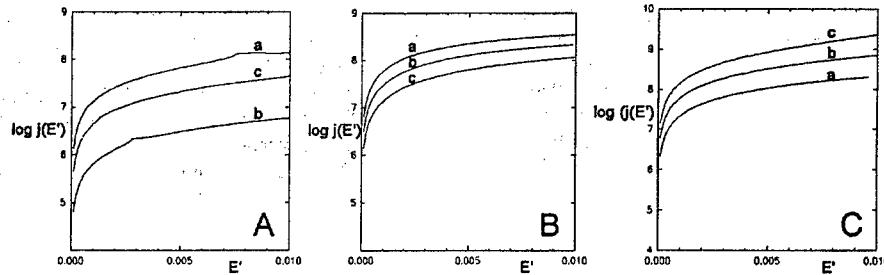
Fig.1. The current-field characteristics for r-$\mathcal{E}$-hopping in a limit of weak electron-phonon interaction. Fig. A - L/D = 0.0; Fig. B - L/D = 0.75; Fig. C - L/D = 1.5; curves a - $\sigma_{\mathcal{E}}$ = 3kT; curves b - $\sigma_{\mathcal{E}}$ = 6kT; $\sigma_{\mathcal{E}}$ = 12kT. Number of centres in the simulation box N = 100.
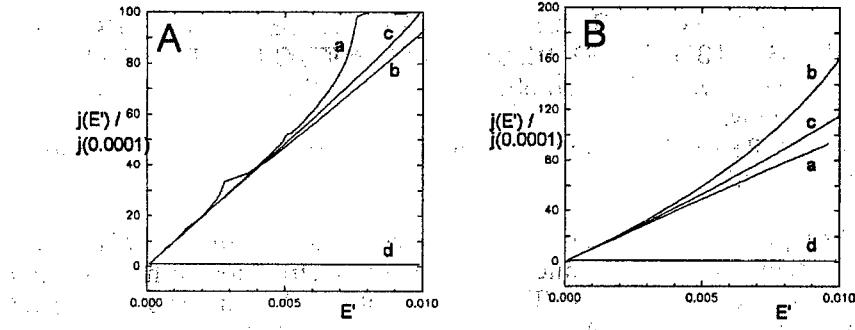
Fig.2. The characteristics of Fig. 1A (Fig. 2A), and of Fig. 1C (Fig. 2B), normalised to the current values at a very low field, $E' = 0.0001$ (curves a,b,c). The curves d) in both figures correspond to $\sigma_{\mathcal{E}} = 0$ (r-hopping).

3. Concluding remarks.

The presented above initial fragments of the current-field characteristics for r-$\mathcal{E}$-hopping transport in the limit of a weak electron-phonon interaction show a significant degree of causality, due to a very small number of centres in the simulation box (note no systematic dependence of the currents slopes on the width of the energetic distribution in Fig.2, and a remarkable dispersion in the current values themselves in Fig.1). However, the influence of the energetic disorder is evident, resulting in an important change of the curve character. In order to understand better the influence of the energetic disorder on the conductivity of the considered systems further efforts are necessary. The possibility of performing simulations for much higher number of centres, in a wider range of electric fields is here of a crucial importance. Numerical calculations in quadruple precision could probably allow a significant progress in the subject.

References

Bottger H and Bryksin V V 1980 Phil. Mag. B 42 297
Bottger H and Bryksin V V Hopping conduction in solids, Akademie-Verlag, Berlin 1985
Bottger H and Wegener D 1984 Phil. Mag. B 50 409
Mancini G, Rybicki J and Chybicki M 1993 J. Phys. CM 5 4475

CURRENT - VOLTAGE CHARACTERISTIC OF Si-SiO$_2$ SYSTEMS CHANGES, INDUCED BY PULSED MAGNETIC FIELD TREATMENT.

V.M. Maslovsky, A.V. Vorobyov, Y. A. Klimov, J.O. Lichmanov, N.S. Samsonov.
Zelenograd Research Institute of Physical Problems, Zelenograd, Moscow 103460, RUSSIA.

As reported in [1,2] the pulsed magnetic field treatment (PMFT) of Si-SiO$_2$ systems (thermodynamic nonequilibrium structure with considerable internal mechanical stresses (IMS)) stimulates IMS relaxation in Si-SiO$_2$ systems, which lasts for about a week. It appeared that structural changes were in a good agreement with the variation of MOS-structure electrophysical parameters characterizing the changes of minority carrier generation rate and dielectric leakage currents.

The PMFT phenomenon under consideration is particular interest as:

- at room temperature the interaction energy of the field with the electron magnetic moment at magnetic field amplitude 0.1 MA/m is 3 orders less than the thermal energy;
- the major variation of structure parameters was observed after the end of PMFT.

This paper presents for the first time the experimental results of current-voltage characteristic changing of Si-SiO$_2$ system. To study processes induced by short-term PMFT effects in MOS-structures with dioxide layer formed by phosphorus-dopes Si substrates with 20 Ohm×cm resistivity and (100) orientation, thermal oxidation in dry oxygen at 950° C were used. Dioxide thickness was 30 nm and Al-electrode area was S=1 mm^2. Capacitance-voltage characteristics were measured also and histograms of MOS-structure flat-band voltage V$_{fb}$ were analyzed.

These structures were under the influence of some PMFT pulses with amplitude of H= 0.1-03 MA/m, 0.02-0.05 ms duration and pulse frequency 10 Hz. It was detected that there were no appreciable variations of the parameters just after short-term treatment (less than 10 s).

One of the general PMFT effect on Si-SiO$_2$ was dielectric leakage current-voltage characteristic evolution (Fig. 1). Current-voltage I-V characteristics were measured at positive Al-electrode voltage which corresponded to tunnel injection of electrons from the semiconductor into the oxide. Fig. 1 showed prolonged I-V characteristics changes for two typical structures. The direction of I-V characteristics shift along the axis of the applied field appeared to be different. Before PMFT the I-V characteristics for all structures corresponds the curve 1 in Fig. 1 (the results of multiple testing of every structures leakage current in I < 100 nA range). After approximately 5 days of PMFT almost 20 percent of MOS-structures were characterized by I(E) shown in Fig.1 on the left-side of the curve 3. Such I(E) characteristics where similar to those of initially defective MOS-structure and was depicted by power dependence of current verses voltage in contrast to the known Fowler-Nordheim dependence for defect-free MOS-structure.
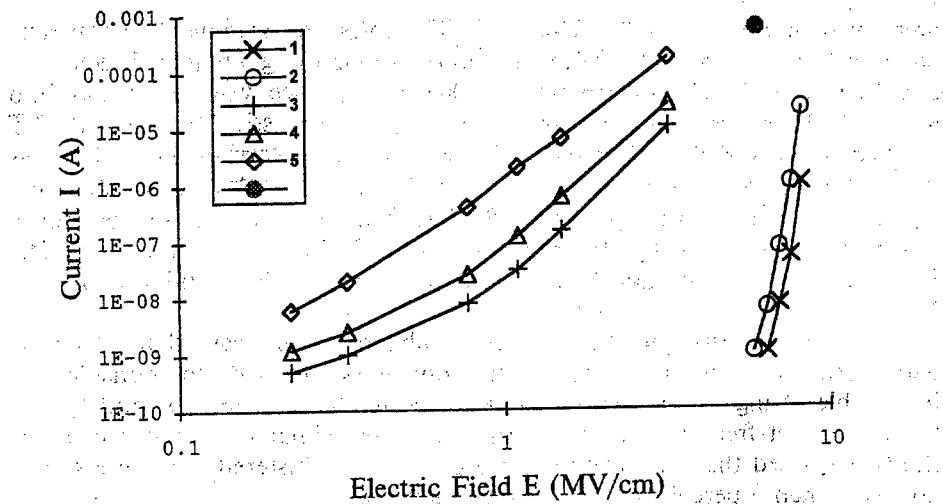
Fig.1. Dielectric leakage current vs. electric field for MOS structures: curves 1 - before , 2 and 3 - in 3 and 6 days after PMFT respectively; 4 - the same of 3, but heated to 375 K, 5 for initially defective MOS structure.

Such conductivity is due to electron transfer via localized states at microcrack surfaces formed by high density broken bonds ($N_t \approx 10^{14}$ cm^{-2}). According to the theory of electron conduction through microcrack in dielectric the current-voltage dependence may be expressed as [3]:

$$I = \sigma_m l \frac{V_t}{d} (\frac{V}{V_t})^{T_t/T+1}$$

where $\sigma_m = 0.1 q^2/h$ was the minimal two-dimensional metallic conductivity; T_t is the temperature characteristic of localized states energy distribution; q is electron charge, $V_t = qN_t d/C_0$, $C_0 \cong \frac{\varepsilon_d}{\pi}$, ε_d is the dielectric constant; l is microcrack length. Heating to T=375 K enabled detection I(E) extrapolated characteristics intersection in higher current region. This characteristics intersect at the electric field $E = E_t = 6$ MV/cm. Therefore, comparing the experimental values of that curve we concluded that the microcrack length was $l \approx 0.1$ μm. Only the existence of defect regions near silicon surface with dimension much more than l makes possible the generation of such mickrocracks. Depending upon microdefect type there could be both compressive and tensile stresses. Relaxation of those stresses resulting in microcrack generation in dielectric was in agreement with the IMS relaxation in Si-SiO$_2$ systems discovered in [1] by Raman scattering.

The density of microdefects over 0.3 mm was not more than 30 cm^{-2} in accordance with scanning electron microscopy investigations, and irreversible microcrack generation caused by IMS changes in smaller size microdefect

areas was hardly probable. Thus, PMFT induced prolonged parameters changes both for defective MOS-structures (containing elongated defects) and "defect-free" (if semiconductor-dielectric interface was not taken into account). Defect reaction in the microdefect region stimulated by PMFT resulted in microdefect electrical activity: anomalous carrier generation was observed in depleted semiconductor layer. The Raman scattering spectra were registered during some days after PMFT. The IMS values in subsurface regions were evaluated by the frequency shift of 520 cm^{-1} phonon line. The IMS increased monotonously during 6 days after PMFT and attained 60 MPa.

The peculiarity of the observed phenomenon was that structure parameters, due to impurity-defect complexes, tended to considerable irreversible change while parameters not due to those complexes and typical for the defect-free structures returned to approximately initial values. It should be noted that the relative variations of the registered parameters were not more then 5 percent for untreated structures.

The degradation of MOS-structure electrophysical parameters was caused by high concentrations of fast diffusion impurities and intrinsic defects. The estimated prolonged processes are in agreement with the idea about the defect structure evolution due to the decay of impurity-defect complexes in subsurface region of Si [1,2], accompanied by a generation of fast diffusing impurity and intrinsic defects (vacancies). These defects diffuse through the crystal and are captured by strained bonds formed by mickrodefects. That results in a changing of electron state of mickrodefects at the $Si-SiO_2$ interface, in IMS changes and in the positive built-in dielectric charge increase. The decay of impurity-defect complexes is due to the influence of nuclear spin system polarization on singlet-triplet (S-T) evolution of defect complexes. Taking into account that such S-T evolution takes places mainly when the field is finished, one can consider that polarization of nuclei "remembers" PMFT since its relaxation time is many orders of magnitude larger than relaxation time of electron spin polarization due to effective spin-lattice interaction [1,2].

Therefor our experimental results shows that the PMFT can leads to formation of mickocracks in the mickrodefect area. In agreement with [2] the appearance of considerable vacancy concentration at $Si-SiO_2$ interface observed by DLTS technique are registed after PMFT. The growth of vacancy concentration results in formation of mickrocrack in IMS region, that's in an agreement with I-V characteristics changing inducted by PMFT.

References

1. Y.A. Klimov, V.M. Maslovsky, L.B. Borisova, N.S. Samsonov, Prolonged structural changes in semiconductor systems inducted by pulsed magnetic field, in International Conference on Advanced and Laser Technologies, ALT-92, Moscow , book of summaries, part 5, pp.58-60, 1992.
2. Levin M.N., Maslovsky V.M., Correlation of electric parameters change and structural changes induced in silicon systems by pulsed magnetic field treatment. Mat. Res. Soc. Proc. 1993 Fall Meeting. Boston. vol 319, pp 119, 1994.
3. Maslovsky V.M., Lichmanov J.O., Simanovich E.V. Influence of extended defects on breakdown of MOS-structures with thin oxide layer. Pisma v zhurnal tekhnicheskoi fiziki, vol 19, N24, pp. 11-16, 1993.

CHARGE ACCUMULATION IN MONOS-STRUCTURES WITH NON-UNIFORM DISTRIBUTION OF CAPTURE CENTERS IN SILICON NITRIDE

V.M. Maslovsky*, E.A. Vorobyova*, S.V. Matorin**

* Zelenograd Research Institute of Physical Problems, Moscow, 103460, Russia
** Scientific Research Institute "Submicron", Block 313a, Moscow, 103482, Russia

Investigation of charge accumulation and leakage in silicon nitride (SN) shows non-uniform distribution of capture centers through SN width [1]. This is due to the non-uniform distribution both of weak quasi-hydrogenous bonds Si-H-Si and of oxygen as a result of the influence of interphase boundaries. For small SN widths (less than 40 nm) influence of this non-uniform distribution of capture centers becomes very significant. In this work for the first time the charge accumulation in MONOS-structures is modelled with account of arbitrary distribution of capture centers. Proposed model is the modification of existing model [2] in which electrons injected from semiconductor through dioxide layer are captured by capture centers. These capture centers are positively charged. The new model modifies the existing one by means of setting arbitrary distribution of capture centers in SN.

The accumulation of electrons in SN is described by the system of the following equations:
- the equation for full current I;
- Shockley-Read equation for the kinetic of the positively charged centers filling f(x) (when Pool-Frenkel effect is took into account);
- Poisson equation.

The initial condition is the uniform distribution of electric field in SN. The boundary conditions are:

1. The dependence of the injection current from electric field in dioxide (that is Fowler-Nordheim tunnelling current)

2. The constant voltage applied to the structure.

Concentration of capture centers in SN near Si-SiO$_2$ boundary (less then 2 nm from SN surface) determined by measuring retention characteristics of MNOS-structures by method developed in [3] was about 2-3·10^{19} cm^{-3}. But the results of work [1] show that concentration of them in volume (more than 4 nm from the boundaries) is about 6-9·10^{18} cm^{-3}. This discrepancy allows to assume non-uniform character of capture centers spatial distribution.

The results of modelling show that there is significant influence of capture centers distribution character on charge accumulation characteristics. In accordance with above mentioned experimental results we assumed in our models that capture centers concentration decreases exponentially:

$$N(x) = (Ns - Nv) \exp(-x/\lambda) + Nv,$$

where Ns is the concentration of capture centers near surface and Nv is their concentration in volume, λ is the character distance (about 2-4 nm).

The temporal dependence of flat-band voltage shows that this dependence is more steep when capture centers are localised near interphase boundary with dioxide. The comparison with experimentally determined charge accumulation characteristics (Fig.1)

and full current prolonged relaxation shows that such exponential distribution of capture centers gives better correspondence. The parameters of the best correspondent distribution of capture canters and their energy level (Φ) were the following:

$Ns = 2 \cdot 10^{19}$ cm^{-3}, $Nv = 7 \cdot 10^{18}$ cm^{-3}, $\Phi = 1.45$ eV.

Similar accumulation characteristics may be obtained with uniform distribution only for concentrations about $1.4 \cdot 10^{19}$ cm^{-3}.
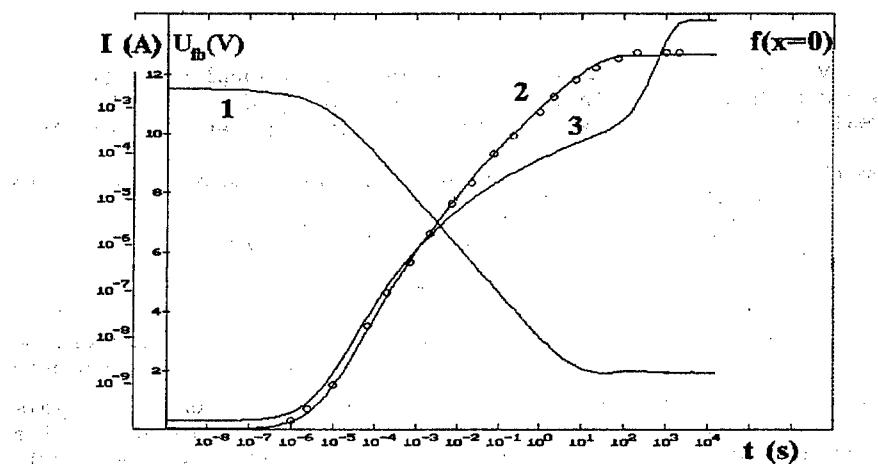
Fig.1. The temporal characteristics of charge accumulation in MONOS-structures for applied voltage U = 30 V. o - the experimental points. Curves: 1 - I; 2- U$_{fb}$; 3 - f(x=0).

REFERENCES:

1. A.P. Aganin, V.M. Maslovsky, A.P. Nagin. Determination of capture centers parameters in silicon nitride in MNOS-structure by electron injection from gate, Mikroelektronika (in Russian), vol. 17, pp. 348-352, 1988.
2. V.M. Maslovsky, E.V. Simanovich. Prolonged storage of electrons in MONOS-structures, Mat. Res. Sos. Symp. Proc., vol.284, pp. 159-166, 1993.
3. V.M. Maslovsky, A.P. Nagin, V.V. Pospelov et al. Spatial distribution of charge MNOS-structure's dielectric, Mikroelektronika (in Russian), vol. 5, pp. 240-249, 1976.

STATISTICAL SELF-SIMILARITY IN LIQUID CTYSTALS

M. Massalska-Arodż

Institute of Nuclear Physics
31-432 Kraków, Radzikowskiego 152

Systematic analysis of the dielectric absorption $\varepsilon''(\nu)$ and dispersion $\varepsilon'(\nu)$ data in many disordered materials has allowed to reveal the power-law type of the frequency dependence of electric permittivity $\varepsilon^{*} = \varepsilon' - i\varepsilon''$ with two fractional exponents in low and high frequency limits

$$\varepsilon''(\nu) \sim (\varepsilon'(\nu) - \varepsilon'(\infty)) \sim (\nu/\nu_{max})^{n-1} \qquad \nu \gg \nu_{max} \quad ,$$

$$\varepsilon''(\nu) \sim (\varepsilon'(0) - \varepsilon'(\nu)) \sim (\nu/\nu_{max})^{m} \qquad \nu \ll \nu_{max} \quad .$$

The $\varepsilon'(0)$ and $\varepsilon'(\infty)$ means the low and high frequency limits of the real part of electric permittivity. The ν_{max} is the frequency of maximum of absorption. Among the analyzed disordered materials there were glassy and plastic phases, materials composed of the molecules bounded by the hydrogen bonds and finally the liquid crystalline phases [1]. Such behaviour observed thoroughly by Jonscher [2] differs essentially from that predicted by the Debye model characterized by $n = 0$ and $m = 1$. There are reasons to belive that the deviations of the fractional exponents from values typical for the Debye model are caused by the fact that the molecular relaxation in those materials should be regarded as a cooperative process. In scope of many body Dissado-Hill model [3] of relaxation the values of n and 1-m are the measures of the local and long range correlations in reorientational motions of molecules. The frequency dependence of electric permittivity in the phases mentioned points to existence of correlations on both level of sample morphology. Especially the local correlations are detected to be large.

Power-law frequency dependence of electric permittivity means non-exponential decay of the electric response function of the disturbed system towards equillibrium. In the first stage of relaxation (i.e. for $t < \tau$) the response is proportional to t^{-n} that means it is faster than the Debye decay. For the second stage of relaxation (i.e. for $t > \tau$) the response goes according to the function $t^{-(1+m)}$ that means it is much slower than predicted by exponential decay. Recently, the theoretical models [4] have appeared which show that anomalous power-law type of electric response function can be found for systems with fractal-like properties of structure and microscopical dynamics.

It has been found that the self-similar symmetry typical for fractal objects can be traced in the distribution of the topological

defects in liquid crystalline phases [5,6]. The defects in form of points and lines appear in nematic and smectic phases during the phase transitions when the full rotational symmetry of the isotropic liquid phase is broken. The defects occur in those places of the sample where the arrangement of the long axes of molecules leads to discontinuity of their orientation. They can be easily observed by the polarizing microscope due to the structural anisotropy of the liquid crystalline phases. The details of the image from the polarising microscope depends on the arrangement of elongated molecules and on geometry of the observation.

For the so-called Schlieren texture of the nematic phase the image is created by irregular bright and black areas. Brightness means the elongated molecules are parallel to the polariser or analyser. Points where four black areas meet themselves identified the defects of ±1 type what means that when one traverses the loop around the linear defect going through the point the orientation of the long molecular axes performs 2π angle. The distribution of the point-like defects on the plane of the image seems to be completely random.

In order to trace the fractal type of distribution of defects the boxing method can be used [7] in which the number N of points/defects is counted in several square boxes of the side length L. The slope of the logN vs logL dependence allows for determination of the fractal dimensiomality D_f describing the distribution. The analysis of the images of the nematic phase of MBBA observed by Nagaya, Hotta, Orihira and Ishibashi [8] at several moments after the transition from the isotropic phase shows the fractal distribution of point-like topological defects. The logN vs logL gives $D_f = 1.4$ for each image taken during the relaxation of the defect structure towards equillibrium. The first analyzed image has been taken at 50s after the phase transition while the last at 200s. The defects of the opposite sign anihilate in time. The fact that D_f occured to be the same for all analyzed images means that the relaxation of the defect structure proceeds respecting the rules of self-similarity. Of cource the self-similarity is of the statistical sense only and the range of changes of L where the fractal-like distribution has been found is limited up to the 0.6 mm of linear size of the sample.

In smectic A and C phases the topological defects form the ellipses with perpendicular hyperboles going through their focuses. Observation of defects by polarizing microscope allows to see that various sized ellipses fill the plane of image in accordance to the so-called Appolonian packing of circles [9]. That means the areas between three circles/ellipses of the first generation are filled by the smaller circles/ellipses of the second generation which leave empty areas between them for smaller circles/ellipses of the third generation and so on. The distribution of the elliptical defects on the images recorded by D.Demus et al. [10] has been checked using the boxing method. The slope of the logN vs logL has given $D_f = 1.2$. For Appolonian packing the fractal dimensionality estimated by

the same method has been equal to $D_f = 1.3$ in good agreement with the literature value [9].

The self-similar symmetry found in the distribution of the defects means the existence of the correlation of the defects positions on the plane of the image illustrating the correlations in the sample itself. The results are in agreement with the high values of the n and 1-m correlation parameters evaluated from the dielectric relaxation spectrum for disordered structures. In fact the appearance of correlations in the dipolar materials corresponds to appearance of some forms of order in their structure.

References:
[1]   M. Massalska-Arodź, Mol. Cryst. Liq. Cryst. **214** 171, 1992.
[2]   A. K. Jonscher, Nature **267** 673, 1977; A. K. Jonscher, 1983 Dielectric relaxation in solids (London: Chelsea Dielectrics).
[3]   L. Dissado and R. M. Hill, Chem. Phys. **111** 193, 1987.
[4]   P. Niklasson, J. appl. Phys. **62** R1, 1987;
S. Halvin and D. Ben-Avraham, Adv. Phys. **36** 695, 1987.
[5]   J. B. Fournier and G. Durand, J. Physique Coll. **51** C7-157, 1990.
[6]   M. Massalska-Arodź, Nukleonika, **41** 1994.
[7]   D. J. Robinson, and J. C. Earnshaw, Phys. Rev. A, **46** 2045, 1992.
[8]   T. Nagaya, H. Hotta, H. Orihira and Y. Ishibashi, J. Phys. Soc. Jpn. **60** 3511, 1992.
[9]   B. Mandelbrot, The Fractal Geometry of Nature (San Francisco: Freeman) p 166, 1982.
[10] D. Demus and L. Richter, 1989 Textures of liquid crystals (New York: Verlang Chemie); D. Demus, 1989 private information.

INFLUENCE OF SUBSTRATE - IDUCED ORDERING ON ANCHORING ENERGY IN NEMATIC LIQUID CRYSTALS

L.V. Mirantsev

Institute of the Problems of Mechanical Engineering,
Academy of Sciences of Russia, St.Petersburg,199178,
RUSSIA

It is known that the solid substrates determine the
boundary conditions for the nematic liquid crystals
(NLC) used in various displays and have an effect on
their threshold fields and relaxation times. The
substrate action on NLC is phenomenologically
descriebed by the so - called anchoring energy and
the determination of it's magnitude is one of central
topics of the surface physics of NLC.
The anchoring energy determined from the electro -
(magneto) -optical effects is of order of ~ 0.001 - 1
erg/cm2. However from the dimensional reasons this value
should be several orders larger. In order to solve this
paradox a simple layered model for the NLC region near
the substrate surface is considered. The surface free
energy profile is determined. It is shown that though
the magnitude of the total surface free energy is within
the interval of ~ 10 - 100 erg/ cm2 it's major part is
localized in first surface layer with thickness of order
of the molecular length. Since this energy is much
larger than the possible energy of the NLC elastic
deformation per one layer, first liquid crystal layer
near the substrate is insensitive to the deformations in
the nematic bulk caused by the external electric
(magnetic) field. The magnitude of the rest part of
the surface free energy distributed in other layers of
the surface region coincides in order with the anchoring
energy determined from the electro (magneto) - optical
effects in NLC.
In addition the influence of the substrate - induced
smectic - A structure on the anchoring energy is
investigated. It is shown that the appearance of the
surface smectic - A phase above the first order nematic
to smectic - A phase transition point gives rise to the
considerable decrease in the anchoring energy. The
binary mixture of polar liquid crystals 9 CB and 10 CB
can be considered as a possible candidate for the
experimental verification of this theoretical prediction.

DIELECTRIC RELAXATION PROPERTIES
OF MAIN CHAIN LIQUID CRYSTALLINE POLYMERS

M. Mucha
Faculty of Process and Environmental Engineering, Technical University of Łódź,
ul. Wólczańska 175, 90-924 Łódź, Poland

When studying the dielectric relaxation of liquid crystalline polyesters of nematic and smectic order*, special attention was paid to the dynamics of molecular mobility connected with the presence of dipole moments (ester group mainly) in the polymer chain. This mobility depends on phase transitions of the polymers. Relaxation processes β and α are associated with the transverse component of the dipole moment. A co-operative mobility of side groups and segments below the glass transition temperature and in its vicinity, forms $\alpha + \beta$ process. Process δ depends on the mobility of longitudinal component of the dipole moment in the vicinity of mesomorphic phase transitions of the liquid crystalline polymers. Weak process γ or ($\gamma + \beta$) is a result of the molecular mobility inside the aliphatic chain.

Dielectric relaxation studies in the frequency range from 10^{-3} to 10^5 Hz and at temperature from -160°C to 160°C were carried out using Du Pont Dielectric Analyser. Samples of diameter 0.025 m and thickness 60 μm were placed between two parallel gold plated electrodes. Temperature stabilization and measurements were fully computer-controlled.

A set of curves ε', ε'', tgδ and σ was obtained as a function of temperature and frequency. Results were analyzed and activation energy of relaxation processes α, β, δ was calculated.

Dielectric relaxation spectroscopy is a sensitive and important method for characterization of polymers, in particular of liquid crystalline polymers.

---

* Liquid crystalline polyesters were synthesized in the laboratory of Prof. A. Blumstein, University of Massachusetts, Lowell, USA, where the dielectric relaxation measurements were also made.

DIELECTRIC BEHAVIOUR OF GLASSES
CONTAINING TRANSITION METAL IONS

L. Murawski and R. J. Barczyński
Faculty of Applied Physics and Mathematics
Technical University of Gdańsk, 80-952 Gdańsk, Poland

1. Introduction

Many glasses containing transition metal ions, for instance iron or vanadium, are electronically conducting semiconductors [1]. A general requirement for semiconducting is capability of coexistence of transition metal ions in more than one valence state, so that the conduction can take place by the transfer of electrons from low to high valence states. Such charge transport usually considered in terms of small polaron hopping theory [2]. An interesting property of these glasses is that the dielectric and mechanical relaxation processes have the same activation energy as their d.c. conductivity [3]. This suggests that the same mechanism, associated with the electron hopping between transition metal ions, is responsible for all three phenomena. In this paper we discussed these correlation in terms of a new theory of relaxation in glasses that has been published by Hunt [4, 5].

2. Experimental

We have prepared four different sets of samples (in mole %): I. $50P_2O_5$-$(50-x)FeO-xMO$; (where M = Mg, Ca, Ba; x = 0, 10, 20, 30, 40); II. $50P_2O_5$-$(50-x)V_2O_5$-xMO (M = Mg, Ca, Sr, Ba; x = 0, 10, 20, 30, 40); III. $(100-x)P_2O_5$-xV_2O_5 (x = 40, 50, 60, 70); IV. $(100-x)TeO_2$-xV_2O_5 (x=40, 50). A capacitance bridge (Gen. Rad. 1615A) has been used for a.c. measurements in the frequency range from 20Hz to 100kHz while for higher frequencies a VHF bridge (Tesla BM431E) was used, covering the range from 10^5 to 10^8Hz. At frequency near the relaxation peak the dielectric loss current is usually much smaller then the conduction current. This makes it very difficult to observe the dielectric relaxation spectra - it is impossible to separate the dielectric loss current from the total current measured by the a.c. bridge. To avoid this difficulty we have applied the absorption current method. The dielectric loss is then obtained from the discharge current and no separation from the conduction current is necessary. The dielectric relaxation spectra can be observed at very low frequencies down to 10^{-4} Hz.

3. Results

Figure 1 shows a typical dielectric loss spectra obtained in a transition metal oxide glass. The loss factor $\varepsilon_1''(\omega)$ is calculated from the results of the absorption current measurements by means of the Hamon approximation [6]. The results of the a.c. bridge measurements are shown in Figure 2. We used the electric modulus representation [7] in which the complex electrical modulus $M^*=1/\varepsilon^*=M'+jM''$, where $\varepsilon^*=\varepsilon'-j\varepsilon''$ is the complex permittivity. The conductivity $\sigma_t=\sigma_{dc}+\sigma_{ac}$ is related to ε'' by

$$\varepsilon'' = \frac{\sigma_t}{\omega\varepsilon_o} = \frac{\sigma_{dc}}{\omega\varepsilon_o} + \varepsilon_1''(\omega) \quad (1)$$

and

$$\sigma_{ac}=\omega\varepsilon_o\varepsilon_1''(\omega) \quad (2)$$

The temperature dependences of the peak frequencies for the dielectric relaxation ε_1'', the electric modulus M'' as well as the internal friction Q^{-1} are shown in Figure 3. The plot of log f_m versus $1/T$ indicates a linear relationship within the temperature and frequency range investigated, so that we expect that f_m is given by a simple Arrhenius formula $f_m=f_{mo}\exp(-W/kT)$. As seen in Table I the activation energies W of the dc conductivity, the dielectric relaxation and the internal friction are all of the same value within the experimental error.

Figure 1 Dielectric loss factor versus frequency at various temperatures for $50P_2O_5$-$30FeO$-$20CaO$ glass.

We have found that the dielectric loss peaks obey the B-N-N [8, 9, 10] relation:

$$\sigma_{dc}=2\pi f_{mD}\varepsilon_o(\varepsilon_s-\varepsilon_\infty)p \quad (3)$$

where p is constant. Namikawa has shown [10] that in electronically conducting glass p=1. If we assume that this is also true in our glasses then the BNN relation is fulfilled for $\Delta\varepsilon = \varepsilon_s-\varepsilon_\infty = 11.4 \div 13.4$ in the system with CaO and for $\Delta\varepsilon = 17.6 \div 18.7$ in glass containing BaO.
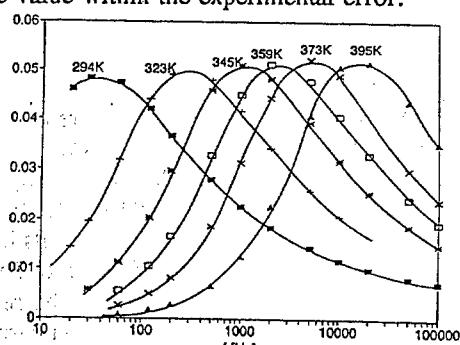
Figure 2 M" as a function of frequency at various temperatures for $50P_2O_5$-$50FeO$ glass.

4. Discussion

Recently, Hunt [4, 5] has published a new theory of dielectric relaxation in electronic and ionic conducting glasses. His basic concept is to distinguish two relaxation processes in two frequency ranges: below and above the dielectric loss

Table I Activation energy of dc conductivity (W_{DC}) dielectric loss (W_{RD}) electric modulus (W_M) and internal friction (W_{IF}) in glasses from set I.

x [mol%]	10CaO	20CaO	30CaO	10BaO	20BaO	30BaO	0
W_{DC} [eV]	0.64	0.72	0.76	0.58	0.71	0.70	0.63
W_{RD} [eV]	0.68	0.69	0.70	0.62	0.68	0.74	0.63
W_M [eV]	0.64	0.72	-	0.65	0.66	-	0.61
W_{IF} [eV]	0.67	0.70	0.74	0.48	0.52	0.68	0.59

peak. In the high frequency range (above the peak), the relaxation processes have a local (parallel) character - it means that the carier hopping takes place between the centers being in close pairs. In this range a distribution in relaxation time with an exponential

dependence on random variables, i.e. R - the hopping distance, is known to give a non-Debye behaviour with $\sigma_{ac} \propto \omega^s$, s < 1 [11]. The cross - over frequency is the frequency of peak ω_m, at which the individual (parallel) pair processes percolate and thus necessitate the consideration of series processes. The series processes in the low frequency range are non-local and can be treated as percolation of individual particles over macroscopic distances in clusters or chains. For $\omega < \omega_m$ a fractal structure of clusters is responsible for relaxation currents and the conductivity has a form:

$$\sigma_t(\omega) = \sigma_{dc}\left[1 + K(d)\left(\frac{\omega}{\omega_m}\right)^r\right] \quad (4)$$

where $r = 1 + d - d_f > 1$; d is the dimensionality of the space containing relevant clusters, d_f is the fractal dimensionality of such clusters. K(d) is a dimensionally dependent constant related to the statistics of the contributing clusters. For $\omega > \omega_m$ the pair approximation holds and the conductivity is given by:

$$\sigma_t(\omega) = \sigma_{dc}\left[1 + A\left(\frac{\omega}{\omega_m}\right)^s\right] \quad (5)$$

Figure 3 The temperature dependence of dielectric relaxation (●), electric modulus (○) and internal friction (*) for typical glasess from group I.

where s < 1 and A is constant.

We have applied this theory to our results of dielectric loss measurements in transition metal oxide glasses. The results of the numerical calculation of K(d), r, A, and s are given in Table II. These parameters are obtained by fitting the theoretical expression for $\varepsilon_1''(\omega)$ to the experimental curves from Fig. 1. From (4) and (5) $\varepsilon_1''(\omega)$ can be deduced: for $\omega < \omega_m$

$$\varepsilon_1''(\omega) = \sigma_{dc}K(d)\frac{\omega^{r-1}}{\varepsilon_o\omega_m^r} \quad (6)$$

and for $\omega > \omega_m$

$$\varepsilon_1''(\omega) = \sigma_{dc}A\frac{\omega^{s-1}}{\varepsilon_o\omega_m^s} \quad (7)$$

The values of s and r are reasonable and may confirm the applicability of Hunt theory to our glasses. If transport takes place in three dimensions it

Table II Parameters of numerical fitting for $50P_2O_5$-$30FeO$-$20CaO$ glass.

t [°C]	K(d)	r	A	s
17	-	-	0.045	0.67
27	0.001	1.44	0.065	0.665
42.5	0.0012	1.30	0.053	0.67
62	0.0019	1.4	-	-
86.5	0.0025	1.22	-	-

is possible to calculate d_f which is the fractal dimensionality of cluster. Using the average values r = 1.4 and d = 3 (from Table II) one obtains $d_f = 2.6$. This means that in clusters the percolation paths have also three dimensional character.

One can notice in eq. (7) that $\sigma_{ac} \propto \sigma_{dc}$ if take into account B-N-N relation. With

$\omega_m = \sigma_{dc}/\varepsilon_o \Delta \varepsilon$ the result obtained for σ_{ac} is:

$$\sigma_{ac} = A(\omega \varepsilon_o \Delta \varepsilon)^s \sigma_{dc}^{1-s} \quad (8)$$

This yields that in log-log scale $\sigma_{ac} = f(\sigma_{dc})$ should be linear with a slope of (1-s). Figure 4 shows these dependences for all investigated glasses measured by a.c. bridge. From the slope we have obtained $s = 0.70$ for $f = 10$kHz, $s = 0.74 \div 0.76$ for $f = 1$MHz and 10MHz. These values correspond to the average s obtained from the frequency dependent $\sigma_{ac} = A \omega^s$ measured at the same temperature.

In conclusion: we believe that the Hunt theory explains the correlation between internal friction, dielectric relaxation and dc conductivity.
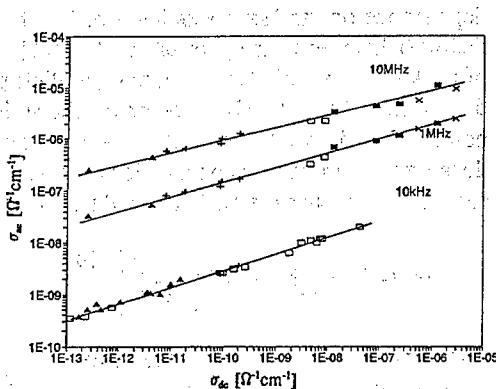
Figure 4 Room temperature conductivity $\sigma_{ac} = f(\sigma_{dc})$ in groups of samples: I - (▲, +); II - (□); III - (■) and IV - (×).

References

1   L. Murawski, C.H. Chung and J.D. Mackenzie, *J. Non-Cryst. Solids*, **32** (1979) 91.
2   N. F. Mott, *J. Non - Cryst. Solids*, **1** (1968) 1.
3   W. Chomka, D. Samatowicz, *J. Non - Cryst. Solids*, **57** (1983) 327.
4   A. Hunt, *J. Phys.: Condens. Matter*, **2** (1990) 9055; **3** (1991) 7831; **4** (1992) 6957.
5   A. Hunt, *J. Non - Cryst. Solids*, **134** (1991) 267; **144** (1992) 21.
6   B. V. Hamon, *Proc. Inst. Elec. Eng. (London)*, **99** (1952) 115.
7   P. B. Macedo, C. T. Moynihan, R. Bose, *Phys. Chem. Glasses*, **13** (1972) 171.
8   J. L. Barton, *Verres Refr.*, **20** (1966) 328.
9   T. Nakajima, *Annual Report, Conf. on Electric Insulation and Dielectric Phenomena*, (National Academy of Sciences, Washinton, DC, 1972), p. 168.
10 H. Namikawa, *J. Non - Cryst Solids*, **18** (1975) 173.
11 M. Pollak, G. E. Pike, *Phys. Rev. Letters*, **28** (1972) 1449.

XEROGRAPHIC DRIFT MOBILITY MEASUREMENTS IN DLC THIN FILMS

W. Mycielski, E. Staryga and A. Lipiński
Technical University of Łódź, Institute of Physics,
Wólczańska 219, 93-005 Łódź (Poland)

Diamond-like carbon (DLC) films obtained by r.f. plasma decomposition from hydrocarbons (e.g. methane CH_4) have a number of unique properties that predict this material for technical and industrial applications. Recently, the DLC layers are considered as a substitute of the traditional semiconductors in microelectronics [1,2]. It is evident that eventually application of DLC layers depends on their properties, particularly on the electronic transport properties.

The carrier drift mobility is the most important parameter characterizing the electronic properties of insulators and high ohmic semiconductors (e.g. DLC films). In this work the results of the electron drift mobility obtained from xerographic time-of-flight experiment in thin DLC films are presented.

Experimental details

The DLC thin films were prepared by r.f. glow discharge from methane at the pressure 50 Pa. The applied negative self-bias voltage V_e depended on the discharge power was from 80 to 250 V. As the substrates platinum, gold or low-resistivity silicon were used. The thicknesses of the layers (determined by an interferometer method) were $0.06 \div 0.60$ μm. The technology of the thin DLC layers preparation was described in detail elsewhere [3, 4, 5].

For the drift mobility measurements the so called xerographic or open-circuit technique was applied. This method was first proposed and described by Batra *et al.* [6] and its equivalence with conventional time-of-flight technique was presented by Enck and Abkowitz [7]. More details of the xerographic time-of-flight technique were given by Vaezi-Nejad [8]. In this technique, the free surface of the sample is initially charged to voltage U_o. Next this voltage decreases due of transport of charge carriers. According to the theory [6] for negative charging the $U = f(t)$ and $dU/dt = f(t)$ dependences are given by:

$$U(t) = U_o(1 - t/2t_{tr}), \tag{1}$$

$$\text{for } t < t_{tr}$$

$$dU/dt = - U_o/2t_{tr} \tag{2}$$

and

$$U(t) = (D^2/2\mu)(1/t), \tag{3}$$

$$\text{for } t > t_{tr}$$

$$dU/dt = - (D^2/2\mu)(1/t^2), \tag{4}$$

where t_{tr} is the transit time of the leading charge front, D - thickness of the sample and $\mu = D^2/t_{tr}U_o$ is the electron drift mobility. The transit time may be determined from Eq.1 (t_{tr} is the time when the voltage has decayed to half its initial value) or from Eq.2 using the value of derivative dU/dt, initially independent of time.

In our experiment the samples were placed in vacuum and charged by low--energetic (~1 keV) electron beam (in the works [6] and [7] a corona charging devices were used). The decaying surface voltage U(t) was measured using FET preamplifier connected to 20 MHz digitizing transient recorder MC 101 (MesComp, Poland). The transient recorder was interfaced with AT computer for registration of the U(t) dependences and their further numerical analysis.

The apparatus was tested using amorphous layers of selenium, which material is very convenient for xerographic measurements. The obtained electron drift mobility at room temperature is in a very good agreement with the one reported by other authors. The mean value of the electron mobility calculated from a number of publications [9 - 13] is 6.2×10^{-3} cm²/Vs whereas our result is 7.0×10^{-3} cm²/Vs.

Results and discussion

Figure 1 displays a typical discharge curve U(t) for DLC films (D = 0.6 μm, V_e = 250 V) and the derivative dU/dt for the same sample. As can be seen, the shape of these dependences is in good agreement with theoretical predictions, i.e. the derivative dU/dt for $t < t_{tr}$ is practically time independent (Eq.2). Numerical calculations for the time $t > t_{tr}$ have shown that U(t) ~ 1/t and dU/dt ~ $1/t^2$ according to Eqns. 3 and 4 with the correlation coefficient greater than 0.99 and 0.95, respectively .
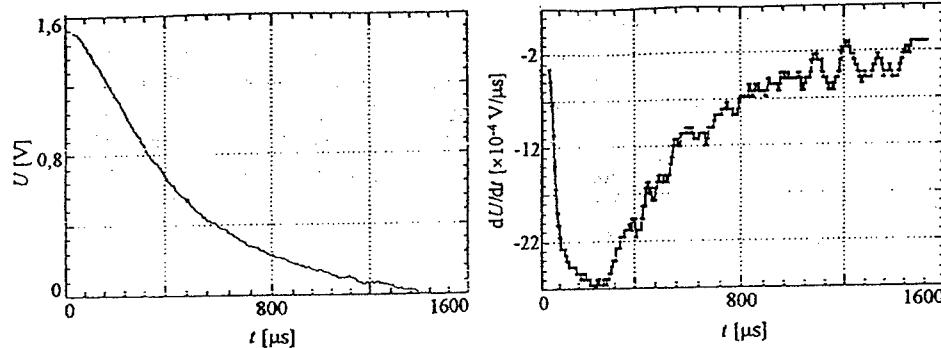

Fig. 1. The time dependence of surface voltage U(t) and the derivative dU/dt for diamond-like film at room temperature (D = 0.6 μm, V_e = 250 V).

Table 1 presents the mean values of the electron drift mobility μ for the DLC films prepared at different negative self-bias voltages V_e. All measurements were carried out at room temperature. No influence of the substrate material on the experimental results of the mobility has been observed.

TABLE 1. *The electron drift mobility in DLC films (T=300 K)*

Negative self-bias voltage V_e [V]	Electron drift mobility μ [cm^2/Vs]
80	1.6×10^{-6}
150	2.3×10^{-6}
250	8.0×10^{-6}

The electron drift mobility values obtained in our experiment are from 1.6×10^{-6} to 8.0×10^{-6} cm^2/Vs. These mobilities in DLC films are very low in comparison with the ones reported by other authors for diamond films ($\sim 10 \div 50$ cm^2/Vs) [14 - 16]. It is evident that this difference is a result of quite different structure of diamond-like and diamond films. The values of mobility of the order $10^{-7} \div 10^{-6}$ cm^2/Vs are rather typical for polymers [17 - 19]. Such mobilities indicate that the hopping may be predominant mechanism of the charge carrier transport in the DLC films according to Robertson's suggestions [20].

References

1. G. SH. Gildenblat, S.A. Grot and A. Badzian, *Proc. IEEE Electron Device*, 79 (1991)647
2. Y. Tzeng, M. Yoshikawa, M. Murakawa and A. Feldman in *Aplications of Diamond Films and Related Materials*, Elsevier, Amsterdam, 1991
3. Z. Haś, S. Mitura and B. Wendler, *Proc. Int. Ion Eng. Congress ISIAT-IPAT '83*, Kyoto, 1983, p.1143
4. Z. Haś, S. Mitura, M. Clapa and J. Szmidt, *Thin Solid Films*, 136 (1986) 161
5. E. Staryga, A. Lipiński, S. Mitura and Z. Haś, *Thin Solid Films*, 145 (1986)17
6. I.P. Batra, K. Keiji Kanazawa and H. Seki, *J. Appl. Phys.*, 41 (1970) 3416
7. R.C. Enck and M. Abkowitz, *J. Non-Cryst. Solids*, 66 (1984) 255
8. S.M. Vaezi-Nejad, *Int. J. Electronics*, 82 (1987) 370
9. W.E. Spear, *Proc. Phys. Soc.*, 76 (1960) 826
10. J. I. Hartke, *Phys. Rev.*, 125 (1962) 1177

11. W.E. Spear, *J. Non-Cryst. Solids*, 1 (1969) 197
12. J. Schottmiller, M. Tabak, G. Lucovsky and A. Ward, *J. Non-Cryst. Solids*, 4 (1970) 80
13. M.D. Tabak, *Phys. Rev. B*, 2 (1970) 2104
14. K. Okano, H. Kiyota, T. Iwasaki, Y. Nakamura, Y. Akiba, T. Kurosu, M. Iida and T. Nakamura, *Appl. Phys. A*, 51 (1990) 344
15. C.A. Hewett and J.R. Zeidler, *Diamond Relat. Mater.*, 1 (1992) 688
16. A.T. Collins, *Mater. Sci. Eng. B*, 11 (1992) 257
17. Y. Kanemitsu and J. Einami, *Appl. Phys. Lett.*, 57 (1990) 673
18. L.B. Schein, A. Peled and D. Glatz, *J. Appl. Phys.*, 66 (1989) 686
19. M. Stolka and M.A. Abkowitz, *J. Non-Cryst. Solids*, 97&98 (1987) 1111
20. J. Robertson, *Prog. Solid St. Chem.*, 21 (1991) 199

DIELECTRIC PROPERTIES OF POLYURETHANE MODEL NETWORKS - PRESSURE DEPENDENCE

J. NEDBAL[1], J. FÄHNRICH[1], M. ILAVSKÝ[2] and B. STOLL[3]

[1]Department of Polymer Physics, Faculty of Mathematics and Physics, Charles University, Prague, Czech Republic
[2]Institute of Macromolecular Chemistry, Academy of Sciences of the Czech Republic, Prague, Czech Republic
[3]Department of Physics, University of Ulm, Ulm, FRG

Polyurethane networks based on poly(oxypropylene)triols and diisocyanate have been used as model systems for testing the relation between the network structure and its relaxation behaviour. It was found that the temperature and frequency position of dielectric and mechanical functions in the main transition region of these networks are affected mainly by the concentration of polar urethane groups [1-3]. This quantity may be controlled easily by changing the initial ratio r_H of hydroxyl to isocyanate groups involved in the reaction. The deviation of r_H from its stoichiometric value leads to pronounced reduction of network density , which can be observed in the relaxation measurement, mainly in the mechanical case. The temperature shift of absorption peak position in the main transition region was adequately described by Vogel-Fulcher-Tammann (VFT) formula [4]. Further extension of the experimental information about structure of these networks can be achieved from the pressure dependence of dielectric relaxation process [5, 6].

In this contribution we study the dielectric properties of polyurethane networks based on poly(oxypropylene)diols(POPD) or poly(oxypropylene)triols (POPT), 4,4'-diphenylmethane diisocyanate (MDI),triiso-cyanate-tris(4-isocyanatophenyl)thiophosphate (TI) and trimethylolpropane (TMP). Three different types of networks have been prepared. The first group of networks was prepared from POPT s and MDI, the second one from PPD s and TI and the third one from PPD s, MDI and TMP.

The networks under study were prepared at various ratios of OH and NCO reactive groups, r_H. Networks were cured at 353 K for time t ≈ 24 h at the presence of dibutyltin dilaurate catalyst up to the highest possible conversion of minority groups.

Dielectric measurements of real ϵ_1 and loss ϵ_2 parts of complex permittivity $\epsilon^* = \epsilon_1 - j\epsilon_2$ at different pressures and temperatures were performed in the frequency range 0.02 Hz - 200 MHz [6]. The temperature varied between 240 - 325 K, the applied pressures covered the range 1 - 5000 bar.

The dielectric data may be represented with reasonable accuracy as a superposition of two terms - the dielectric and the conductivity contributions. The dielectric contribution is given by the Havriliak-Negami formula [7]. The conductivity becomes dominant at low frequencies and high temperatures. The temperature shift of the relaxation region in the main transition zone was processed by the standard procedure based on the VFT formula [4] for each applied pressure separately. This result is in agreement with the free-volume concept of the glass transition. From thus evaluated measurements we have estimated the values of the basic parameters characterizing the relaxation behaviour: VFT temperature T_0, the dielectric increment, parameters of the Havriliak-Negami distribution and conductivity parameters. Then the influence of the pressure on all these parameters is discussed. Generally, with increasing deviation from stoichiometry (decreasing crosslinking density) at constant pressure VFT temperature decreases and the width of transition zone increases. On the other hand, with increasing pressure at constant temperature VFT temperature increases and width of transition decreases. In our contribution special attention is paid to the free volume approach and to the testing of its validity.

REFERENCES
[1] M.Ilavský, K.Dušek: Polymer 24, 981 (1983)
[2] M.Ilavský, K.Dušek: Macromolecules 19, 2139 (1986)
[3] A.Havránek, M.Ilavský, J.Nedbal, M.Böhm, W.v.Soden, B.Stoll: Coll. Polym. Sci. 265, 8 (1987)
[4] G.Tammann,G.Hesse:Z.Anorg.Allg.Chem. 156, 245 (1926)
[5] G.Williams, Trans.Faraday Soc. 61, 1564 (1965)
[6] W.M.Heinrich: Disertation, University of Ulm (1987)
[7] S.Havriliak, S.Negami: J. Polym. Sci. C, Polym.Symp. 14, 99 (1981)

EXTENSION OF THE GRAIN CONSOLIDATION MODEL TO ACCOUNT FOR INTERFACE EFFECTS

B. Nettelblad and G.A. Niklasson[§]

Physics Department, Chalmers University of Technology,
S-412 96 GÖTEBORG, SWEDEN

§: Present address: Teknikum, Uppsala University, Box 534, S-751 21 Uppsala, Sweden

It has been reported in several cases that the permittivities of porous, liquid-filled solids (such as rocks or ceramics) can be extremely high at low frequencies [1-3]. Such behaviour may be dismissed as 'electrode effects', but it has also been proposed that 'bulk' polarisation of the internal interfaces may be the origin of this behaviour. One way of determining the main cause of the high permittivity values is to cut one specimen into several samples of different thickness and compare the results from measurements of apparent permittivity and conductivity. By doing so, it has been shown [3, 4] that at least sometimes these effects emanate from the 'bulk' of the sample.

When solid particles are dispersed in an electrolyte, the permittivity at low frequencies increases considerably [5], just as for impregnated porous solids. In this case, several theories have been presented [6, 7] that explain the high permittivity values as effects of diffusion and polarisation in the electro-chemical double-layer around the particles. The double-layer can be described as consisting of a thin layer of counterions at a fixed distance close to the charged surface of the solid and a diffuse layer of ions further out.

The difference between liquid impregnated porous solids and dispersions of solid particles is that the volume fraction of solid material is much higher in the porous medium, making the solid phase continuous, but otherwise both systems are in principle equivalent. Yet, little work has been done on impregnated porous solids, compared with what has been done on dispersions, probably because the intricate geometry of the pores makes porous materials difficult to characterise whereas dispersions can often be treated as dilute.

One model for porous materials is the so called 'Grain Consolidation Model' (GCM), that was proposed by Roberts and Schwartz [8]. This simple structural model treats the solid phase as spherical grains, growing homogeneously until they touch each other and then, continuing to grow where they do not intersect (see Fig. 1a), until the appropriate porosity is attained. The calculations are considerably simplified if the grains are placed on a regular lattice. Shen et al. [9] gave a useful method for calculating the permittivity or the conductivity of such a lattice, using a Fourier expansion technique. In the original papers it was assumed that the porous material only had two phases, each phase having the same properties throughout their volume. Tyč et al [10] added a third layer at the solid-liquid interface, considered to consist of platy grains that acted as clay particles. In a previous paper [4], we used another approach, where we modeled the electrochemical double-layer as a thin interface layer, having different electric properties

than the bulk liquid (see fig. 1b). We showed that we got results in satisfactory agreements with experiments.
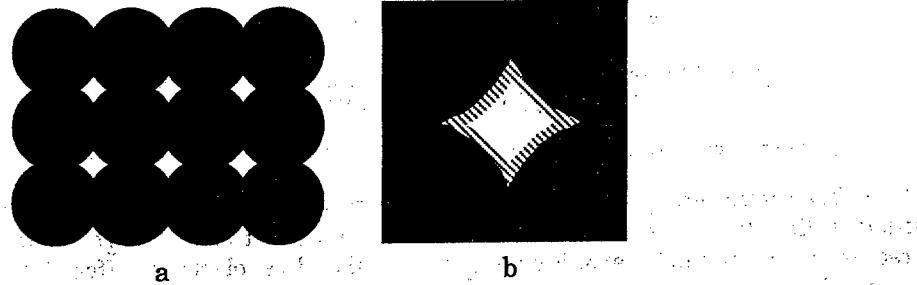
Figure 1.a) Cross-section of one layer in the lattice in the GCM. b) The model of the interface and double-layer (not necessarily drawn to scale)

In this paper we discuss more thoroughly this three-component GCM and the complications that arose when we developed it. We also give comparisons to predictions of effective-medium theories.

To get a faster convergence in the summation of the Fourier series, Shen et al. expressed the electric field as a sum of two terms:

$$E = E_1(r)\theta_1(r) + E_2(r)\theta_2(r) , \qquad (1)$$

where $\theta_1(r)$ equals one in material 1 and zero in material 2 (and the reverse for $\theta_2(r)$). Since the values of $E_1(r)$ in material 2 and of $E_2(r)$ in material 1 are of no interest, these functions can be smooth. The functions are expressed in Fourier series:

$$E_1(r) = \sum_m C_{1m} e^{ib_m \cdot r} \qquad \theta_1(r) = \sum_m T_{1m} e^{ib_m \cdot r}$$
$$E(r) = \sum_\alpha \sum_m \sum_n T_{\alpha n} e^{ib_n \cdot r} C_{\alpha m} e^{ib_m \cdot r} \qquad (2)$$

The T's can be calculated for a certain geometry, but the C's are unknown and have to be calculated by solving Maxwell's equations with the condition that the spatial average of the electric field be equal to the applied field.

In the Fourier plane, Maxwell's equations can be written:

$$b_n \times \sum_\alpha \sum_m T_{\alpha n-m} C_{\alpha m} = 0 , \qquad b_n \cdot \sum_\alpha \sum_m \varepsilon_\alpha T_{\alpha n-m} C_{\alpha m} = 0 \qquad (3a,b)$$

We now take each component of $n \leq N$ and each component of $m \leq M$, where N is so large that the number of equations exceeds the number of unknowns. The equations are then solved by the least square method.

Our purpose was now twofold: We wanted to study the frequency-dependent complex dielectric properties, including a conduction loss. We also wanted to extend the model to include a third component: an interface

layer. We did this by adding the functions $E_3(r)$ and $\theta_3(r)$ to the problem, yielding:

$$E = E_1(r)\theta_1(r) + E_2(r)\theta_2(r) + E_3(r)\theta_3(r) \, , \tag{4}$$

$\theta_3(r)$ has the value one within the interface layer and is zero elsewhere, while $\theta_1(r)$ and $\theta_2(r)$ equal zero in the interface layer.

Calculating the complex dielectric constant doubles both the number of equations and the number of unknowns. Still, if we assume the grains to be placed on a regular lattice (for simplicity, we assumed a simple cubic lattice), we can use the symmetries to decrease the number of unknowns. If the applied field is in the z-direction and we denote the x component of $C_{[a,b,c]}$ by $C^x_{[a,b,c]}$ (and analogously for other components) then we see, e.g., that:

$$C^x_{[-a,b,c]} = - C^x_{[a,b,c]} \, ; \, C^y_{[-a,b,c]} = C^y_{[a,b,c]}; \, C^z_{[-a,b,c]} = C^z_{[a,b,c]} \tag{5}$$

Still, there are problems at low frequencies, where the dominating part of ε will be the imaginary part: $i\sigma/(\omega\varepsilon_0)$, that diverges at zero frequency. In equations (3b) above, there is a factor ε_α that does not appear in equations (3a). This means that at low frequencies the equations (3b) are more heavily weighted in the least-squares calculations than the equations (3a). We solved this problem by dividing equations (3b) with $\sqrt{(\varepsilon_1-\varepsilon_2)^2 + (\frac{\sigma_1-\sigma_2}{\omega\varepsilon_0})^2}$.
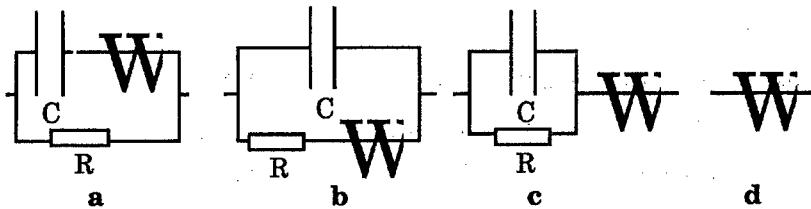
Figure 2. The equivalent circuits used for modelling the behaviour of the interface layer. The 'W' is symbolising a Warburg impedance.

Several equivalent circuits were tested for the electrical behaviour of the interface layer. Each included a Warburg impedance to account for the diffusion effects. A capacitor and a resistor were normally included in the equivalent circuit to render the high-frequency properties of the layer equal to those of the bulk liquid, ignoring any high-frequency interface conductivity. In Fig. 2, we show the different equivalent circuits used. Circuit b) was found to give best agreement with experiments, but circuit c) was not much inferior. The circuits a) and d) gave poor agreement with experiments.

Finally, we present a comparison with the Bruggeman unsymmetrical formula [11]. We treated the solid material as inclusions and the water as host material and let the interface layer be included either in the guest (having
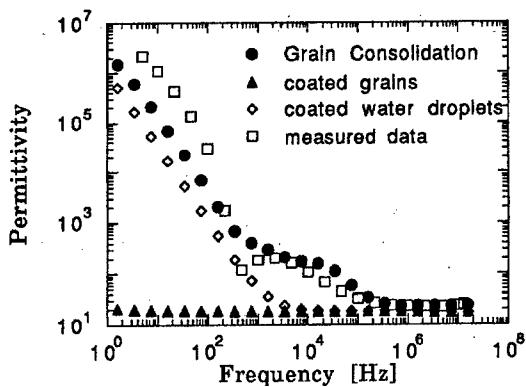
Figure 3. Comparison between experimental data, the GCM and effective medium theory.

the guest as coated spheres) or in the host material (coated water droplets). In the calculations, we used the same conditions (31 % porosity, water conductivity 12 mS/m, sphere diameter 0,25 mm) as in our previous paper [4]. To calculate the effective dielectric constant of a coated sphere (or a coated droplet) we used the Maxwell-Garnett theory [11]. As is seen if Fig. 3, the GCM gives good agreement with experiments, the coated water droplets model has inferior agreement and the coated spheres model totally disagree with experiments at low frequencies. This difference may be due to the fact that the interface layer is not continuous in the coated spheres model.

REFERENCES

1. F. Brouers, A. Ramsamugh, V. V. Dixit, *J. Mater. Sci.* **22**, 2759 (1987).

2. D. A. Lockner, J. D. Byerlee, *J. Geophys. Res.* **90**, 7837 (1985).

3. C. Ruffet, Y. Gueguen, M. Darot, *Terra Nova* **3**, 265 (1991).

4. B. Nettelblad, G. A. Niklasson, *Solid State Commun.* **90**, 201 (1994).

5. L. A. Rosen, D. A. Saville, *Langmuir* **7**, 36 (1991).

6. W. C. Chew, P. N. Sen, *J. Phys. Chem.* **77**, 2042 (1982).

7. E. H. B. DeLacey, L. R. White, *J. Chem. Soc. Faraday Trans. II* **77**, 2007 (1981).

8. J. N. Roberts, L. M. Schwartz, *Phys. Rev. B* **31**, 5990 (1985).

9. L. C. Shen, C. Liu, J. Korringa, K. J. Dunn, *J. Appl. Phys.* **67**, 7071 (1990).

10. S. Tyč, L. M. Schwartz, P. N. Sen, P.-Z. Wong, *J. Appl. Phys.* **64**, 2575 (1988).

11. R. Landauer, Electrical conductivity in inhomogeneous media, C. W. Garland, D. Tanners, Eds., Conference on Electrical, Transport and Optical Properties of Inhomogeneous Media (ETOPIM) (Columbus, Ohio, USA, 1977), pp. 2-43.

THE "UNIVERSAL RESPONSE" AND SELF-SIMILARITY PRINCIPLE.

by prof. Raoul R. Nigmatullin
Kazan State University, Kazan, Tatarstan, Russia.

1.The "universal" response phenomenon which has been discovered experimentally more than 20 years ago [1] caused again the considerable interest in connection with the "penetration" of fractal conception into solid state physics [2],[3]. In spite of considerable progress which has been achieved in understanding of physical grounds of this phenomenon from theoretical point of view [4],[5] the nature of its "universality" remains hidden and unclear. From another side the fractal conception stimulated the interest to investigations the processes of relaxation in heterogeneous systems where relaxation is far from usual exponential law of relaxation. Here alongside with "universal" response we can remind the "stretched" exponential law of relaxation

$$\phi(t)=\exp[-(t/\tau)^{v}], \qquad 0 < v < 1 \qquad (1)$$

which also observed in wide class of materials [6]. The "universal" behaviour of complex susceptibility in certain interval of frequencies is usually expressed as

$$\chi(j\omega)=\chi(0) - (j\omega/\Omega_{p})^{m} \quad \text{for } 0 << \omega/\Omega_{p} <<1 \qquad (2a)$$

$$\chi(j\omega)=(j\omega/\Omega_{p})^{n-1} \qquad \text{for } 1<< \omega/\Omega_{p} << \infty \qquad (2b)$$

Here $0< m,n <1$, Ω_{p} coincides approximately with the peak loss frequency. The formulas for the relaxation function in the corresponding temporal interval has the form

$$\phi(t) \propto t^{-1-m} \qquad \text{for } \Omega_{p} t >> 1 \qquad (3a)$$

$$\phi(t) \propto t^{-n} \qquad \text{for } \Omega_{p} t << 1 \qquad (3b)$$

These relationships which are observed in wide class of heterogeneous materials allows us to formulate the questions concerning the nature of such "universality".

Q1. Is there a general property of heterogeneous materials which can lie in the grounds of these "universal" mechanisms of relaxation?

Q2. What kind of corrections one can expect to the functions $z^{\pm v}$ in (1)-(3) if the boundaries of frequency or temporal interval is increased?

Q3. How this "universal" relaxation behaviour is related to microscopic relaxation functions?

Q4. What is the general nature of exponents v,m,n, which determine the relationships (1)-(3)?

Q5. Are there some practical realizations of this phenomenon in physics and technics?

The *main purpose* of this abstract is to demonstrate the close relationship between the *"universal" response and self-similarity principle* and outline the direction which helps to find the answers for the questions formulated above.

2. The system is called *self-similar* if the number of objects $N(\xi)$ of a less scale ξ generated in the region of a space of the scale η $(\eta > \xi)$ depends only on the ratio $N(\eta/\xi)$. The system which obeyed this definition (principle) which is called self-similar. Consider the sum of the type

$$S_N(z) = \sum_{j=0}^{N} b^j f(z\xi^j) \qquad (4)$$

One can prove that —

The "universal" behaviour of the type (2) or (3) is closely related with the "universal" properties of the sum $S_N(z)$.

We shall try to find the general principles of the appearance of the sum $S_N(z)$ as the function of variable z. This sum is rather general and can arise as the result of *additive summation* of a physical value distributed over a fractal structure.

The physical systems with fractal geometry occupy an intermediate position between discrete and continuum cases because from one side a fractal system has an indivisible and uncorrelated structural unit and from another side the availability of gaps differ these systems from continuum.

We consider some physical process which is described by the function $f(z/z_j)$. z_j is size variable forming the j—th part of the fractal system considered, z is an *intensive* variable which can characterize the system at whole. For example z can coincide with time, frequency, pressure, temperature and etc.

Let us suppose that $z_j = aV_j$ where V_j is a fractal volume of the j—th generation. As it follows from the results which are known from fractal geometry V_j is expressed as

$$V_j = G_f p^j (\Lambda/k^j)^{d_z} = G_f \eta^{d_z} (\Lambda/\eta)^{D_r} \qquad (5)$$

where $G_f (\Lambda/k^j)^{d_z}$ is a volume of a fractal of the scale $\eta = (\Lambda/k^j)$.

$p^j = (\Lambda/\eta)^{D_r} = M_j$ is a number of figures of the scale η, G_f is the geometric form—factor, j is a number of self—similar generations (j = 0,1,2,...,N). The last stage j = N is related to the minimum scale $\lambda = \Lambda/k^N$. Taking into account all remarks made above we can present the sum $S_N(z)$ in the form

$$S_N(z)/N_A = \sum_{j=0}^{N} M_j f(z/z_j) = \sum_{j=0}^{N} p^j f(z/aV_j) = \sum_{j=0}^{N} b^j f(z\xi^j) \qquad (6)$$

Here $b = p$, $\xi = k^{d_z}/p$, $z \Rightarrow z/(aG_f \Lambda^{d_z})$, N_A is a number of homogeneous

regions of the scale Λ. Schematically the process of additive summation is shown on **Fig.1.** The detailed investigations of sum (6) have lead to the following result:

$$S_N(z) = A(v)z^{\pm v} + B(v) \qquad (7)$$

Here $z=j\omega$ for all cases, the values of constants $A(v),B(v)$ and interval of z are given in the **Table 1.**

These results has been used in [7] for calculations the impedance of self–similar RC circuits. If $z=t/\tau$ and we consider the relaxation process in time–domain then the invariant properties of the sum $S_N(z)$ is conserved. As we see the final result is *insensitive* to concrete form of microscopic relaxation function $f(x)$ and so the "universal" properties of this sum is correct for the wide class of functions $f(x)$. The exponent $v=\ln b/\ln\xi$ is not changed under the transformations $b\Rightarrow b^k$, $\xi\Rightarrow\xi^k$ and so we have a right to call the invariant property of the sum $S_N(z)$ as **fractal or self–similar invariant.** If a process includes in itself two or more exponents it is sufficient to consider the sum of the type

$$S_{N_1 N_2}(z) = \sum_{j_1=0}^{N_1}\sum_{j_2=0}^{N_2} b_1^{j_1}b_2^{j_2} f(\xi_1^{j_1}\xi_2^{j_2}z) \qquad (8)$$

From physical point of view the sum (8) represents itself an additive distribution of two types of fractal structures related with a microscopic process $f(z)$. By analogy one can show that depending on the values b_1, ξ_1, b_2, ξ_2 the sum $S_{N_1 N_2}(z)$ admits the existence of 4^2 invariants. Calculations have lead to the result

$$A(v_1,v_2)z^{\pm v_1} \pm B(v_1,v_2)z^{\pm v_2} \pm C(v_1,v_2) \qquad (9)$$

which is correct for the certain interval of $z=j\omega$ and wide class of functions $f(x)$ having the finite Mellin's image. The last result can reproduce CPA and FPR branch for various values v_1, v_2.

3.The "stretched" exponential law of the type (1) is related closely with parallel relaxation and also has "universal" character. Consider the product

$$\phi(z) = \prod_{j=1}^{K} [g(z/j^{\delta})]^{n_0 j^{\gamma}} \qquad (10)$$

Here $z=t/\tau$, γ, $\delta > 0$. This type of relaxation is typical for the branching process of relaxation when the process is determined by two factors-the rate of relaxation in channel and number of channels (branches) in the next generation. The first factor is determined by the exponent δ and the second one by γ. The function $g(y)$ which describes the microscopic process of relaxation satisfies the following conditions $g(0)=1$, $dg'(y)/dg<0$.

At rather general conditions imposed on the the function $g(y)$ at small and large values of y one can obtain the following result

$$\phi(z) = \exp\{-\gamma(v)(t/\tau)^v + B(v)(t/\tau)\} \qquad (11)$$

Here

$$\gamma(v)=\frac{n_0}{\delta v}\int_0^\infty y^{-v}\frac{|g'(y)|}{g(y)}\,dy, \quad B(v)=\frac{n_0 a_1}{\delta(1-v)}\varepsilon^{1-v} \qquad (12a)$$

$$v=(1+\gamma)/\delta, \quad 0<v<1, \quad \varepsilon=1/K^\delta <<1 \qquad (12b)$$

The boundaries of intermediate asymptotic are determined by the expression

$$\left|\frac{A_1 n_0}{g(1+v)\delta}\right| << \frac{t}{\tau} << \left|\left[\frac{2\delta(2-v)}{n_0(2a_2-ca_1^2)\varepsilon^{2-v}}\right]^{1/2}\right| \qquad (13)$$

So the "stretched" exponential law of a type (11) alongside with "universal" functions (7),(9) is rather general and applicable for wide class of microscopic relaxation functions f(x) and g(x). The second term in (11) determines the small correction to usual exponential law decreasing the rate of relaxation. One can prove that the translation and rotational symmetry of local atoms is not essential for relaxation and so this theory applicable not only to regular structures but to wide class of disordered systems also. The same result (11) can be obtained for fractal structures if we consider the product

$$\phi(z)=\prod_{j=0}^N [g(z/\xi^j)]^{n_0 b^j} \qquad (14)$$

and based on the estimations of sum (6) and results of **Table 1** determine the interval of z and the exponent $v=\ln b/\ln\xi$.

4. So the self-similarity principle is closely related with the "universal" laws of relaxation (1),(3) and can be applied to the more wide class of heterogeneous media than it was supposed before [6]. Based on the results (2) one can suggest the new passive two-pole elements of electric circuits realizing the operation of fractional integration and differentiation in t-domain region and predict the new types of waves propagating in "poor" conductors.

REFERENCES
1.A.K.Jonscher, Dielectric relaxation in solids, Chelsea Dielectric Press, London,1983.
2.J.Feder,Fractals, Plenum Press, New—York and London,1988.
3.G.A.Niklasson,Comparison of dielectric response functions for conducting materials,J.Appl.Phys.,vol.66,pp.4350—4359,1989.
4.L.A.Dissado and R.M.Hill,The fractal nature of the cluster model response functions, J.Appl.Phys.,vol.66,pp. 2511—2524,1989.
5.J.C.Dyre,Universal low—temperature ac conductivity of microscopically disodered nonmetals,Phys.Rev B, vol.48,pp.12511—12526,1993.
6.J.Klafter and M.Shlesinger,On the relationship among three theories of relaxation in disordered systems, Proc.Natl.Acad.Sci.,USA, vol.83,pp.848—851,1986.
7.R.M.Hill,L.A.Dissado and R.R.Nigmatullin, Invariant behaviour classes for the response of simple fractal circuits, J.Phys.Condens.Matter, vol.3,pp.9773—9790,1991.

The results of estimations of sum (6) presented in brief in **Table 1.**

[Case A] $\xi, b < 1$, $\xi < b < 1$, $\varepsilon = \xi^N << 1$, "CPA" response for $z \in [1,\infty)$, $v = \ln b / \ln \xi$

$$S_N(z) \approx [G(v)/(1-\xi)]z^{-v} - [f(0)\varepsilon^v/v(1-\xi)]$$

for interval z

$$[A_1/(1-\xi)(1-v)] << |z| << 1/\varepsilon$$

[Case B] $\xi > 1$, $b < 1$, $b\xi > 1$, $E = \xi^N >> 1$, "FPR" response for $z \in [0,1]$,
$v = \ln(1/b)/\ln\xi$

$$S_N(z) \approx [f(0)/|v|(\xi-1)] + [G(-|v|)/(\xi-1)]z^{|v|}$$

for interval z

$$[A_1|E^{-(1+|v|)}/|v|(\xi-1)(1+|v|)] << |z| << [|v|(\xi-1)(1-|v|)/|C_1|]$$

[Case C] $\xi, b > 1$, $1 < b < \xi$, $E = \xi^N >> 1$, "CPA" response for $z \in [0,1]$, $v = \ln b / \ln \xi$

$$S_N(z) \approx [G(v)/(\xi-1)]z^{-v} - [f(0)/v(\xi-1)]$$

for interval z

$$[A_1|E^{-(1-v)}/(\xi-1)(1-v)] << |z| << [(\xi-1)(1+|v|)/|C_1|]$$

[Case D] $\xi < 1$, $b > 1$, $b\xi < 1$, $\varepsilon = \xi^N << 1$, "FPR" response for $z \in [1,\infty)$,
$v = \ln(b)/\ln(1/\xi)$

$$S_N(z) \approx [f(0)/\varepsilon^v|v|(1-\xi)] + [G(-|v|)/(1-\xi)]z^{|v|}$$

for interval z

$$[A_1/|v|(1-\xi)(1+|v|)] << |z| << [|v|(1-\xi)(1-|v|)/|C_1|\varepsilon^{1-|v|}]$$

Here $G(v)$ represents itself the Mellin transform of the function $f(x)$ i.e.

$$G(v) = \int_0^\infty x^{v-1} f(x) dx \qquad (A1)$$
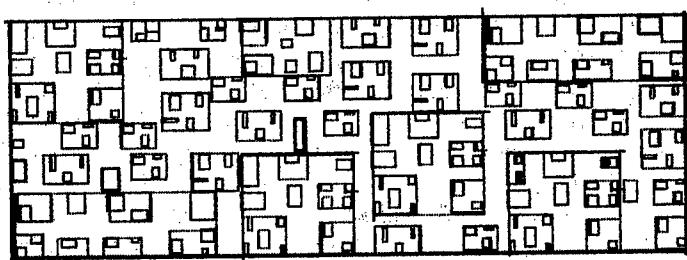
Figure1 shows the process of additive summation over the correlated regions and explaining the origin of the sum (6).

ELECTRODE INJECTED IONIC CURRENTS IN LIQUID CRYSTALS AND POLYMERS

M. Olejnik, J. Michalski, Chair of Physics, Technical University of Rzeszów
W.L. Szymański, Cracow Institute of Technology, Krakow
A.B. Szymański, Chair of Physics, TU Rzeszów and Cracow Institute of Technology

Abstract.

The interest in finding and application of electrodes capable of injecting ions to organic materials is of interest, for a long time [1,2,3,4].However the electrical low frequency response of the sample subjected to such electrodes is often noisy and poorly reproducible. So, for such studies ,a suitable measuring set-up is needed. By means of time domain , fully automated apparatus [5] , the above studies were undertaken, once again, in our group. The problem of ion-injecting electrodes was solved by means of application of porous glass plates [6], filled with gel rich of dissolved salt, particularly NaCl. The sample construction enable us of decrease of sample thickness. In present experiment the sample thickness controlled by pieces of optical fiber, was in the range of 200 mm. The experiment has been carried for following materials: 6CB /hexylcyanobiphenyl/ and cholesteryl oleate. For comparison the sample supplied with SnO electrode has been measured. These electrode act as blocking electrodes to these materials [7]. The comparison of particular response of the samples of cholesteryl oleate with injecting and blocking electrodes is shown in fig.1 and 2. As one can see from the figures,the sample response is quite different. The magnitude of DC current is considerable is case of ion injecting electrode and the current - voltage dependence is nonlinear one /see Fig. 2/. For long times the slope of the current I vs time t is of importance. This can be approximated, with good accuracy, by straight line in log i-log t scale. In case of SnO_2, after subtracting of DC current the charging and discharging slopes are identical.Is not the case of injecting electrode,where big differences in charging/discharging slopes is observed. The aim of the use of ion injecting electrode is to observe ionic space charge limited currents [2,3,4]. To meet this condition certain restrictions are put on sample thickness, voltage applied and the material . The theory of these currents [8] and restrictions put on measurements has been discussed.
   The Authors would like to express his gratitude to Dr E. Szwajczak and Dr M. Leśniak for their interest and helpful discussions.
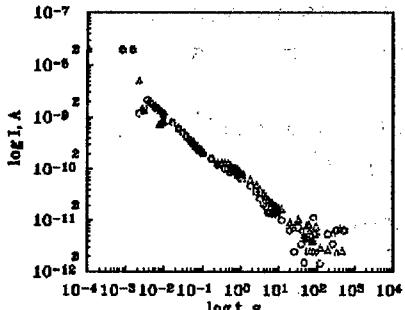
Fig.1. Current vs time (log-log scale) for cholesteryl oleate supplied with SnO$_2$ electrodes. Voltage applied 7 V, temperature 298 K.
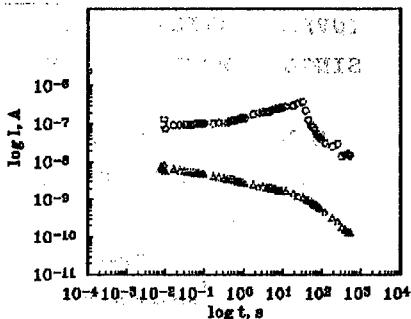
Fig.2. Current vs time (log-log scale) for cholesteryl oleate supplied with injecting electrode. Voltage applied 10 V, temperature 298 K.

Bibliography

[1]. B.I. Sazin,W.P. Szuwaew, Elektrochimja, 1966, 2, 831,

[2]. M. Lesnia et al. in Adv.in Liquid Crystal Research and Appl. Pergamon Press, Oxford, 1979

[3]. M. Lesniak et al. Mol.Cr.Liq.Cr.1980,Vol.61,241

[4]. M. Lesniak et al. Chemia Stosowana ,(1987),XXXI,603

[5]. W.L. Szymanski,A.B. Szymanski, Abstract of the Conference "Dielectric and Related Phenomena" Zakopane, Poland, 12-16.09.1994, pp.19.

[6]. M. Olejnik, A. Blahut, A.B. Szymanski, presented on The Seminar On Properties of Silica Glasses, PGL'94, Karpacz-Poland, 6-10. 06. 1994

[7]. W.L. Szymanski, A, Adamczyk, to be published

[8]. M.A. Lampert, P. Mark, Current Injection in Solids, Acad. Press, N.York, London,1970

INVESTIGATION OF DIELECTRIC PROPERTIES OF NdGaO$_3$ SINGLE CRYSTAL IN THE TEMPERATURE RANGE 80-350 K

V.M. Pashkov, V.N. Borisov, D.I. Savitskii[*],
V.P. Bovtun, S.B. Ubizskii[*]

Kiev Politechnical Institute, KPI-2240,
37 Pobeda avn., Kiev 252056, Ukraine

[*]Research Production Amalgamation "Carat",
202 Stryjska str., L'viv 290031, Ukraine

Possibility of use of some oxide single crystals with perovskite-like structure (such as NdGaO$_3$, LaGaO$_3$, LaAlO$_3$, YAlO$_3$ and others) as substrates for epitaxial growth of HTSC films has coused an increased interest to investigation of their properties. It is focused on those properties which determine the efficiency of their using first of all in cryoelectronics and those which have not been adequately studied before.

This work is devoted to investigation of dielectric properties of neodimium gallium perovskite (NGP) single crystals at radio frequencies and at microwave ones in the temperature range 80 to 350 K, the information of which is incomplete yet.

The NGP single crystals (space group *Pbnm*) were obtained by Czochralsky technique from stoichiometric charge. The twin-free crystals were grown in [110] direction and reached two inches in diameter.

The measurements were performed by resonant techniques - by capacitor method using Q-meter in radio frequencie range and by the dielectric resonator method with $TE_{01\delta}$ oscillation mode [1] in microwave range. The samples were prepared in the form of wafers with evaporated cooper electrodes in the first case and in the cylinder form in the latter one. The error of measurement of dielectric permeability (ε) and of tangent of dielectric losses ($tg\delta$) at radio frequencies did not exceed 2-3% and 7-10%

respectivelly. The additional calibration and using of the correction curves (see [1]) allow to reduce the microwave measurement error of ε and $tg\delta$ up to 3-5%.

It was established that NGP crystal exhibits low losses and practically linear dependence $\varepsilon(T)$. The dispersion of ε was not observed in the range of 10-30 GHz. Such behaviour at microwaves are analogous to aluminates of rare earth elements [2,3], that allows to consider aluminates and gallates as one group of high quality double oxides of rare earth [see Table 1]. But a more sharp rise of $tg\delta$ of NdGaO$_3$ with frequency increase permits to suppose its dispersion frequency to be significantly lower than that for aluminates of rare earth.

Table 1

Dielectric parameters of some gallates and aluminates
crystals at room temperature and at frequencies 0.5 MHz
(RGaO$_3$) 15 MHz (RAlO$_3$) 10 GHz (RGaO$_3$) and 40 GHz (RAlO$_3$)

Composi-tion	ε_{RF}	$tg\delta_{RF}$, $\cdot 10^{-4}$	$TF_{\varepsilon_{RF}}$, $\cdot 10^{-6}K^{-1}$	ε_{MV}	$tg\delta_{MV}$, $\cdot 10^{-4}$	$TF_{\varepsilon_{MV}}$, $\cdot 10^{-6}K^{-1}$
NdGaO$_3$	22.7	2-3	+150	22	1.0	+70
LaGaO$_3$	25	2-3	–	–	–	–
LaAlO$_3$	24.5	6	+200	27	1.0	+90
PrAlO$_3$	25	40	+500	24.7	0.8	+80
NdAlO$_3$	22.5	60	+200	22.2	0.5	+70
EuAlO$_3$	22.5	10	+200	21.8	1.0	+200
GdAlO$_3$	19.5	10	–	19.3	1.0	+240
SmAlO$_3$	19.0	10	+200	18.5	3.0	+90
YAlO$_3$	17.0	3	–	–	–	–

The second specific feature of NGP single crystal is a considerable rise of $tg\delta$ with temperature lowering below 160 K (see Fig.1a) that was observed also in [4]. One of proposal explaining of such behaviour made in [4] connects it with spin ordering of neodimium ions on law $1/T$. The course of temperature dependence $tg\delta$ near 80 K on different frequencies (Fig.1a) allows to think that a peculiarity of

dependence having a non-relaxation nature can take place at $T<80$ K. The results of [5] are evidence of that too. The increase of $tg\delta$ is accompanied by a slightly expressed that minimum of $\varepsilon(T)$ dependence near 100 K that was observed in the extremum form of resonant frequency dependence. Its nature is not clear at the present.

The significant difference between the values of temperature factor of ε TF_ε at microwaves and at radio frequencies (Table 1) suggests that the relaxation losses in NGP crystal take place. It is confirmed by investigation in radio frequency range. In all samples even with high structure perfection a maximum of $tg\delta$ near 230 K occures. It lies just above as the frequency is increased that is an evidence of its relaxation nature. And the activation energy estimation connects this relaxation maximum with ion subsystem of crystal.
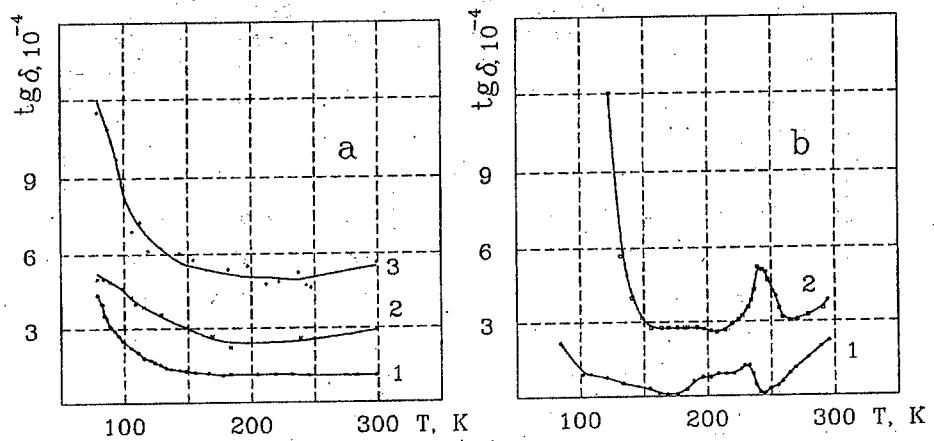
Fig.1. The $tg\delta$ temperature dependencies of NdGaO$_3$ single crystal in microwave (a) and radio frequency (b) range: curves 1, 2 and 3 on (a) correspond to frequencies 10, 16, 30 GHz, and 1 and 2 on (b) - to 0.5 and 3 MHz.

The investigation of crystals with various non-point defects (twin boundaries, mechanical stesses, dislocations and microcracks) shows a sensitivity of the common level of dielectric losses at radio frequencies in the range 80-350 K

to structural perfection of NGP crystal. The losses in such crystals are higher and the appearence of some local maxima on dependence $tg\delta(T)$ occures. As the frequency increases the sensitivity of $tg\delta$ to the structural perfection of sample falls. In spite of presence of defects and relaxation phenomena the dielectric losses of NGP single crystals remain to be relatively low.

Thus, the main features on temperature dependences of studied dielectric parameters of $NdGaO_3$ single crystal in the range 80 to 350 K are the rise of losses level at all frequencies at temperature below 160 K and the presence of local maxima in temperature range 180-240 K that have probably a relaxation nature. To clear up these phenomena some additional investigations including other methods are necessary.

REFERENCES

1. V.G. Tsykalov, V.M. Pashkov, V.P. Bovtun, Investigation of thermostable dielectric resonators with $TE_{01\delta}$ oscillations, Dielectric and semiconductors, Kiev, Vyshcha shkola, 1979, N 15.

2. V.P. Bovtun, Dielectric and semiconductors, Kiev, Vyshcha shkola, 1983, N 23, p. 33-42.

3. Yu.M. Poplavko, V.M. Pashkov, V.P. Bovtun, The high permeability dielectrics in microvawe engineering, Kiev, Znanie, 1982.

4. J. Konopka, I. Wolff, Dielectric properties of high-T_C substrates up to 40 GHz, IEEE Trans. Microwave Theory Techn., vol. 40, pp. 2418-2423, 1992.

5. H.Y. To, G.J. Valco, K.B. Bhasin, 10 GHz $YBa_2Cu_3O_{7-\delta}$ superconducting ring resonators on $NdGaO_3$ substrates, Supercond. Sci. Technol., vol.5, pp. 421-426, 1992.

Angular velocity correlation function of ellipsoidal particles.
Molecular dynamics simulation and theory

K. Pasterny and A. Bródka

Institute of Physics, University of Silesia,

Uniwersytecka 4, 40-007 Katowice, Poland

We carried out molecular dynamics simulation of 256 ellipsoidal molecules interacting via the Gay-Berne potential model [1]. From the simulation results the angular velocity and angular velocity sign reversal correlation functions were calculated. Due to the similarity of these two correlation functions we applied the model worked out for translational velocities by Variyar et al. [2]. The simulated distribution of time intervals between successive angular velocity reversals was analysed using theoretical expression [2] based on uncorrelated consecutive velocity reversals, and one adjustable parameter was estimated. This parameter allowed us to reproduce the main features of the simulated angular velocity correlation function.

[1] J.G. Gay and B.J. Berne, J. Chem. Phys., 74 (1981) 3316.

[2] J.E. Variyar, D. Kivelson, G. Tarjus and J. Talbot, J. Chem. Phys., 98 (1992) 593.

DIELECTRIC RELAXATION PHENOMENA IN POLYMERS
INVESTIGATION OF ELECTRET BEHAVIOUR IN POLYACRYLONITRILE
(PAN)

J. POSPÍŠIL

Department of Polymer Physics, Faculty of Mathematics and
Physics, Charles University,
V Holešovičkách 2, 180 00 Prague, Czech Republic

Objectives
The thermally stimulated depolarization currents (TDSC)
method has been widely used as a tool to monitor and
analyze the complex relaxation phenomena occuring in
polymer [1,2].
TSDC method has been exploited to put in evidence
possible electret behaviour of polyacrylonitrile (PAN),
which has relevant technological applications and is
endowed by the large dipole moment (3.4 D) of the nitrile
side groups present along its main chain.

Experimental

The polyacrylonitrile (PAN) polymer, manufactured by
Aldrich (M_v = 140 000) has been used for the sample
preparation. The 1 mm thick pellets were prepared by
molding-compresion at 155°C and the thin films by casting
on a glass substrate from a PAN viscous solution in
dimethyl formamide solvent (DMF). The viscous PAN
solution in DMF was prepared in the 1:10 weight ratio.
The PAN thin films were dried in a dry box for 24 hours
in vacuum (10^{-3}torr).

Results and conclusions

TSDC results and conclusions
Either pellets and thin films of PAN show a complex TSDC
spectrum in which two regions, A and B, can be isolated.
The former (temperature range 77-400K) is the region of
the molecular mobility of PAN polymer in amorphous phase
and the latter (temperature range > 400K) is the
paracrystalline region. In the A region the spectra can
be decomposed by a proper choice of the poling conditions
(T_P) into three peaks, α, β, and γ. The α peak,
occuring at 380K in the pellets, corresponds to the
glass-transition and is due to dipolar relaxation in the
amorphous phase. In the thin films it is shifted to
360K. The α peak is broad: such a feature might be
meaningful of a wide distribution of molecular weights in
PAN polymeric material. The β peak occurs at 240K, i.e.
below T_g, and can be related to local motions of-C≡N side
groups, The γ peak, at 175K, is probably caused by impu-
rities, e.g. water, see figs. 1a,b,c,d
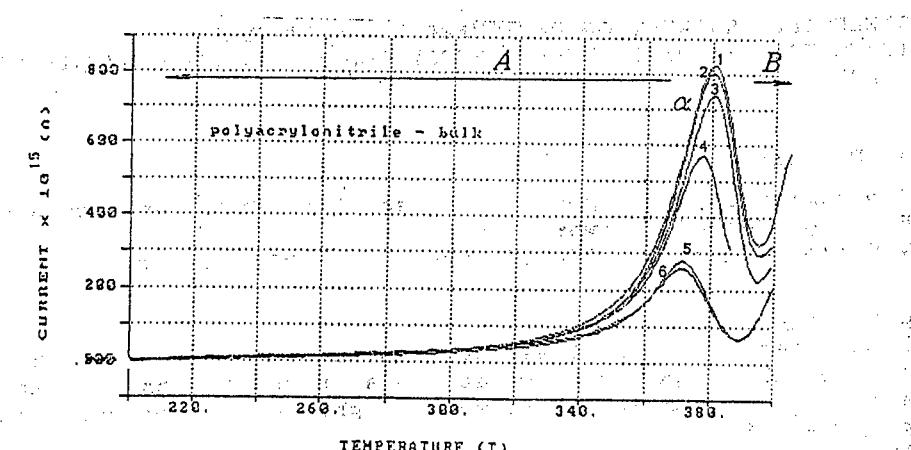
Fig. 1 a - TSDC curves in amorphous region of PAN: $E_p = 25V$, d=1.05 mm, $t_p = 180$ sec, T_p 391, 382, 376, 365, 361, and 358 K for curves 1, 2, 3, 4, 5, and 6 respectively.
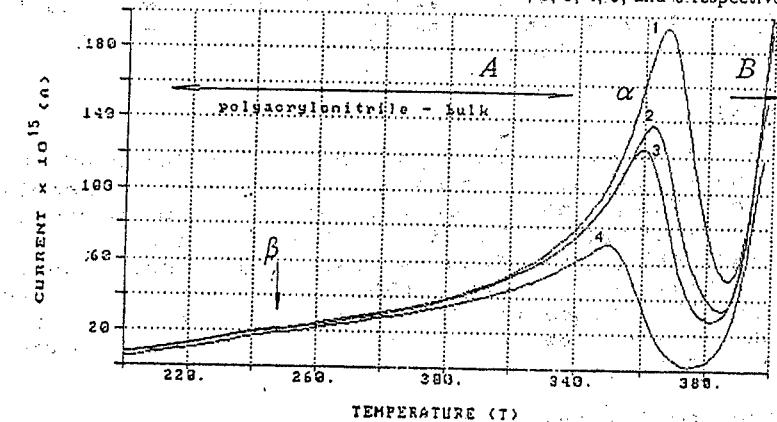

Fig. 1 b - TSDC curves in amorphous region of PAN $E_p = 25V$, d = 1.05 mm, $t_p = 180$ sec, $T_p = 353$, 351, 347, and 338 K for curves 1, 2, 3, and 4 respectively.
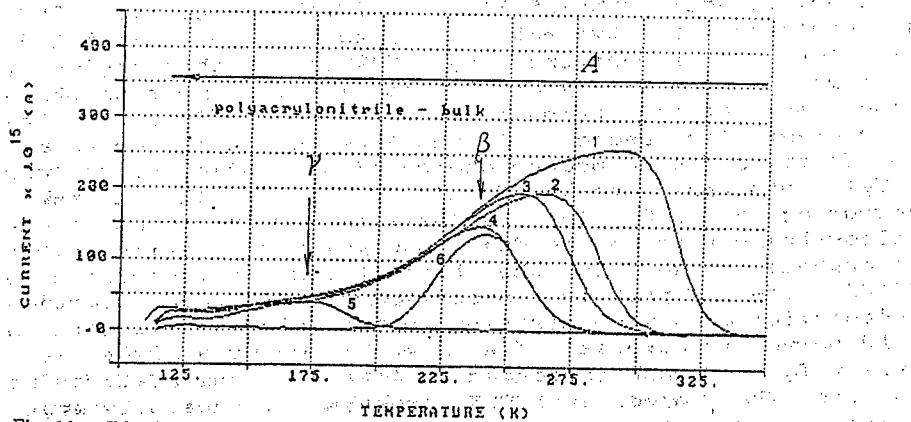
Fig. 16c - TSDC curves in amorphous region of PAN $E_p = 250V$, $t_p = 180$ sec, d = 1,05 mm, $T_p = 294$, 264, 250, 234, 189, and 213 for curves 1, 2, 3, 4, 5, and 6 respectively.
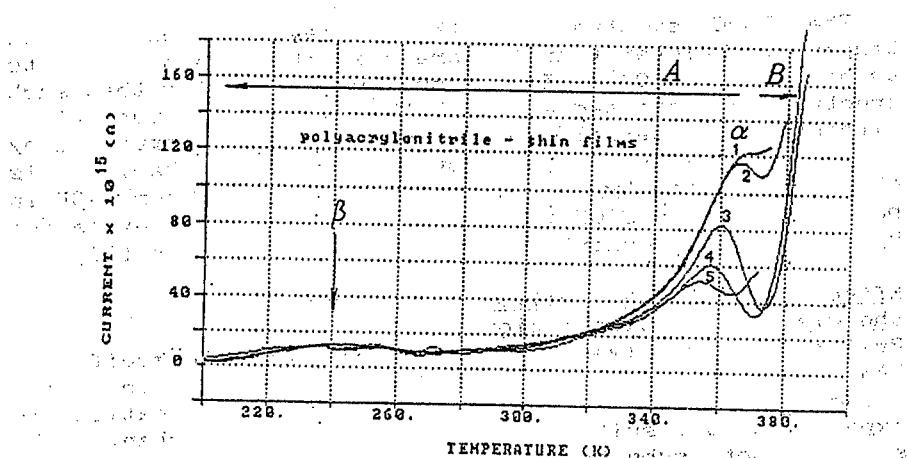
Fig. 1 d - PAN thin film; $E_p = 2V$, $d = 30 \ \mu m$, $t_p = 210 \ sec$, $T_p = 363, 361, 352, 347$, and 343 K for curves 1, 2, 3, 4, and 5 respectively.
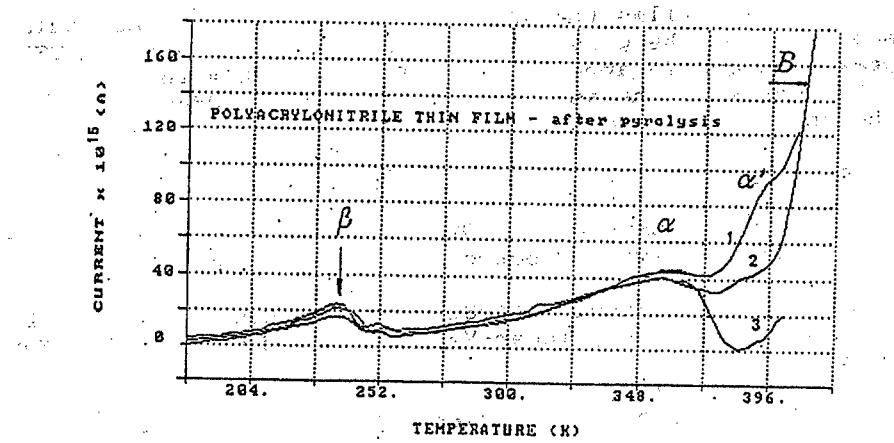
Fig. 2 - Polyacrylonitrile (PAN) thin film after pyrolysis at $T = 230C$ and for $t = 15$ min in air. Polarization conditions: $E_p = 2V$, $t_p = 210 \ sec$, $T_p = 384, 377$, and 362 for curves 1, 2, and 3 respectively.

113

The TSDC spectra in the B region, occuring at temperature higher than T_g, are characterized by currents as higher as $3x10^{-9}$A. It is worthwhile noticing that such spectra are detected even in the blank TSDC runs (i.e. without any external field) and cannot be suppressed by the procedure reported above. Such a behaviour is observed in both types of samples, starting from 400K in pallets and from 370K in thin films, and can be explained by PAN chain alignment in paracrystalline region [3]

Effects induced by pyrolysis on the molecular mobility in the glass-transition region

Preliminary experiments have been performed to modify the PAN structure by pyrolysis at 230°C in air. A ladder-like structure with -electron conjugation is expected as a result [4]. The dramatic color change (the samples not submitted to the thermal treatment are colorless and become yellow, brown, and black brown for increasing times of treatment) is accompanied by deep changes of the i.r. spectrum as well. TSDC measurements on samples submitted to the pyrolysis process show that in the thin films the α peak (related to the molecular mobility) in the glass transition decreases and new TSDC peak α' above T_g appears, see fig.2. Such effects are in agreement with the assumption that in a ladder structure the chains are less mobile.

References

[1] J. van Turnhout, (1977) In: Thermally Stimulated Discharge of Polymer Electrets, Elsevier, Amsterdam

[2] J. van Turnhout, (1980) In: Electrets, edited by G. M. Sessler (Springer-Verlag, Berlin-Heidelberg-New York), p.80

[3] S. I. Stupp, S. H. Carr: J. Appl. Phys. 46, 4120 (1975)

[4] J. Pospišil, M. Samoc, J. Zieba, P.N. Prasad : Third order of nonlinearity in PAN ladder polymer. Submitted to Polymer

DIELECTRIC PERFORMANCE AND LUMINESCENCE OF SILIKA POROUS GLASSES WITH SILICON IMPREGNATIONS

Ya.O.Roizin[*], E.Rysiakiewicz-Pasek[**], A.B.Korlyakov[*]

[*]Odessa State University, 270100 Odessa, Ukraine,

[**]Wroclaw Technical University, 50-370, Wroclaw, Poland

New porous materials for optical and electronic application have been obtained and investigated. The starting materials were porous silica samples obtained by three different technologies. In the first case sodium-borosilicate glasses with initial phase separation were etched in acid solutions to fabricate porous SiO_2 matrixes. The samples of second and third groups were obtained by thermal oxidation of porous silicon which was fabricated by means of electrochemical etching and spark-discharge processing of crystalline silicon, respectively. The thickness of fabricated porous specimens ranged from 30 to 500 micron. They consisted of practically pure silica and had similar size dictributions of pores with maxima at 20-30 A. The further technological steps consisted in filling the volume of voids with amorphous carbon by means of thermal decomposition of glucose at $220^\circ C$ and in thermal annealing of thus obtained composite material at $600-750^\circ C$. The samples that had a typical black colour after carbon deposition retained their initial transparence and behaved as typical dielectrics after the annealing procedure. The a.c. conductivity measured in a wide frequency domain increased several times compared with initial porous glasses, thus indicating the presence of inclusions polarized by the applied a.c. voltage. The volume of voids could be deduced from capacitance measurements and the calculated values agreed well with the results obtained for initial samples by other techniques. It confirmed the fact that sintering of porous glasses was not pronounced for the employed annealing temperatures. This contrast with the mentioned above results significant changes were observed in course of our luminescent measurements for porous glasses subjected to carbon filling-annealing procedure. An increase of the luminescence intensity up to two orders of magnitude was observed. This fact and also typical shifts of the luminescence band maximum strongly suggest that the origin of the light emission is connected with quantum-confinement effects in silicon clusters formed in the SiO_2 matrix by carbon reduction of porous silica. The kinetics of liminescence decay depended upon the energy of UV excitation quanta E_i. A model is proposed to account for the large (up to 10 seconds) relaxation times in case E_i exceeded the absorption gap of silica glasses.

ALTERNATING CURRENT HOPPING CONDUCTIVITY IN SALT-ZWITTERIONIC MIXTURES

S.A.Rozanski, F.Kremer

FB Physik (Abt. PAF), Universität Leipzig
Linnéstr. 5, 04103 Leipzig, FRG

P.Koberle, A.Laschewsky

Université Catholique de Louvain, Département de Chimie
Place L.Pasteur 1, B-1348 Louvain-la-Neuve, Belgium

Introduction

In electrically conducting polymers the frequency and the temperature dependence of the complex dielectric functions, and hence the complex conductivity, allows to draw conclusions concerning the mechanisms of charge transport . The electrical characteristic of ionically conducting materials are often studied by ac techniques to avoid the necessity of developing the non-blocking ion-conducting electrodes that are needed for dc measurements.

One of the most characteristic properties of electrical conduction in disordered solids is strong dispersion of the conductivity. At low frequencies one observes a constant conductivity while at higher frequencies the conductivity becomes strongly frequency dependent, varying approximately as a power of the frequency where the exponent is less then but close to one as the temperature goes to zero.

A particularly interesting case is given for zwitterionic polymers [1]. In such polymers, all ions are fixed to the polymer backbone, and low-molecular-weight counterions are missing. The high density in dipolar units affords a number of specific properties to these polyzwitterions: very high glass transition temperature, strong polarity, the ability to dissolve inorganic salts in stochiometric amounts, and very high affinity for water. Solubility of polybetaines depends on the nature of the anions and cations of low molecular weight salt. The interaction of salts and polyzwitterions observed in solution can be extended to the behavior in bulk. It enables the preparation of equivalent amounts of inorganic salt and polyzwitterions.

The dielectric properties of zwitterionic polymers and hence their conductivity are only briefly explored. By employing broadband dielectric spectroscopy the frequency and temperature dependence of the complex dielectric function is measured. This enables the underlying mechanisms of charge transport to be investigated and the influence of the inorganic salt concentration on this process to be studied.

Experimental

To elucidate the influence of inorganic salt concentration on the dielectric properties and conductivity in ionic side chain polymers we have studied isomeric polymethacrylates at several concentration of sodium iodine salt (formula of polymer is shown in Fig. 1). The synthesis of monomers and polymers, and the preparation of the polymer blends of polymer with inorganic salts has been described previously [1]. All measurements was made below Tg temperature which is higher then chemical stability temperature (453 K) of the polymer.

$$CH_3$$
$$|$$
$$(-CH_3-C-)_n \qquad CH_3$$
$$| \qquad\qquad |$$
$$COO-(-CH_2-)_{11}-N^+-(CH_2)_3- SO^-_3$$
$$|$$
$$CH_3$$
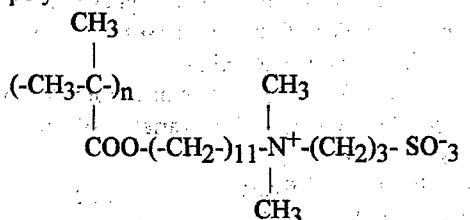
Fig.1

For the dielectric measurements, polymer films were placed between two gold plated stainless steel electrodes that were pressed together by a micrometer screw. The polymer films with different NaI molar contents and with a thickness ranging between 40 μm and 80 μm were cast directly from 2 ml 1:1 mixtures of 2,2,2 trifluorethanole with water on to one of the electrodes and the solvent was evaporated for 2 h at 323 K. To provide good contact with the upper electrode of the sample condenser a graphite 16 mm diameter disk spacer was placed on to the polymer film. For the dielectric measurements ($10^2 \div 10^7$ Hz) an impedance analyser (HP 4192A) was employed. The measurement system used a custom-made cryostat, which allowed the sample temperature to be adjusted between 100 K and 400 K by using a temperature - controlled nitrogen gas jet (stability $\pm$ 0.02 K). The sample temperature was measured with a platinum temperature sensor mounted in one of the condenser plates (temperature resolution $\pm$ 0.01 K). Before measurements samples were heated in the nitrogen atmosphere, at a temperature about 400 K to remove all water.

Fig.2

Results and Discussion

The influence of the salt concentration on the conductivity contribution has been derived from the frequency dependence of ε'' according to equetion $\sigma' = Re(\varepsilon_0\omega\varepsilon^*)$. Fig.2 and Fig.3 shows the real part of the complex conductivity as a function of frequency at different temperatures for pure polymer and with 200 mol% NaI salt concentration. The effect of enhancement the conductivity of pure zwitterionic polymethacrylate with adding a stoichiometric amount of NaI salt on about two orders of magnitude is observed. The real part of the conductivity increases with increasing

Fig.3

Fig.4

Fig.5
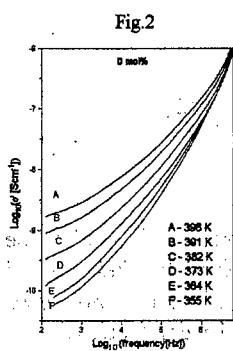
frequency, temperature and inorganic salt concentration. For high salt concentration and temperatures the conductivity is almost constant at low frequencies while at higher frequencies the conductivity becomes strongly frequency dependent, varying approximately as a power of the frequency ($\sigma \sim \omega^s$, $0.67 < s < 1$). For high frequencies changes of the conductivity with temperature in pure polymer are smaller then in polymer with 200 mol% NaI salt concentration. The ac conductivity is less temperature dependent then dc, suggesting that ac conduction is dominated by processes with activation energies smaller then dc conduction.

To describe the frequency and temperature dependence of the complex conductivity variety of theoretical approaches have been proposed, with the main focus on hopping models. We compare two models for the complex conductivity i.e., a microscopic model proposed by Funke [2] and the random free - energy barrier model proposed by Dyre [3].

Funke modified the Debye-Hueckel-Onsager-Falkenha-gen theory of conduction in electrolytes for solid ionic conductors. In his model, the hopping motion of the mobile charged defects is largely determined by their mutual repulsive interaction. As a consequence, correlated forward-beckward hopping processes takes place. They are responsible for the observed dispersion of the conductivity. An expression for the real part of the conductivity behavior can be obtained from the following equetion (low frequency limit):

$$\sigma'(\omega) = \sigma(0) + \sigma(0)(\omega/\omega_s)^s, \qquad (1)$$

where $\sigma(0)$ is the dc conductivity, ω_s is the characteristic frequency for the onset of ac conduction, s describes the slope of the dispersion region. Now the critical frequency ω_s can be found by inspection of the ac conductivity data since $\omega = \omega_s$ when $\sigma(\omega_s) = 2\sigma(0)$.

Dyre have proposed a random free-energy barrier model for ac conduction in disordered solids. This model assumes conduction takes place by hopping, where the hopping charge carriers are subject to spatially randomly varying energy barriers. The model is solved in the continuous time random walk approximation (CTRW). The disorder is taken into account by a distribution of waiting times between succesive

118
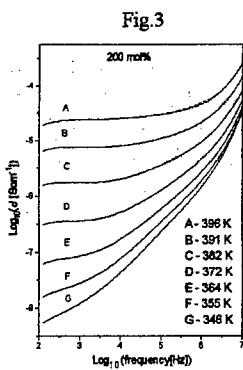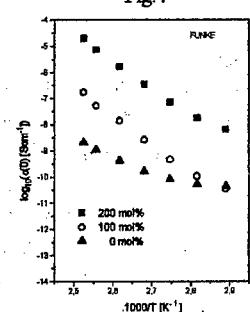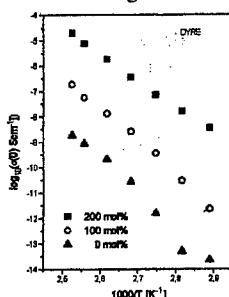
jumps. The real part of the conductivity in random free-energy barrier model solved within CTRW approximation is given by:

$$\sigma'(\omega)=\sigma(0)(\omega\tau)\arctan(\omega\tau)/(\{\ln[1+(\omega\tau)^2]^{1/2}\}^2+[\arctan(\omega\tau)]^2), \qquad (2)$$

where $\sigma(0)$ is dc conductivity and $\tau=1/(\gamma_{min})^{-1}$ - low frequency cutoff.

The conductivity data on Fig.2 and Fig.3 were fitted using equations (1) and (2). The temperature and concentration dependence of the parameters of the best fits to the conductivity data are shown in Fig. 4, 5, 6, 7. $\sigma(0)$ and ω_s increases with increasing both temperature and salt concentration. The activation energy for the critical frequency is about 0.38 eV - 3.03 eV and for the conductivity is about 0.94 eV - 2.89 eV. ω_s is thermally activated following the same Arrhenius-like behavior as the $\sigma(0)$ conductivity.

Fig.6

Fig.7

The best fits of the experimental data are obtained only for high temperatures and high salt concentration then for pure polymer and low temperatures slight deviation from the simple power-low behavior appear.

Conclusions

The frequency and temperature dependence of the conductivity in salt-zwitterionic mixtures can be described by a model proposed by Funke [2] and Dyre [3]. Both models are in quantitative agreement with experimental results and yield nearly identical fit parameters. However, detailed examination of the fits shows that Funke model fit better present data then the model proposed by Dyre. The difference is sufficient only in low temperature region where the relative deviation of fit parameters is about two times poorer then those obtained using Funke fitting. The main part of the misfit arises probably from the fitting of the dc conductivity. Nevertheless, based on the above experimental data it is not justified to give a preference to any one model.

Acknowledgment

Rferences

1. P.Koberle, A.Laschewsky, T.D.Lomax, Makromol.Chem. 12, 427 (1991)
2. K.Funke, R.Hoppe, ISSI Letts. 1, 9 (1990)
3. J.C.Dyre, J.Appl.Phys. 65, 2456 (1988)
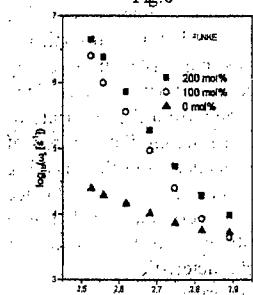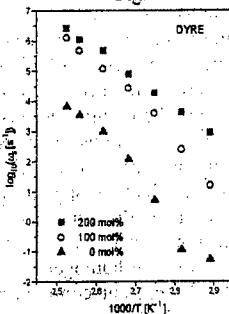
NUMERICAL STUDY OF NON-OHMIC R-HOPPING CONDUCTIVITY IN MACROSCOPICALLY NON-UNIFORM RANDOM SYSTEMS.

J. Rybicki, G. Mancini and M. Chybicki

Istituto di Matematica e Fisica, Universita' di Camerino, Camerino (MC), Italia

1. Introduction.

The current-field and conductivity-field characteristics of random three dimensional r-hopping systems can be calculated numerically within a model proposed by Bottger and Wegener (1984). The authors of the model have published only few exemplary curves for a random, but macroscopically uniform centres distribution over the sample (simulation box). However, in most real cases an extremely thin layer can only hardly be thought to be a macroscopically uniform one, because of a relaxation of the density of structural defects due to differences in bond lengths, diffusion of atoms from the substrate or chemical reactions. All these reasons make it necessary to consider the case of random distributions of hopping centres, with their macroscopic density varying as a function of the distance from the injecting contact. Such a spatial non-uniformity in the centres distribution has been proved to influence remarkably the transient currents measured in the classical time-of-flight experiment for hopping transport (Rybicki et al. 1992, 1993). Thus, it seems to be interesting to investigate also the influence of the layer non-homogeneity on stationary current-field and conductivity-field characteristics.

In the present communication we describe in short the results of the numerical simulation of the current-field, and conductivity-field characteristics for r-hopping transport for a strong electron-phonon coupling (small polarons), and for a weak electron-phonon coupling (band-like transport) in macroscopically non-uniform amorphous thin layers.

2. Basic equations.

The basic equations describing the hopping conductivity (Bottger and Bryksin 1985) are as follows. For an electric field E of arbitrary strength, the density j of the dc hopping current is given by

$$j = \tfrac{1}{2\Omega} \sum_{m,m'} (R_m - R_{m'}) \cdot i(m',m),$$

where R_m is the position of the m-th hopping site, Ω - volume of the system, N - total site number within volume Ω, and i(m',m) is the current running from site m' to site m. The latter may be written as

$$i(m',m) = e W_{m'm} \Big[\rho_{m'}(1 - \rho_m)\exp\big(\beta V_{m'm}/2\big) -$$
$$\rho_m(1 - \rho_{m'})\exp\big(-\beta V_{m'm}/2\big)\Big],$$

where $V_{m'm} = V_{m'} - V_m$, $V_m = \mathcal{E}_m + e u_m$, $\mathcal{E}_m$ - energy of the m-th site, u_m - potential of the external field E at the point R_m, $\beta = kT$, k - Boltzmann constant, T - temperature, ρ_m - the occupation probability of site m, $W_{m'm}$ - the symmetrized hopping probability. The latter in the limits of strong and weak electron-phonon interactions may be expressed as:

$$W_{m'm} = W_0 \cdot \exp\big(-2\alpha |R_{m'm}|\big),$$

and

$$W_{m'm} = W_0' \Big[\sinh |V_{m'm}| \beta / 2\Big]^{-1} \cdot \exp\big(-2\alpha |R_{m'm}|\big),$$

respectively, where α is the reciprocal Bohr radius, and the prefactor W_0 depends only weakly on the external electric field E, as well on the site position R_m and energy $\mathcal{E}_m$. We resolve numerically the above equations together with

$$\sum_{m'} i(m',m) = 0,$$

under the normalisation condition

$$N^{-1} \sum_m \rho_m = n,$$

where n is the concentration of electrons in the system. In our model calculations we use the exponentially decreasing in space average density of hopping centres:

$$N_h(x) = N_0(D) \cdot \exp(-x/D),$$

where x is the distance measured from one of the electrodes, $0 < x < L$, L - the layer thickness, and D is a characteristic length of the site concentration decay. The centre concentration at $x = 0$, $N_h(0)$, for each value of D, is chosen in such a way that the total number of hopping centres within the simulation box is constant. The parameters, which are common for all the curves are: the concentration of electrons in the system $n = 0.5$, the system dilution $\alpha/N^{1/3} = 15$ ($N = N/\Omega$); N = 500.

3. Numerical results and discussion.

3.1. Small polarons.

Fig.1 shows current-electric field characteristics for various degrees of non-uniformity L/D for a strong electron-phonon interaction ($E' = eE\beta\alpha^{-1}/2$, current in arbitrary units). The characteristics obtained for non-uniform centres distributions, with L/D in the range 1.0 - 2.5, reveal an N-like course, showing a current maximum at fairly low fields, followed by a current decay down to a minimum value, and by a subsequent exponential current increase. The overall shape of the curves remains similar. The quantities which depend remarkably on L/D are the position and the depth of the current and conductivity minima. With increasing sample non-uniformity the current minima occur for increasing fields, and the minimal current values become lower.

Fig.2 shows differential conductivities $\sigma(E')$ corresponding to the j vs E' characteristics of Fig.1 (normalised to $\sigma(E'=0)$. The curves corresponding to L/D > 1.0 practically coincide, and thus the relative differential conductivity variations in the function of the applied field do not depend on the degree of spatial non-homogeneity in the centres distribution, assuming a specific shape, common to all sufficiently non-uniform systems. The point to be noted is that the conductivity saturation occurs at a certain critical value of the applied field, E'_c, only weakly dependent on L/D (for $E'_c \approx 0.2$). The non-uniform systems become thus ohmic, at least up to the fields consistent with the assumption of constant carrier concentration. Such a behaviour is quite different from the case of uniform systems, where there is no conductivity saturation, but the local conductivity minimum is followed by the exponential conductivity increase. There is also no negative-conductivity region, in contradistinction to the non-uniform systems. In order to understand such a behaviour we have studied the histograms of the average (for 10 successive subintervals of the layer thickness) occupation probabilities of the centres in the function of E', for each value of L/D (Mancini et al 1993). For L/D ≥ 1.0, the field range over which the average occupation in the central part of a layer tends to about one, corresponds to the conductivity decay towards zero. On increasing field the spatial extension of the region with almost fully occupied centres increases, and the differential conductivity assumes its negative values. Finally, the increasing field is again able to enforce the effective carrier motion, and the current increases slightly, so that the conductivity assumes small positive values (spatial extension of the fully occupied region begins to shrink). For spatially uniform systems, in the whole field range the average occupation of centres over all the layer thickness remains well below one.
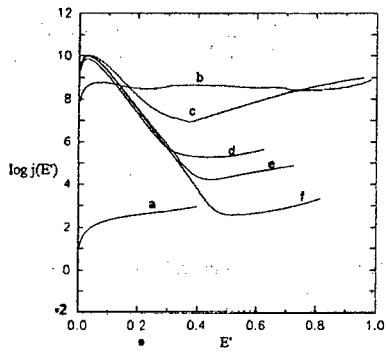
Fig.1. Current-field characteristics in their dependence on the non-homogeneity parameter L/D: a) L/D = 0.0; L/D = 0.5; c) L/D = 1.0; d) L/D = 1.5; e) L/D = 2.0; f) L/D = 2.5. Strong electron-phonon coupling.
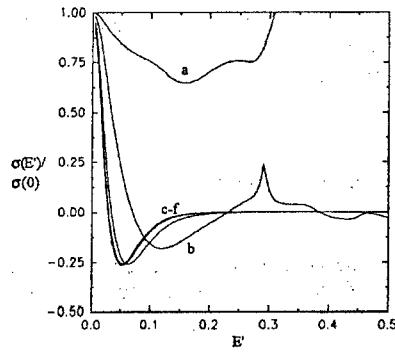
Fig.2. Differential conductivities $\sigma(E')/\sigma(E'=0)$ calculated from characteristics a - f of Fig 1.
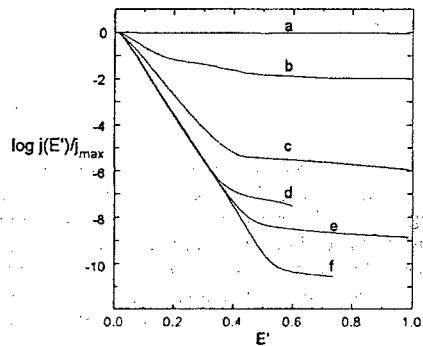
Fig.3. Current-field characteristics in their dependence on the non-homogeneity parameter L/D: a) L/D = 0.0; L/D = 0.5; c) L/D = 1.0; d) L/D = 1.5; e) L/D = 2.0; f) L/D = 2.5. Weak electron-phonon coupling.
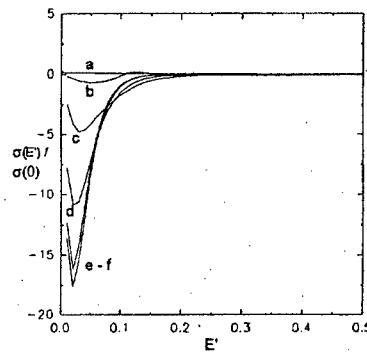
Fig.4. Differential conductivities $\sigma(E')/\sigma(E'=0)$ calculated from characteristics a - f of Fig.3.

3.2. Band-like transport.

Fig.3 shows current-field characteristics for various values of L/D for a weak electron-phonon interaction (normalised to j_{max}). All the characteristics consist of a very narrow ohmic region (for E' << 0.01), showing a current maximum at fairly low fields, followed by a current decay down to the minimum (saturation) value. The quantities which depend remarkably on L/D are the values of the saturation current, and the field, at which the saturation occurs. With increasing sample non-uniformity the current reaches its saturation value for systematically increasing fields. The final current values is lower for higher L/D.

Fig.4 shows differential conductivities $\sigma(E')$ corresponding to the j vs E' characteristics of Fig.3 (normalised to $\sigma(E'=0)$). Here, in contradistinction to the case of a strong electron-phonon coupling, the curves corresponding to different L/D values do not coincide, retaining, however, their typical shape: the conductivity decreases, reaches its minimum, and then approaches a small negative value. The depth of

the conductivity minimum depends dramatically on L/D. A study of the histograms of the average occupation probabilities of the centres in the function of E', for each value of L/D shows, that for L/D ≥ 1.0 the field range in which the average occupation in the central part of a layer tends to about one (over about 10% of the layer thickness), corresponds to the conductivity decay towards its minimum value. On increasing field the spatial extension of the region with almost fully occupied centres increases, and the differential conductivity begins to increase. In contradistinction to the case of a strong electron-phonon interaction, the increasing field is not able to enforce the effective carrier motion, and the current always decays, so that the conductivity has a small negative value up to the maximum fields (assumption of constant carrier concentration). The described behaviour of non-uniform systems is only quantitatively different from the behaviour of macroscopically uniform samples, where the conductivity also remains negative, but the conductivity minimum is much less deep than for the non-uniform samples. The average occupation histograms show, that for the uniform systems the full occupation is never reached. Up to the highest fields, the average centre occupation does not exceed 0.7 in any of the slices. The shallow conductivity minimum (occurring at E' = 0.06), however, corresponds to somewhat higher centre occupations (about 15% of the layer thickness has the average centre occupation ≈ 0.8 in the field range 0.05 < E' < 0.1).

4. Concluding remarks.

The considered model of hopping transport is rather difficult to be treated numerically. In order to get fully realistic results one should perform calculations involving - as we estimate - at least 10^6 hopping centres in the simulation box. However, the increased remarkably number of sites in the simulation box, in addition to increase strongly the difficulty of operating numerical methods, would demand extremely long CPU times, and thus such calculations are practically impossible. We think, however, that even somewhat oversimplified numerical results reveal qualitative behaviours of real physical systems. In the base of the results discussed above we can state a significant both quantitative and qualitative changes due to quasi continuous variations in the average centre concentration over the sample thickness.

References

Bottger H and Bryksin V V 1980 Phil. Mag. B 42 297
Bottger H and Bryksin V V *Hopping conduction in solids*, Akademie-Verlag, Berlin 1985
Bottger H and Wegener D 1984 Phil. Mag. B 50 409
Mancini G, Rybicki J and Chybicki M 1993 J. Phys. CM 5 4475
Rybicki J, Feliziani S, Mancini G and Chybicki M 1992 J. Phys. CM 4 3783
Rybicki J, Rybicka A, Mancini G, Feliziani S and Chybicki M 1993 J. Phys. CM 5 5027

A MONTE-CARLO STUDY OF R-HOPPING CARRIER TRANSPORT IN NON-UNIFORMLY DOPED CRYSTALS

J. Rybicki, A. Rybicka and S. Feliziani,
Istituto di Matematica e Fisica, Universita' di Camerino, Camerino (MC), Italia

M. Chybicki
Faculty of Technical Physics and Applied Mathematics,
Technical University of Gdańsk, Narutowicza 11/12, 80-952 Gdańsk, Poland

1. Introduction.

One of the most widely used methods for the determination of the microscopic transport parameters, is the analysis of the results obtained in the classical time-of-flight (TOF) experiment (Scher and Montroll 1975, Schmidlin 1977a,b, Arkhipov and Rudenko 1982, Rudenko and Arkhipov 1982a,b). The classical theory of the TOF experiment describes transient currents in thin layers, which are assumed to be spatially homogeneous on the macroscopic scale, and permits to perform an extensive analyse of the transients measured in macroscopically uniform layers (*e.g.* Marshall 1983, Marshall and Main 1983, Marshall *et al.* 1985, Weissmiller 1985, Muller-Horsche *et al.* 1987, Di Marco *et al.* 1989, Seynhaeve *et al.* 1988). However, a number of phenomena introduce the macroscopic scale variations of the total density of hopping centres over the layer thickness. Thus, the straightforward application of the theory developed for spatially uniform layers can not be fully reliable. For the multiple-trapping transport mechanism, the influence of the spatial non-uniformity of the trap distribution on the transient currents has been investigated by Rybicki and Chybicki (1988, 1989), Rybicki *et al.* (1990), and some simple formulas for determination, or at least estimation of the spatial distribution of multiple-trapping centres have been proposed.

The TOF measurement interpretation for the hopping transport mechanism is more difficult than in the case of the multiple-trapping transport (*e.g.* Bassler *et al.* 1982, Bassler 1984, Yuh and Stolka 1988). Computer experiments, in particular Monte Carlo simulations, are often performed in order to elucidate certain features of the hopping transport in materials characterised by diagonal or/and off-diagonal disorder (*e.g.* Adler and Silver 1982, Marshall 1978, 1981, Marshall and Sharp 1980, Ries and Bassler 1987, Pautmeier *et al.* 1989, Richert *et al.* 1989, Rybicki *et al.* 1992, 1993).

In the present contribution we report on the results of the Monte Carlo simulation of the time-of-flight (TOF) experiment for r-hopping transport in thin non-uniformly doped crystalline layers (substitutional disorder). The density of the substitutions is assumed to depend on the distance from the contacts, and to be constant in the plains perpendicular to the applied electric field. In particular, the density of r-hopping centres is assumed to change exponentially as a function of the from the injecting electrode. The results of simulations performed for various system dilutions, and various degrees of the layer spatial non-uniformity, are discussed.

2. Simulation results.

The TOF signals were calculated according to the algorithm described in Ries and Bassler 1987 and Rybicki *et al* 1993. The transient currents were calculated from the time and spatial evolution of the injected carrier packet n(x,t) during its motion towards x = L, according to the expression:

$$j(t) = -\frac{1}{n_0}\frac{d}{dt}\int_0^L n(x,t)dx + \frac{1}{n_0 L}\frac{d}{dt}\int_0^L xn(x,t)dx$$

(*e.g.* Leal Ferreira 1977), where j(t) is the particle current per one carrier, n_0 is the number of injected carriers. The carrier packets n(x,t) were obtained by averaging the random walks of 3000 individual carriers (20 carriers for each of 150 site generations). Simulations have been performed for systems of various transport centres concentrations c in the range 0.1 ÷ 1.0, and various degrees of spatial non-uniformity of the centre density (from uniform samples to the samples revealing e^3 - fold change of the substitutions concentration over the layer thickness).

Prior to presenting the influence of the spatial macroscopic-scale non-homogeneity of the total centre concentration on the TOF transient currents, we will show separately the pure effect of decreasing centre concentration. In Fig.1 the transient currents correspond to the x-independent average spatial centre density (L/D = 0), and the only parameter being changed is the average centre concentration c. The slopes of the final current decay decrease remarkably in the range of c from 1.0 to 0.1, and the overall shape of the characteristics indicates the dispersion increase on decreasing doping. The histograms of the total numbers of jumps performed by the carriers during their walk from x = 0 to x = L (Rybicki *et al.* 1994) show that the dispersion of the total numbers of hops increases rapidly with decreasing site concentration, in accordance with increasing dispersive character of the transients in Fig. 1.

In order to investigate qualitatively the influence of the macroscopic non-uniformity of the r-hopping centre spatial distribution, we performed our simulations for exponential variations of the centre concentration in the function of x, the total number of centres within the sample being held constant. Thus, the initial values of currents obviously depend on the actual degree of non-uniformity, because the number of hopping centres near the injecting contact (x = 0) is different from one curve to another. In particular, the concentration $N_h(x)$ of hopping centres is given by

$$N_h(x) = N_0(D) \cdot S(x), \qquad (1)$$

where

$$S(x) = \exp(-x/D), \qquad (2)$$

or

$$S(x) = \exp[-(L-x)/D], \qquad (3)$$

D is the concentration decay (increase) parameter, and $N_0(D)$ is the L/D-dependent normalisation factor. Figures 2 and 3 show the influence of the degree of the layer spatial non-uniformity for c = 0.2, and Figure 4 - for c = 0.1.

Let us consider at first the case of decreasing in x (eqs. (1)-(2)) total concentration of hopping centres (Fig. 3, and Fig 4, curves a, c). Here the carriers moving towards x = L enter the region of lower centre density, and thus their motion is slowed down for higher x. With increasing degree of non-uniformity, L/D, the slopes before the effective time-of-flight increase, whereas after the effective time-of-flight - decrease. For high degree of spatial non-uniformity (L/D = 3.0), the effective time-of-flight is difficult to be determined (for times of order of the effective time-of-flight the current decay of slope close to -1). Thus the increase of L/D acts qualitatively as the increase of the system dilution, and the overall shape of the transient is governed by the minimum density region.

For the increasing in x total centre density (eqs. (1)-(3)), the effect of spatial non-uniformity is more interesting (Fig 2, and Fig. 4, curves a, b). The increasing in x centre density makes the carrier motion easier for larger distances from the injecting contact. The characteristic feature is the occurrence of current maxima immediately before the final current decay. The current peaks become the current plateaux for sufficiently diluted systems (c ≈ 0.1) of sufficiently high L/D value.

The comparison of the curves for the same ratio L/D, centre average concentration c, but obtained for reversed spatial centre distributions, eqs. (1)-(2), and (1)-(3), respectively, shows a remarkable polarity dependence of transient currents. Note, that the slope of the final current decay does not depend on the polarity (the final parts of the pairs of curves denoted with b's, c's, and d's, in Figures 2, and 3, and also the final parts of the curves b, and c in Fig. 4, are parallel).

The effective mobility of the carriers is time-dependent, and in the case of the exponential decrease of the centre density may be approximated as (Rybicki et al. 1992):

$$\mu_{eff}(t) = \frac{\mu_0}{1 + [2(\alpha'-1)/(3D)]\,\mu_0 E\,t}, \qquad (4)$$

where μ_0 is proportional to $\exp(-2\alpha')$, α' is the reciprocal Bohr radius expressed as $N_0^{-1/3} / R$, R is the Bohr radius of the localised state, N_0 is the centre concentration at x = 0, and E is the applied electric field. The latter formula is valid for not too high value of L/D, and only prior to the effective time-of-flight. The currents calculated in the base of (4) approximate well the Monte Carlo results shown in the above figures (Rybicki et al. 1994). Having to disposal even so simplified analytical expression, one can determine the parameter D from the currents measured in the TOF experiment, assuming of course a priori the functional shape of the hopping centres distribution (1)-(3).
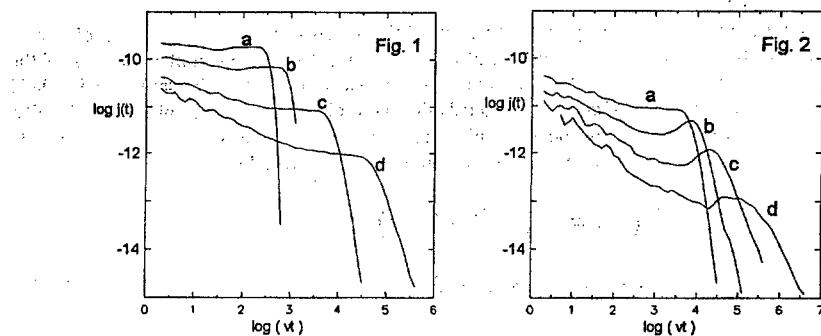
Fig.1. r-hopping transient currents for various transport site concentrations c for spatially uniform (L/D=0) systems: a) c=1.0; b) c=0.5; c) c=0.2; d) c=0.1.

Fig.2. r-hopping transient currents for the average centre concentration c = 0.2, spatial centre distribution (1)-(3): a) L/D = 0.0; b) L/D = 1.0, c) L/D = 2.0; d) L/D = 3.0.
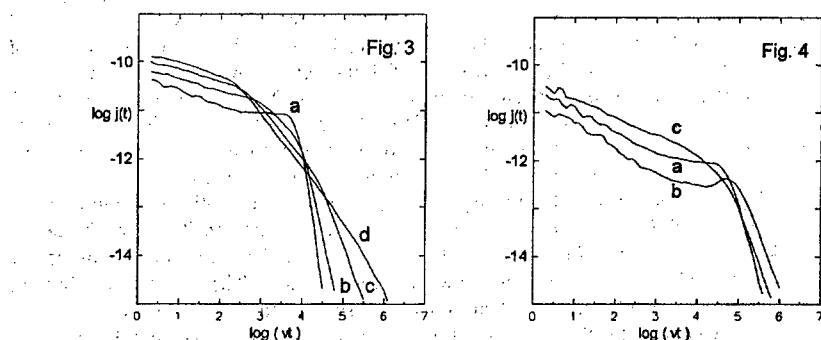
Fig.3. r-hopping transient currents for the average centre concentration c = 0.2, spatial centre distribution (1)-(2). a) L/D = 0.0; b) L/D = 1.0, c) L/D = 2.0; d) L/D = 3.0.

Fig.4. r-hopping transient currents for the average centre concentration c = 0.1. a) uniform centre distribution L/D = 0.0; b) centre distribution (1)-(3), L/D = 1.0; c) centre distribution (1)-(2), L/D = 1.0.

4. Concluding remarks.

r-hopping transient currents measured in the classical TOF experiment in crystalline thin layers are highly sensitive to spatial macroscopic-scale variations of the total hopping centre concentration. The detailed shape of the transients depends in a complicated way on the system dilution, and spatial variations of the centre concentration. It seems that even having to disposal precise analytical expressions for the currents, it would be very difficult to determine reliably the spatial centre distribution from the measurement results obtainable within the TOF experiment alone. However, following the simple, but general considerations of Rybicki *et al.* (1992), the formulas like (4) can be easily developed for several other shape functions S(x). Thus, if it is possible to assume *a priori* S(x) in the form of a family of one-parameter functions, one can fit the parameter value to get the closest coincidence between the measured and calculated curves, establishing in that manner a possible spatial hopping centre distribution responsible for a particular shape of the observed current.

References

Adler J and Silver M 1982 Phil. Mag. B 45 307
Arkhipov V I and Rudenko A I 1982 Phil. Mag. B 45 189
Bassler H 1984 Phil. Mag. 50 347
Bassler H, Schonherr G, Abkowitz M and Pai D M 1982 Phys. Rev. B 26 3105
Di Marco P, Kalinowski J, Giro G and Rybicki J 1989 Thin Solid Films 182 271
Leal Ferreira G F 1977 Phys. Rev. B 16 4719
Marshall J M 1978 Phil. Mag. B 38 335
------ 1981 Phil. Mag. B 43 401
------ 1983 Phil. Mag. B 47 323
Marshall J M, Barclay R P, Main C and Dunn C 1985 Phil. Mag. 52 997
Marshall J M and Main C 1983 Phil. Mag. B 47 471
Marshall J M and Sharp A C 1980 J. Non-Crystalline Solids 35&36 99
Pautmeier L, Richert R and Bassler H 1989 Phil. Mag. Lett. 59 325
Richert R, Pautmeier L and Bassler H 1989 Phys. Rev. Lett. 63 547
Ries B and Bassler H 1987 Phys. Rev. B 35 2295
Rudenko A I and Arkhipov V I 1982a Phil. Mag. B 45 177
------ 1982b Phil. Mag. B 45 209
Rybicki J and Chybicki M 1988 J. Phys. C: Solid State Phys. 21 3077
------ 1989 J. Phys.: CM 1 4623
Rybicki J, Chybicki M, Feliziani S and Mancini G 1990 J. Phys.: CM 2 3547
Rybicki J, Feliziani S, Mancini G and Chybicki M 1992 J. Phys.: CM 4 3783
Rybicki J, Rybicka A, Mancini G, Feliziani S and Chybicki M 1993 J.Phys.: CM 5 5027
Rybicki J, Rybicka A, Mancini G, Feliziani S and Chybicki M 1994 submitted to Thin Solid Films
Scher H and Montroll E W 1975 Phys. Rev. B12 2455
Schmidlin F 1977a Solid State Commun. 22 451
------1977b Phys. Rev. B16 2362
Schonherr G, Bassler H and Silver M 1981 Phil. Mag. 44 47
Seynhaeve G, Adriaenssens G J, Michiel H and Overhof H 1988 Phil. Mag. B 58 421
Yuh H J and Stolka M 1988 Phil. Mag. B 58 539
Weissmiller J 1985 Phil. Mag. B 51 349

EFFECT OF X-RAY IRRADIATION ON ELECTRIC PROPERTIES OF THERMOTROPIC LIQUID CRYSTALS

B. S. Saburov, S. Shukhiev

Tajik Agricultural University, Dushanbe, Republic of Tajikistan.

Electrical properties of thermotropic liquid crystals of different types - cholesteric (ch), nematic (n) and smectic (sm) were studied in dynamics of x-ray irradiation. Cholesteric ethers - cholesterilacetate (cha), cholesterilpelergonate (chp), cholesterilvaleriate (chv) and also 4-nitrophenil-4-n-octiloxybenzoate (nphob) and 4-n-gexyloxyphenil-4-n-deciloxy-benzoate (gphb) were chosen for the investigation.

URS-60 plant emitting decelerating x-ray irradiation within the range of 0.5-2.5 A° wavelength where spectral maximum fell on 0.75 A° was used as a source of x-rays. Current in x-ray tube was varied from 0.15 to 15 A that guaranteed x-ray irradiation power dose (D) from 0.012 to 1.2 Gr/s. Temperature of the samples was kept to an accuracy of 0.1°C. Intrinsic G_o and additional $\Delta G = G - G_o$ electrical conductivities depending on temperature in different x-ray irradiation power doses were measured with the help of ITN-6 electrometer where G and G_o were conductivities of samples which were affected and unaffected by x-ray irradiation respectively. Special scheme of electrometer made it possible to compensate completely intrinsic conductivity of liquid crystal and to measure value and sign of additional current in the sample.

It is established that x-ray irradiation doses used did not lead to temperature change of phase transitions (to an accuracy of 0.1°C). In addition all the measurements of conductivity observed under x-ray irradiation turned out to be completely reversible after the latter was switched off. Thus one may claim that power doses up to 1.2 Gr/s used in the work did not cause marked destruction of substance (in contrast to gamma and proton irradiation /1.2/) and therefore radiation-induced impurities were not sources of additional charge carriers producing an effect on conductivity of liquid crystals.

In fig. dependences of additional conductivity $\Delta G = G - G_o$ obtained as difference of conductivities both under x-ray irradiation G and its absence G_o are shown. Changes of were due to temperature dependence of intrinsic conductivity in the range of existence of mesomorphic condition including above mentioned polymorphic transformations of the samples under investigation. Besides G_o cholesterilvaleriate was varied by means of multiple cleaning of the sample by recrystallization and chromatographic method and also by doping of 3% addition of n-deciloxypiridine chloride (curve 5). It is seen from the data given in fig. that the value and sign of

additional conductivity arising in liquid crystals under x-ray irradiation depend on the value of G_c of the samples.

Fig. Dependences of additional conductivity on intrinsic one for different liquid crystals under x-ray irradiation power dose D=I.2 Gr/s in temperature range of existance of mesophase and isotropic condition. I-cha; 2-chp; 3-chv; 4-nphob; 5-chv (t=80°C). I'-uncleaned; 2'-single cleaned; 3'-double cleaned; 4'-three times cleaned; 5'-6'-chv with addition of n-deciloxy-piridine chloride (5'-I.0%; 6'-3%).
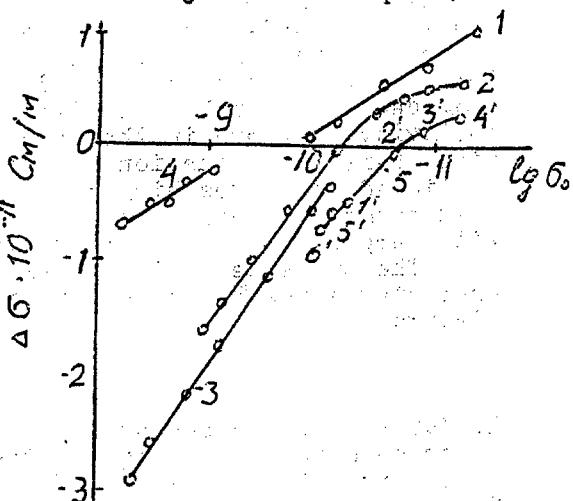
Indeed in the area of high G_o values for all the liquid crystals ΔG is negative in sign under all x-ray irradiation power doses. On the contrary G_o decreases along with temperature lowering or extension of cleaning degree is accompanied by decrease of negative absolute values of G_o and in some cases by ΔG sign inversion to positive when values of G_o are sufficiently low (curves I, 2, 5). Measurements of μ current carries mobility in (chp) both under x-ray irradiation and in its absence with application of transit of charge time between electrodes determined by method of reversal polarity of voltage applied to the sample showed that μ =5·10^{-10}-5·10-II m/v·s discovered in mesomorphic and isotropic conditions of chp remained invariable after irradiation was switched on. Therefore one can approve that charges generated under effect of x-ray irradiation in liquid crystals and reversible effecting on values of samples conductivity have the same mobility as intrinsic current carriers in mesomorphic liquids.

Apparently in the sample under investigation as a result of ionization of liquid crystal molecules under effect of x-ray irradiation both mobile electrones and positive ions can appear. Involvement of positive ions in generation of additional current is scarcely probably as far as rather large dimensions and asymmetrical configuration of liquid crystal molecules together with high viscosity (poises) of anisotropic liquids must ascertain rather low mobility of such ions. At the same time an assumption that recombination of mobile electrones and intrinsic current carriers (additive ions /3/) in liquid crystals is possible allowed to explain experimental results obtained - primarily insignificant quantity

(some per cent of G_o and alternative ΔG sign (fig.)

In fact decrease of conductivity under effect of x-ray irradiation $(\Delta G < 0)$ can be explained by appearance of charges opposite in sign to charges of intrinsic current carriers in the samples under investigation. Recombination possibility of indicated charges assigns negative sign of liquid crystals ΔG. Concentration of charges produced by x-ray irradiation with G_o decrease can become higher than content of intrinsic conductivity carriers in the sample and in this case only partial their recombination is realised. As a result the charges mentioned when reaching anode can provide current increase that causes ΔG sign to be changed from negative to positive with temperature decrease or cleaning of substance.

The suggested point of view is borne out by volt-ampere characteristics (VACH) ΔI and ΔG space dependences between electrodes.

REFERENCES

I. Kurik M.V., Lavrentovich O.D., Linjev S.Z. - Change of phase diagrams in liquid crystals under the effect of ion irradiation. - J. Phys. Chem., v. 6I, pp. I634-I639,I987
2. Kosinov G.N., Kurik M.V., Lavrentovich O.D. - On the effect of proton irradiation on temperature phase transitions in liquid crystals. - Ukr. Phys. Zhurn., v. 30, pp. I8I4-I8I6, I985.
3. Blinov L.M. - Electro- and magnitooptics of liquid crystals. - M., Nauka, 1987.

A POOLE-FRENKEL APPROACH FOR A MOLECULAR HOPPING SYSTEM

Santos-Lemus, Simón J.
Universidad de Oriente, Departamento de Fisica
Cumaná - Venezuela

Poole-Frenkel mechanism has been used to estimate the reduction of the potential barrier in the case of two charged centres separated by a distance R. The calculation arrived to an expression for the activation energy of the form:

$$(1) \qquad \Delta E(F,R) = (\Delta E_0 - e^2/\epsilon_0 \epsilon R) - \beta F^{1/2}$$

where F is the applied electric field and β is the Poole-Frenkel coefficient. The zero electric field activation energy would by:

$$(2) \qquad \Delta E(F=0,R) = \Delta E_0 - e^2/\epsilon_0 \epsilon R$$

ΔE_0 represents the true unperturbed potential barrier height. In a typical molecular hopping system like molecularly doped polymers, $R \to \infty$ limit corresponds to the undoped polymer matrix, so ΔE_0 characterizes the potential barrier height of intrinsic localized states eventually presents in the matrix. Experimental results on drift mobility measurements in N-isopropylcarbazole dispersed in an amorphous polycarbonate matrix[1,2], are in agreement with eq.(2) for activation energies obtained from Arrhenius plots for different dopant content with electric field as parameter. Extrapolation of eq.(1) to zero field give the correspondent activation energy given by eq.(2). Consequently, plots $\Delta E(F=0,R)$ vs 1/R would be a straight line whose extrapolation to $R \to \infty$ would give ΔE_0. In our experiment it was obtained for the polycarbonate matrix $\Delta E_0 = 0.98$ eV, which agree with values obtained from DC dark conductivity measurements.

[1] S. Santos L., J. Hirsch, Phil. Mag., 853, 25, (1986)
[2] S. Santos Lemus, Polymer Eng. and Science, (1994) - in Press

OPTICAL PROPERTIES OF DOPED DIELECTRICS

J. P. Šetrajčić, *D. Lj. Mirjanić**, *S. Lazarev***

Inst. of Physics, Faculty of Sciences, University of Novi Sad
**Medical and Faculty of Technology, University of Banja Luka*
***Higher Chemical and Technological School*

Translational symmetry of the molecular distribution of the exitonic system is broken by the sputtering and due to existence of two boundary surfaces. This symmetry breaking orthogonal to boundaries was treated as a perturbation. The influence of the impurities (or defects) on the relevant characteristics of the unperturbed system was analyzed using Green's functions and the Dzyaloshinskii-Pitaevskii method. The absorption and the refraction indices are calculated and graphically presented. The change in the absorption peak height are estimated, particularly in the range of solar spectrum, which are in good agreement with the experimental data.

THE PROCESSES OF STRUCTURAL RELAXATION IN AMORPHOUS CHALCOGENIDE SEMICONDUCTORS ASSOCIATED WITH RADIATION-INDUCED BOND-BREAKING.

O. I. Shpotyuk, M. M. Vakiv, A. P. Kovalsky, L. I. Shpotyuk, O. Ya. Mrooz

Lviv Scientific Research Institute of Materials, Lviv, Ukraine

Structural relaxation processes in amorphous chalcogenide semiconductors (AChS) based on As_2S_3 and As_2Se_3 induced by influence of high-energy radiation (γ-quanta, accelerated electrons, reactor neutrons and so on) are studied using differential Fourier-spectrometry technique in 400 - 100 cm^{-1} region [1]. It is shown that observed changes of AChS dielectric, mechanical, optical and electrophysical properties are connected with coordination defect formation due to theoretical model proposed in [2]. The whole process of radiation-induced microstructural transformation in AChS can be presented as a totality of following stages:

1. Initial microscopic process - excitation of electron and (or) hole pairs localized at soft atomic configurations [3] or excitation of electron-hole pairs (excitons) [4].

2. Intermediate process - weakening of intermolecular interactions that causes the possibilities to displacements of atoms and atomic blocks.

3. Formation of new metastable state (exciton self-trapping) on the level of short-range order due to observed chemical bonds transformations [1] as well as on the level of middle-range order in accordance with EXAFS data obtained earlier [5].

[1] O.I. Shpotyuk, Zh. Prikl. Spectroscop. **59**, 550, (1993).
[2] O.I. Shpotyuk, Phys. Stat. Sol.(b) **183**, 2, (1994).
[3] M.I. Klinger, Phys. Rep. **165**, 275, (1988).
[4] R.A. Street, Phys. Rev. **B17**, 3984, (1978).
[5] C.Y. Yang, J.M. Lee, M.A. Paesler, D.E. Sayers, J. Non-Cryst. Solids, **97-98**, 1119, (1987).

Currents decay in electrically pre-treated liquid-crystalline samples.

E. Szwajczak, J. Michalski
Chair of Physics, Technical University, Rzeszów, Poland

Dielectric properties of liquid crystals have been investigated for "pure" materials in relaxed state. The measurements have been carried out by measuring the current versus time relations (Fig.1), using computer controlled MS1-A equipment in the time range from ms up 10^4 s or longer. The results have been compared with theoretical ones obtained from Thomson - Thomson relations. Numerical solutions of Thomson-Thomson equations, on an assumption of the lack of space - charge and for short time ranges [2], are shown on Fig.2.

Now we would like to present the current decay curves for electrically pre-treated materials, doped with electroactive dopant. The sample of investigated compound was previously treated by an application "+" (or "-" respectively) polarization with a step voltage, during appropriate time - see figures 3,4.

One can imagine different conditions for ionic transport in the sample, because the samples generally contain many electrolytes with varied kinetics and space charge in thin boundary layer at the electrode. In this way one can expect to realize various distribution of charge throu out the sample (different from "stationary" distribution).

We find in "pure" materials fractional power - law calls by A.K. Jonscher 'the universal law" of dielectric relaxation [3]. This power law has been verified in electrically pre-treated materials.
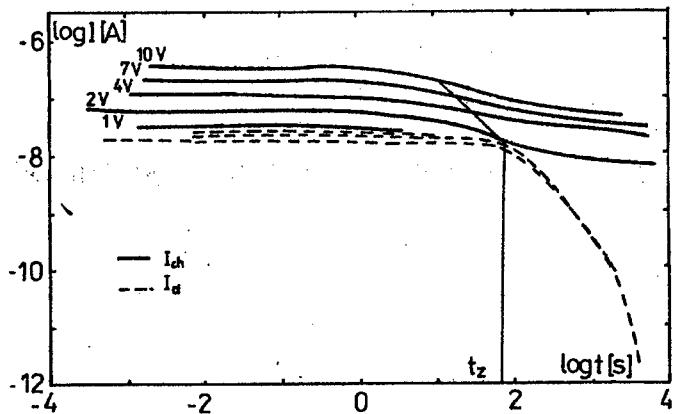

Fig.1. Charging and discharging current in "pure" smectic liquid crystal (8CB - octyl-cyano-biphenyl), for various values of applied voltage.
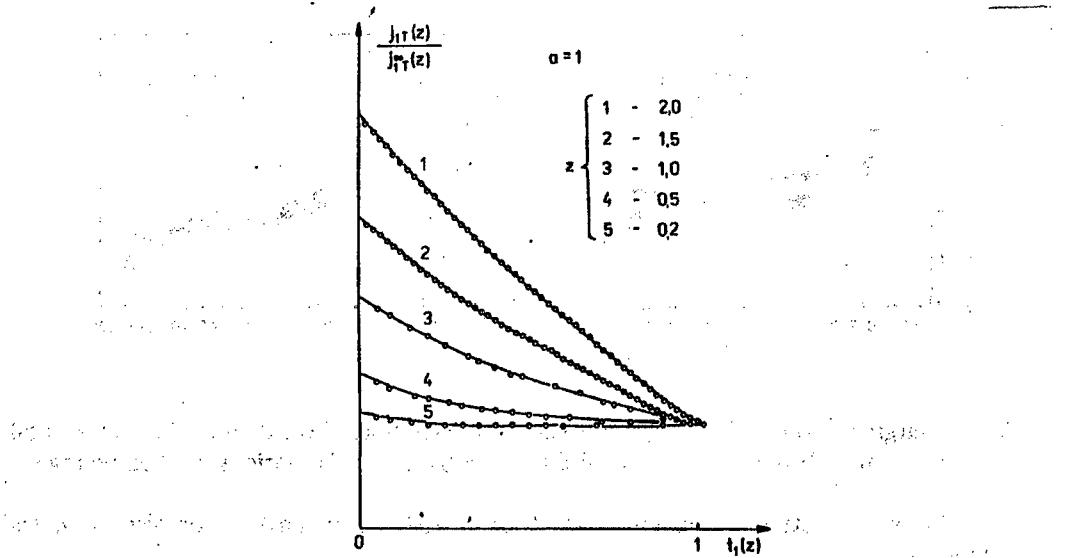
Fig.2. Current-time dependence (in arbitrary units) according to Thomson - Thomson theory, for short time (order τ_T), for different values of electrical field $z=\tau_R/\tau_T$ whre τ_R - chemical relaxation time, τ_T - ionic transit time.
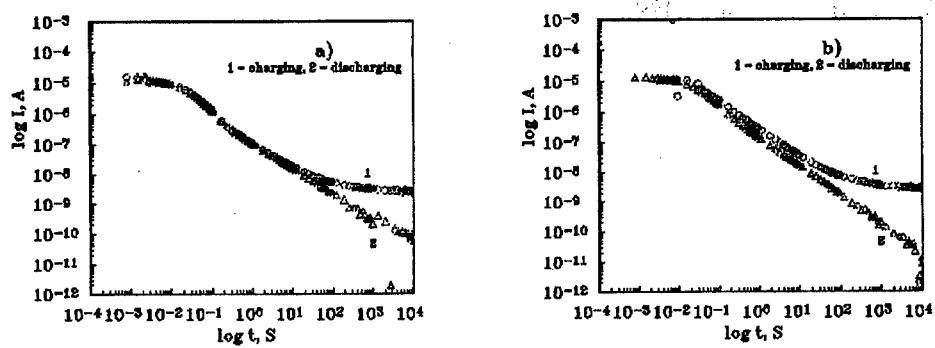
Fig.3. Charging and discharging current in nematic liquid crystals (6OCB - hextyloxy-cyano-biphenyl) doped by tetra-butyl-ammonium-bromide, for measurement voltage $U=+1V$; a) without previous polarization; b) with previous polarization by -1 V during 3h.
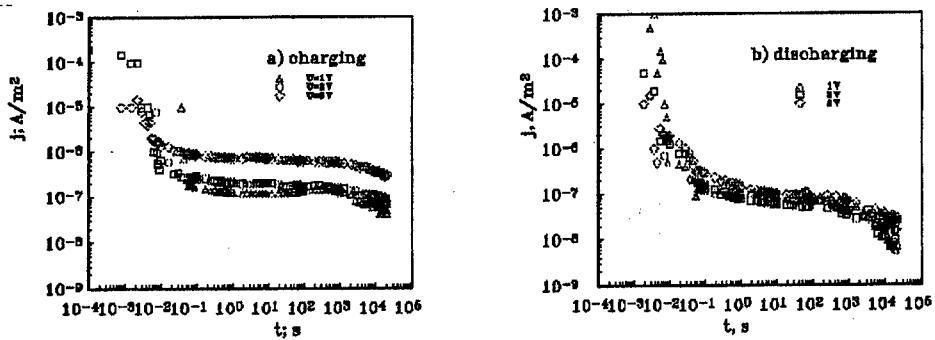
Fig.4. Charging (4a) and discharging (4b) current in cholesteryl oleate doped by tetra-butyl-ammonium-bromide, pre-treated during 3h by +1 V, for various applied voltage.

Authors gratefully acknowledge Prof. A.B. Szymanski for discussion and collaboration.

Bibliography:
[1] E. Szwajczak, A. Szymanski, Mol. Cryst. Liq. Cryst., vol. 139, 253, (1986)
  M. Lesniak, E. Szwajczak, A. Szymanski, Chemia Stosowana, XXXI,4,603,(1987)
  E. Szwajczak, M. Lesniak, R. Sikora, The Conference DRP'92, Zakopane, Poland,
  62, September (1992)
[2] J. Małecki, P. Pierański, Acta Phys. Pol. A, 50, 581, (1976)
[3] A. K. Jonscher, Proc. 3rd Int. Conf. Properties and Application of Dielectric Materials,
  Tokyo, Japan, 1, July (1991)

TIME-DOMAIN STUDIES ON INTERFACIAL IONIC CURRENTS

A.B. Szymański, Cracow Institute of Technology
and Chair of Physics Technical University of Rzeszów.
W.L.Szymański, Cracow Institute of Technology and ELF Sp zo.o.

Abstract.

By means of previously constructed time-domain apparatus [1] current transients ranging from 0.1 ms up to 10 s has been recorded for broad range of sample impedances. The method has been applied for the electrodes:

i/ apparently not exchanging carriers with material of interest /blocking electrodes /

ii/ exchanging carriers with material -ion injecting electrodes

To be sure that the currents flowing are ionic currents liquid crystalline materials were chosen as the model ones. The ionic conductivity of liquid crystalline materials has been studied extensively in the past and is well established. The material used were hexycyanobiphenyl /6CB / and cholesteryl oleate. As the blocking electrodes, SnO_2 interfaces were chosen. This interfaces has been used frequently for the studies of the electrical properties of liquid crystals. As the ion injecting electrodes the modification of previously used electrode [2,3] has been applied. This consisted with porous glass filled with the suitable ion-exchanging material. The samples were sandwich ones. The thickness of liquid crystal layer was controlled by pieces of optical fibers.

The typical current transient for 6CB sample supplied with blocking electrode is shown in Fig.1 [4]. After electrode DC current subtraction charge and discharge curves are identical. Also in cited paper, electrode current i vs voltage applied was evaluated and the relation has been found superlinear one. Similar behavior exhibited cholesteryl oleate samples supplied with blocking electrode. On the contrary, in case of ion-exchanging electrodes, the magnitude of DC electrode current /Fig.2 / as well as charge and discharge current vs time dependence are different. More, in certain cases the current "cusp" is observed,as shown in Fig.3 [5] in linear scale as well as in Fig.4. in log scale. In the experiment only one electrode has the property of exchanging the ions. Therefore the current flow was suppressed for long times.

One of the possible interpretation of this behavior is appearance of injected space charge limited ionic current [2]. These phenomena has been reviewed in the literature [6] and were observed frequently in the case of electrons and holes as the carriers. The same mechanism may be, in principle operational in case of ionic current. However, for ions one can expect the barrier at the electrode [2]. This may obscure the time the injection start to be active. The main reason for studying this phenomena is to use it for investigation of the properties of polymers. In the case of synthetic chitosan /poly(2-amino-2-deoxy- D-glucose), a biopolymer these phenomena are very strong /Fig.5/ [7]. These model studies may be helpful in elucidation of mechanism of other experimental findings. During the studies of carpathian diatomites ,which are natural porous rocks,in respect to the electrode applied two different behaviors is observed. On

application of pressed metal electrode a monotonic decay of charging curve is observed. However on application of silver paint electrode [8] a current "cusp " is observed. The material has been investigated in frequency domain, and as expected, negative capacitance value has appeared on capacitance vs frequency curve. The negative capacitance never has been observed, in frequency domain, in the case of liquid crystalline samples supplied with SnO_2 electrodes. However in other materials there are numerous examples coming from papers of Jonscher and coo workers. The physical mechanism of this findings never has been disclosed.
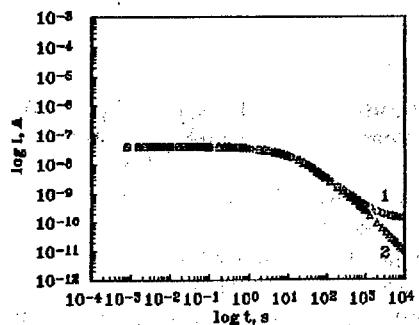

Fig 1. Log of the current I vs log of the time, for 6CB sample supplied with SnO_2 electrode.Voltage applied U=0.3V, temperature T=298 K, sample thickness 70 μm. 1 - charging current, 2 - discharging current.
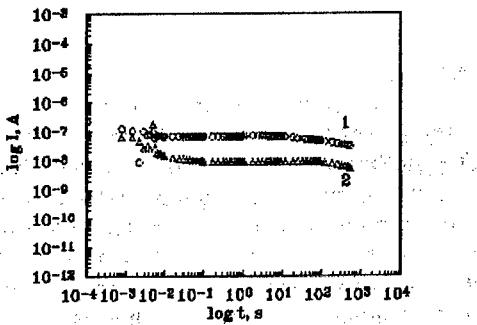
Fig 2. Log of current vs log of time for 6CB supplied with ion-exchanging electrode.Voltage U=9V, temperature=298 K, sample thickness 200 μm. 1 - charging current, 2 - discharging current.
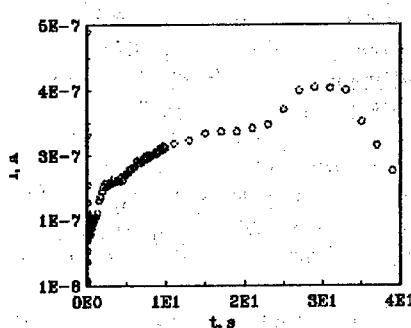
Fig 3. Current "cusp " in cholesteryl oleate - current vs time corresponding to 6V, T=298 K.
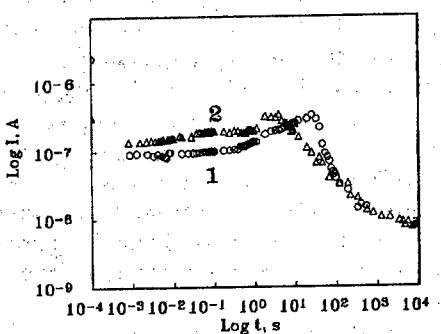
Fig. 4. Current vs time in log-log scale, for the same material and T=298 K. Curve 1 - 6V applied, curve 2 - 10V applied.

Therefore, we would like to conclude a separate role and importance of time domain studies in the cases of carrier exchange at the interfaces and inter facial based flow of ionic currents.
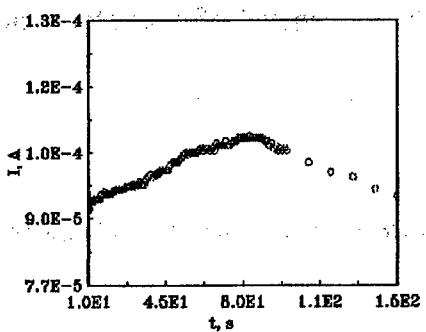
Fig 5. Current "cusp" for the sample of chitosan.
Voltage applied 10V, temperature 295 K. Dry
chitosan supplied with SnO_2 electrodes in
the same conditions exhibited current on 10 A
level.

Bibliography:

[1]. W.L. Szymański, A.B. Szymański, Abstract of the Conference "Dielectric and Related
   Phenomena "Zakopane,Poland,12-16.09.1994, pp.19./The set-up has been demonstrated
   on this meeting,too/.

[2]. M. Leśniak et al. Mol. Cr. Liq. Cr. 1980, Vol.61, 241

[3]. M. Olejnik, A. Błahut, A.B. Szymański, presented on The Seminar On Properties
of Silica Glasses, PGL'94, Karpacz-Poland, 6-10. 06. 1994

[4]. W.L. Szymański, A. Adamczyk, to be published

[5]. M. Olejnik et al. to be presented at this meeting

[6]. M.A. Lampert, P. Mark, Current Injection in Solids, Acad.Press, N.York, London, 1970

[7]. S. Boryniec et.al to be presented at this meeting

[8]. A. Bąk, K. Chłędowska, to be presented at this meeting

Fibre mixtures for improvement of anti-static properties of textile materials

E.Targosz, A.Włochowicz,
Textile Institute, Technical University of Łódź, Branch in Bielsko-Biała

At the present the use of synthetic fibres instead of natural ones is broadly accepted. This may cause the problem in course of fabrication as well as use of textile materials due to static electricity.

Especially in dry condition, static electricity is generate and unpleasant shock on touching metallic objects such as window frames, door handles etc. is well-known.

The property of the preservation of static electricity on textile floor coverings were investigated for mixtures of fibres of different origin. Particularly the mictures of polyamide fibres with polyester, polyacrylic, polypropylene fibres and wool has been investigated. The investigation has been carried by means of measurement of vertical and horizontal resistivities (efficiency of dissipation) of fabrics. That to find the conductive path through the carpet - unhomogeneous material, resistivities in two perpendicular direction - along the length or width of carpet have been measured. The details of fabrication, e.g. tipe of pile, carpet backing, or kind of underlay as well as the participation of polyamide fibres in blend was taken into account.

The measurement has been carried in condition of relative humidity 30% and temperature 21 deg. Centigrade.

It has been found that both vertical and horizontal resistivities are generally smaller if the participation of polyamide fibres in fibre blends decreases. The same has been verified by means of measurements of body voltages built up on a men shuffling carpets.

Determination of temperature characteristics of spontanous polarisation for ferroelectric single crystals

Mariusz Trybus, Władysław Proszak
The Institute of Physics The I.Łukasiewicz Technical University
in Rzeszów. W.Pola 2.

Non linear dielectric (among others ferroelecric monocrystals)
show dielectric hysteresis loop. Basing on the shape of the loop
we can determine some of the ferroelectric parameters
(spontanous polarisation, coercive field, shift field).
In the paper we show a computer measurement system that was set
up basing on two ideas Diamant and Sawyer – Tower bridge
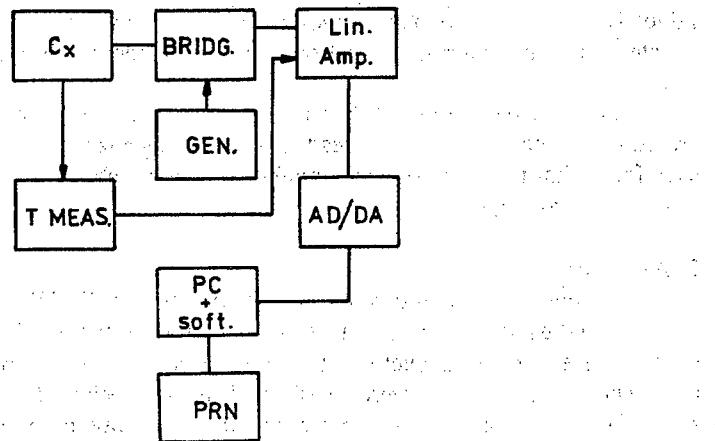
fig.1.
First metod of measurements can be desrcibed as analog combined
digital the second is strict digital.
Different advantages of these methods are analised in the
paper. Typical plots enclosed.

FORMATION OF A STABLE CONDUCTING LAYER DEVELOPED ON BISMUTH SILICATE GLASS BY THERMAL TREATMENT IN HYDROGEN

K. Trzebiatowski

Faculty of Applied Physics and Mathematics
Technical University of Gdańsk, 80-952 Gdańsk, Poland

1. Introduction

It is well known that the structure and therefore electrical properties of the surface of silicate glasses containing lead, bismuth or antymonium oxides can be modified by a special heat treatment in hydrogen [1-3]. This modification can be described as breaking of oxygen-metal ion bonds. As a result, dispersed atoms (Pb,Bi or Sb) appear in the surface layer of glass. These atoms are not connected with the glass matrix and they can migrate to the surface. In the diffusion process they form crystalline grains located near the surface. The grain size can be estimated on the basis of X-ray diffraction measurements [2]. Lead silicate glasses in the reduction process form large crystalline grains of Pb that are separate in a large distance. Hence, their surface conductivity is rather low. The presence of bismuth or antymonium atoms in the glass causes a decrease of the grain size. Subsequently, it leads to an increase of the surface conductivity to the values $10^{-8} \div 10^{-6} S/\square$. We have suggested that the mechanism of electrical conductivity can be interpreted in the terms of electron tunnelling model in discontinuous metal structures [2].

In this paper we report the first results of investigation of reduction and oxidation processes in a new glass without lead, but containing a large amount if bismuth oxide. We have found that in this glass it is possible to obtain a stable conducting layer after thermal treatment in hydrogen.

2. Experimental

Bismuth-silicate glass of the composition (in mol%) $77SiO_2$-$17Bi_2O_3$-$5K_2O$-$1Sb_2O_3$ was prepared using conventional method. The samples had the shape of thin rods. In order to measure electrical conductivity two wire terminals were connected to the ends of the rod. The measurements were performed in a special chamber with a controlled atmosphere. The chamber was constructed in such a way that it was possible to insert the chamber into a furnace or a liquid nitrogen cryostat in any moment of time. The conductivity was measured in the range of temperatures from 80K to 700K. The equipment enables us to observe the kinetics of the change of conductivity during the reduction or oxidation as well as the measurements of the temperature dependence of the electrical conductivity.

3. Results and discussion

Figure 1 shows the time dependence of conductivity in the sample during a different heat treatment processes. Curve 1 in Fig.1 demonstrates the change in the surface conductivity in time ($0 \div 10h$) during heating in hydrogen at temperature $\sim 540K$. Initially, a small jump in the conductivity is observed which takes place in a first three minutes of heat treatment. We suppose that in this time Bi^{3+} ions are reduced to Bi^{2+},

Bi^{1+} or Bi^{o}. The concentration of bismuth atoms Bi^o increases with time. Therefore a jump of conductivity can be explained as a result of an electronic hopping between bismuth ions in different valency states. It should be noticed that the amounts of bismuth ions in lower valency state may increase in a short time. The agglomeration process of Bi ions into grains takes place simultaneously with the reduction of bismuth ions to the atomic state that hamper the increase of conductivity or may cause even its small decrease. After $15 \div 20$ minutes a large increase in the conductivity follows until the saturation state is established. As can be seen from curve 1 the conductivity increases in 5 orders in magnitude if compare with its initial value. Curve 3 shows the change in the conductivity in the first hour of heat treatment. Note that the scale of time is extended 10 times. An increase in the conductivity to the saturation state is similar to the same behaviour observed in a typical lead-silicate glasses [4,5]. It is confirmed that during this stage the amount of crystalline grains increases and the distance between them decreases. This leads to the lowering of the potential barriers in the percolation path of tunnelling electrons. Consequently, the probability of electron tunneling between metallic grains increases. In the saturation stage the reduction process decreases as a result of a very slow diffusion from the bulk. In other words there is a limited number of bismuth atoms that can migrate toward the surface of the glass. We have observed even a small tendency to the lowering of conductivity after 15h heat treatment.
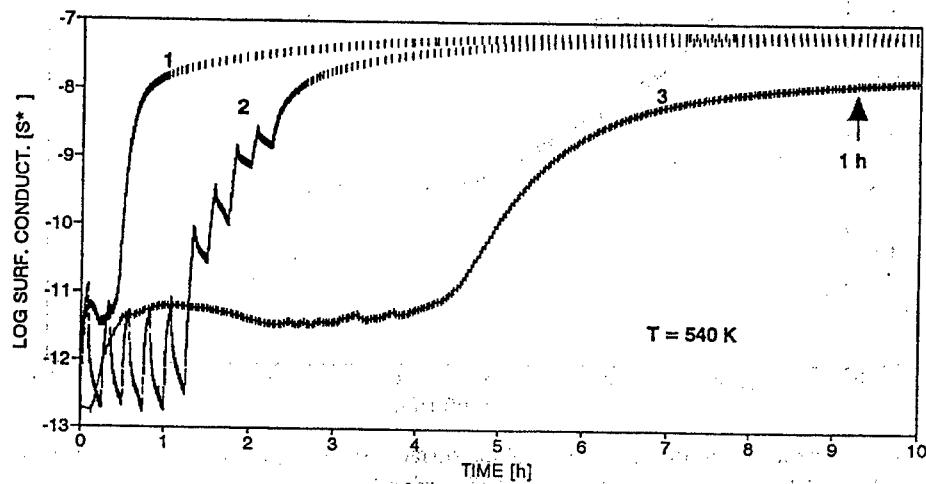
Figure 1 The surface conductivity and the effect of oxidation-reduction atmospheres in bismuth-silicate glass.

Curve 2 shows the time dependence of conductivity when the atmosphere was exchanged in the chamber ($H_2 \rightarrow O_2 \rightarrow H_2 \rightarrow$ etc.) in the first 2 hours. It can be seen that heat treatment in hydrogen always is followed by an increase of conductivity while heating in oxygen induces an opposite effect. This phenomenon was reversible during the first 4 cycles but after one hour a systematic tendency to nonreversible transformation was observed. It led to the successive increase of conductivity. This effect can be explain if consider the oxidation-reduction processes. In the beginning when the sample contains bismuth ions in

a different valency states the influence of the reduction and oxidation is large because it is easy to change the valency states of a single ions. The oxidation of crystalline grains is more difficult because oxygen can react only with bismuth atoms that are located on the surface of the grains.

The reduction process in hydrogen should cause the change in weight of glass because the sample loses oxygen during heat treatment. Figure 2 shows the loss in weight as a function of time of heat treatment in hydrogen. It is shown that maximal change in weight occurs between 1÷5 hours. We suggest that this curve could illustrate the kinetic
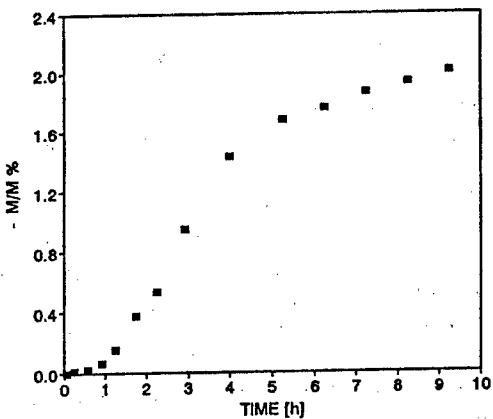
Figure 2 Loss in weight in a sample as a function of reduction time at 540K.
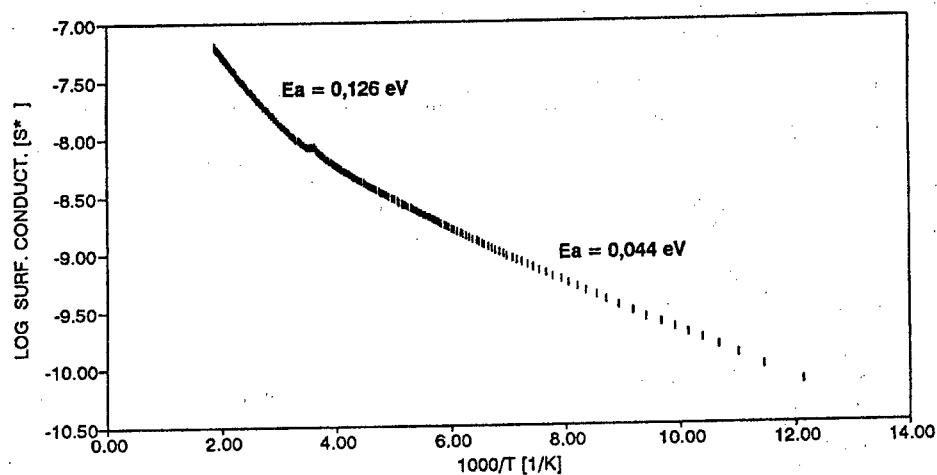
Figure 3 The temperature dependence of the surface conductivity of bismuth-silicate glass after thermal treatment in hydrogen at 540K during 20h

process of the reduction of surface layer.

Figure 3 presents the temperature dependence of conductivity after 20h heat treatment in hydrogen at the temperature 540K. One can see a continuous change of the activation energy from 0.126eV in the high temperature region to 0.044eV at about 100K. We have not observed any hysteresis in this dependency. This behaviour is consistent with the theoretical model of electrical conductivity in discontinuous metal structures based on the tunnelling process of electrons between metal granules [6]. It is believed that the creation of charge carriers is due to thermal processes leading to the transfer of the electrons from one metal granule to a neighbouring one. Therefore the

activation energy is the energy that is needed for the creation of two granules, one positively charged and the second negatively charged. The value of this energy is generally small <0.1eV as in the case of our layer on bismuth-silicate glass.

Acknowledgements.

REFERENCES

1. H.J.L. Trap, Electronic conductivity in oxide glasses, Acta Electronica, vol.14, pp.41-77, 1971.
2. O. Gzowski, L. Murawski, K. Trzebiatowski, The surface conductivity of bismuth contaminated lead-silicate glasses, J. Non-Cryst. Solids, vol.41, pp.267-271, 1980.
3. O. Gzowski, L. Murawski, K. Trzebiatowski, The surface conductivity of lead glasses, J. Phys.D: Appl. Phys., vol.15, pp.1097-1101, 1082.
4. A.M. Then, C.G. Pantano, Formation and behaviour of surface layers on electron emission glasses, J. Non-Cryst. Solids, vol.120, pp.178-187, 1990.
5. B. Abeles, Ping Sheng, M.D. Coutts, Y. Arie, Structural and electrical properties of granular metal films, Adv. Phys., vol.24, pp.407-461, 1975.
6. K. Trzebiatowski, B. Kościelska, M. Chybicki, The growth kinetic of surface conductivity if reduced silicate glasses, Ceramics vol.43, pp.99-103, 1993. Polish Ceramic Bulletin 5.

'NORMAL' AND ANOMALOUS VISCOSITY DEPENDENCE OF THE DIELECTRIC RELAXATION TIME OF LIQUIDS

G. Turky[a], G. Wilke[b], U. Witt[b], A. Ghoneim[a] and M. Stockhausen[b]

[a] National Research Centre, Microwave Physics Department, Cairo (Egypt)
[b] Institut für Physikalische Chemie, Universität Münster (Germany)

$$* * *$$

The dielectric relaxation of non-associating, quasi-rigid molecules in liquids is governed by their reorientational motion, and in the ideal case the dielectric relaxation time τ equals the reorientational correlation time. Already Debye [1] gave an estimation after which for a polar molecule in solution τ depends (in *linear* manner) on the macroscopic viscosity η and the molecular volume. As well known, his relation could not be corroborated quantitatively. However, it is general experience that τ parallels viscosity and molecular size. The aim of the present note is (i) to consider a useful *empirical* correlation between these quantities, and (ii) to present examples where deviating behaviour indicates special interactions.

(i) Empirical τ–η–r_{eff} correlation for quasi-rigid molecules

Often a certain polar molecule in different nonpolar solvents shows relaxation times τ depending in roughly a *sublinear* (rather than a linear) manner on viscosity η [2–4]: $\tau \sim \eta^a$, $a < 1$. Systematic studies by Hufnagel [5, 6] have shown that the exponent a increases as the effective radius r_{eff} of the tumbling entity. The correlation

$$\tau = \tau_0 \left(\frac{\eta}{\eta_0}\right)^{(r_{\text{eff}}/r_0) - k_0}, \tag{1}$$

can be deduced from his material, where the quantities indexed '0' are empirical parameters: $\tau_0 = 0.655$ ps, $\eta_0 = 1.7 \cdot 10^{-4}$ mPa s, $r_0 = 0.6$ nm and $k_0 = 0.27$ [7]. The applicability of Eq. (1) is of course restricted to not too extended η and r_{eff} ranges. Surprisingly enough, it was found that this correlation holds good also for moderate concentrations and even pure liquids consisting of non-associating molecules [7, 8], appearing thus as a general rule, appropriate if the relaxation process under consideration is determined by the tumbling motion of single quasi-rigid entities characterized by r_{eff}. Eq. (1) predicts τ within roughly an octave bandwidth if η and r_{eff} are given, or allows to estimate r_{eff} with an uncertainty of about 0.05 nm from measurements of τ and η.

To demonstrate the applicability of Eq. (1) to concentrated solutions and to pure substances, Tab. 1 presents some 'expected' relaxation times $^e\tau$ in comparison to data which we have measured for some aprotic molecules with relatively high dipole moments. The effective radii r_{eff} are taken from Stuart-Briegleb or corresponding computer models as the minimum radius of a sphere around the molecule's center of

mass chosen such that even its most distant parts (pictured as atomic spheres) are enclosed. The table may show that within the above-mentioned bandwidths there is satisfactory agreement of τ and $^e\tau$.

Tab. 1. Viscosity η and experimental relaxation time τ of some liquids
in their pure state and in 50 vol% solution in 1,4-dioxane, 20 °C.
Effective radius r_{eff} from molecule models.
'Expected' relaxation time $^e\tau$ according to Eq. (1).

Substance [a]	State	η	τ	r_{eff}	$^e\tau$
		mPa s	ps	nm	ps
Dimethylformamide	pure	0.85	10.5	0.35$_5$	10.2
(DMF)	soln.	0.95	12.0		10.5
Propylenecarbonate	pure	2.72	39.5	0.41$_5$	38.8
(PC)	soln.	1.76	37.5		32.3
Methylpyrrolidone	pure	1.78	20.0	0.38$_5$	20.5
(NMP)	soln.	1.45	18.5		19.0
Dimethylethylene urea	pure	2.13	35.0	0.41	32.4
(DMEU)	soln.	1.64	27.0		29.0
Diethylacetamide	pure	1.51	50.0	0.44$_5$	47.7
(DEA)	soln.	1.28	35.5		44.1

[a] In the order of increasing mole volume.

(ii) Systems with anomalous τ–η relation

Significant deviations from the correlation Eq. (1) may be subdivided into two groups.

1. Moderate deviations. The τ–η dependence in a dilution series of a certain substance may be in accord with Eq. (1) inasmuch as τ varies in the same sense as η, but regarding absolute values, there is $\tau > {}^e\tau$ to such a degree that it cannot be reconciled with the tumbling motion of *single* molecules.

This is often found in case of *protic* molecules where it can be ascribed to association. *Example:* Pyrrolidone (in contrast to NMP, Tab. 1) exhibits a relaxation time which is too long for single molecule tumbling motion but is compatible with the motion of dimeric entities [7, 9].

Also some *aprotic* liquids show a similar behaviour, e. g. Dimethylsulfoxide (DMSO). Its experimental relaxation times, $\tau = 18.5$ and 18.0 ps (pure and soln. as in Tab. 1, respectively), both correspond to $r_{eff} \approx 0.38$ nm, which significantly exceeds the model value for a single molecule, $r_{eff} \approx 0.33$ nm, but is, on the other hand, too small for a quasi-rigid dimeric entity. DMSO has a smaller mole volume than the molecules listed in Tab. 1, and possibly its exposed polar group allows for dipole-dipole interactions which cause a slowing down of the relaxation behaviour. The tendency toward self-association has been found also by other methods [10–13].

147

2. As extreme deviations from Eq. (1) we consider cases where τ and η vary in *opposite* sense. In that respect the two systems regarded in the following deserve closer examination. Although studied already previously [14], they are reconsidered here since in the meantime further data have been obtained by extending the concentration range of measurements to dilute solutions.

●● N-Cyanopiperidine and N-cyanopyrrolidine in tetrachloromethane

These systems show some common peculiarities which are especially pronounced with the pyrrolidine derivative. The relaxation times for dilution series of the hetero-cyclic compounds in mixtures with the nonpolar component CCl_4 are shown in Fig. 1. Starting from the pure polar liquids, τ *increases* on dilution and passes through a maximum, whereas η *decreases* monotonously. This feature is related to the choice of the solvent CCl_4; it is not observed *e. g.* with benzene [14]. It may be noted that the relaxation times for *dilute solutions* and for the *pure liquids* are found on roughly one and the same line according to Eq. (1), corresponding to a certain r_{eff} value (Fig. 1). In relation to this there is a 'τ excess', which can be described by an *apparent*, concentration dependent increase in r_{eff} comparable to that mentioned above for DMSO. This is parallelled by a density excess, Fig. 2.
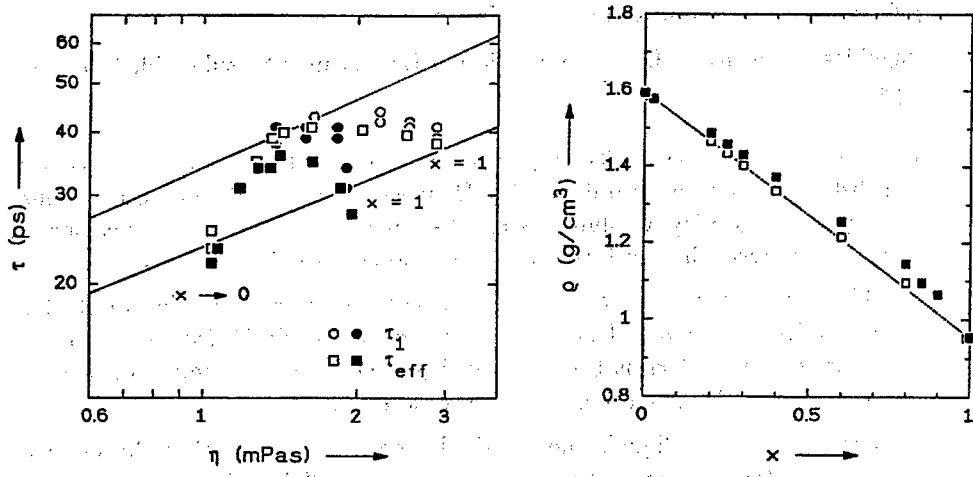
Figs. 1, 2. N-Cyanopiperidine (open symbols) and N-cyanopyrrolidine (full symbols) in the pure state and in CCl_4 solution, 20 °C.

Fig. 1: τ *vs.* η (log-log plot). Straight lines: Eq. (1) for $r_{eff} = 0.435$ (above) and 0.410 nm (below).

Fig. 2: Densities ρ *vs.* mole fraction x of polar component. Straight line indicates linear ρ variation.

The polar molecules under discussion are not rigid, but without doubt the relaxation times considered relate to their overall reorientational motion (minor higher frequency contributions, probably due to flexibility, are disregarded here). In [14] we have discussed the possibility of conformational changes under the influence of the solvent, leading to a *physical* increase in r_{eff}. This interpretation becomes questionable in view of the data on diluted solutions now available. It is feasible, on the other hand, that the rotational motion of the polar molecules is delayed by a special interaction with CCl_4 which leads to transient associations. If so, these must be *short lived* since it is not possible to analyze the results such that a relaxation contribution could be obtained which is slow enough to be ascribed to quasi-rigid, long-lived associates [14]. Since r_{eff} returns to its 'normal' value at low concentration, the transient associates are likely to involve polar molecules as *major* component. It should be mentioned that the relaxation strength, when normalized to concentration, has a minimum around $x \approx 0.8$ (significant at least for cyanopyrrolidine). This indicates a partial moment compensation. Note that the density excess, the sign of which is indicative of attractive hetero-interactions, exhibits a maximum in the same concentration region. According to the tetrahedral CCl_4 symmetry, the short lived associates may therefore be sketched as a preferential arrangement of four polar molecules (cyanopiperidine or -pyrrolidine) surrounding one CCl_4 molecule.

References

1. P. Debye, *Polare Molekeln* (Leipzig 1929).

2. O. F. Kalman and C. P. Smyth, J. Am. Chem. Soc. **82**, 783 (1960).

3. K. Chitoku and K. Higasi, Bull. Chem. Soc. Japan **36**, 1064 (1963).

4. J. Crossley, S. P. Tay, M. S. Walker and S. Walker, J. Chem. Phys. **69**, 1980 (1978).

5. F. Hufnagel, Z. Naturforsch. **25a**, 1143 (1970).

6. F. Hufnagel and Shi Ding He, Z. Naturforsch. **36a**, 505 (1981).

7. E. Dachwitz and M. Stockhausen, Ber. Bunsenges. Phys. Chem. **91**, 1347 (1987).

8. A.-H. Beine, E. Dachwitz, L. Wodniok and M. Stockhausen, Z. Naturforsch. **41a**, 1060 (1986).

9. E. Dachwitz and M. Stockhausen, Ber. Bunsenges. Phys. Chem. **89**, 959 (1985).

10. R. H. Figueroa, E. Roig and H. H. Szmant, Spectrochim. Acta **22**, 587 (1966).

11. J. B. Gill, D. C. Goodall, B. J. Jeffreys and P. Gans, J. Chem. Soc. Dalton Trans. 2597 (1986).

12. H. Bertagnolli, E. Schultz and P. Chieux, Ber. Bunsenges. Phys. Chem. **93**, 88 (1989).

13. E. Cebe, D. Kaltemeier and H. G. Hertz, Z. Phys. Chem. N. F. **140**, 181 (1989).

14. M. Stockhausen and G. Wilke, Ber. Bunsenges. Phys. Chem. **95**, 929 (1991).

ELECTRICAL PROPERTIES OF VACUUM DEPOSITED M/Dy_2O_3/M THIN-FILM SANDWICHES

Tadeusz Wiktorczyk
Institute of Physics, Technical University of Wroclaw
50-370 Wroclaw, Wybrzeze Wyspianskiego 27

1. Introduction

It is very important for dielectric materials, not only from theoretical point of few, but also due to different applications, to have a picture of dielectric polarization mechanisms as well as to know mechanisms of the charge transport. Unfortunately, in many insulating materials a picture of dielectric polarization mechanisms and mechanisms of electical conductivity is far from clear and they still need examinations and explanation. Rare earth oxides belong to this class of dielectric materials [1].
In this paper we report results of dielectric polarization and charge transport studies for dysprosium oxide films (Dy_2O_3). These films belong to sesquioxides of the heavy rare earth metals. Presented results are discussed taking into account properties of the volume as well as properties of metal/insulator (M/I) boundaries.

2. Sample preparation and measurements

All films of Dy_2O_3 and M/Dy_2O_3/M structures were prepared by the method of vacuum deposition. An electron gun was applied for evaporation of these high temperature oxides. Different experimental techniques were applied to electrical examinations, namely:
–Electrical conductivity current, I_o, was measured at equilibrium conditions or during slow cooling of the specimen at fixed voltage bias,
–Transient currents were measured after step voltage application or its removing at isothermal conditions.
–Dielectric studies were carried out in a wide frequency range, from ultra-low frequencies to radio frequencies. Different experimental procedures were applied to this aim [2-4].
–Measurements of thermally stimulated polarization and depolarization currents, TSP and TSD, were performed at linear heating condition.

3. Isothermal charging and discharging currents

Experimental data of isothermal charging currents measured in the time domaim for M/Dy_2O_3/M structures show that these currents follow well known Curie von Schweidler law and after some time achieve a level of equilibrium conductivity current, I_o. In general a shape of $I(t)$ curves depend on a temperature and voltage. The equilibrium currents for examined films were reached after the time of the order seconds at high temperatures (at 500K) and about 10^3 to 10^5 seconds at the room temperature. Such a long dielectric relaxation times observed at the room temperature mean that current is almoust a constant at fixed voltage bias, it is nevertheless a nonsteady

state current.

Examinations of resorption currents in the time domain show, that in the first periot of time currents follow Curie von Schweidler law, $I=A\ t^{-n}$,where n=0.2-0.6. After some time currents become steper,with n>1 [2]. A transition at which $I_d=t^{-1}$ accured is thermally activated with E=1eV. This activation energy corresponds with ionisation of deep traps in insulating film.

4. Temperature dependence of dc currents

As it was mentioned in the previous chapter the measure m ents of the equilibrium dc currents were much time consuming and we applied to this aim the method of dc currents measurements during slow cooling of the pecimen. Fig.1 shows a family of current-temperature curves for $Al/Dy_2O_3/Al$ specimens in logI-1000/T coordinates obtained in the temperature region 150K-500K. It is easily to see that dc current is thermally activated. Values of the activation energy for the conductivity proc e ss evaluated at different voltages are voltage-dependent and decrease from about E=1.1-1.2eV at U=1-6V to about E=0.9eV at 12V.It is obvious that field dependent processes have to be taken account during consideration high temperature conductivity mechanisms. From extrapolation (unshown here) we get E=1.23eV as "zero voltage activation energy" for the conductivity process in $Al/Dy_2O_3/Al$ thin-film sandwiches.
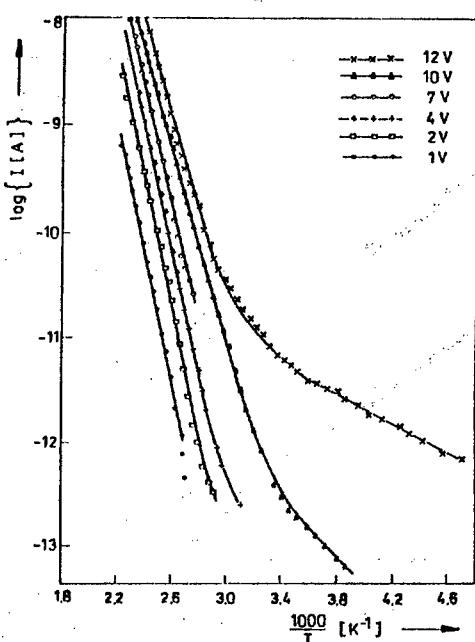

Fig.1 Temperature dependence of the conductivity current for $Al/Dy_2O_3/Al$ thin-film sandwiches (insulator film thickness is 146 nm).

Low-temperature measurements (for T=120-200K) show that the conductivity current is almoust temperature independent. Results presented in logI-1000/T scale give an activation energy of about E=0.01-0.03eV. Such a behaviour indicates that electrical conductivity process in the low temperature region is probably connected with hopping process near Fermi level.Ionistion of the shallow traps is less probable due to the fact that we have insulating films with a "bad" crystalline structure (having deep energy tails in energy gap).

5. Dielectric properties

Experimental data of dielectric reponse of dysprosium oxide thin films were examined by us in frequency range from 10^5 Hz to 10^7 Hz and published elsewhere [2,3]. Here we show, in Fig.2, the normalized dielectric data presented versus the normalized frequency. The low frequency data (below the peak) correspond with properties of M/I boundaries.Results in this range are very sensitive to the measurement conditions (voltage amplitude and its bias). Dielectric dissipation peak appears as an interaction between volume and interface processes. High frequency results correspond with typical volume processes. The peak is thermally activated with activation energy associated with volume processes (E=1eV). High frequency slopes of the real and imaginary part of susceptibility are thermally activated and suggest that an interaction between polarizing spaces take place or another processes give an important contribution to the total dielectric response.
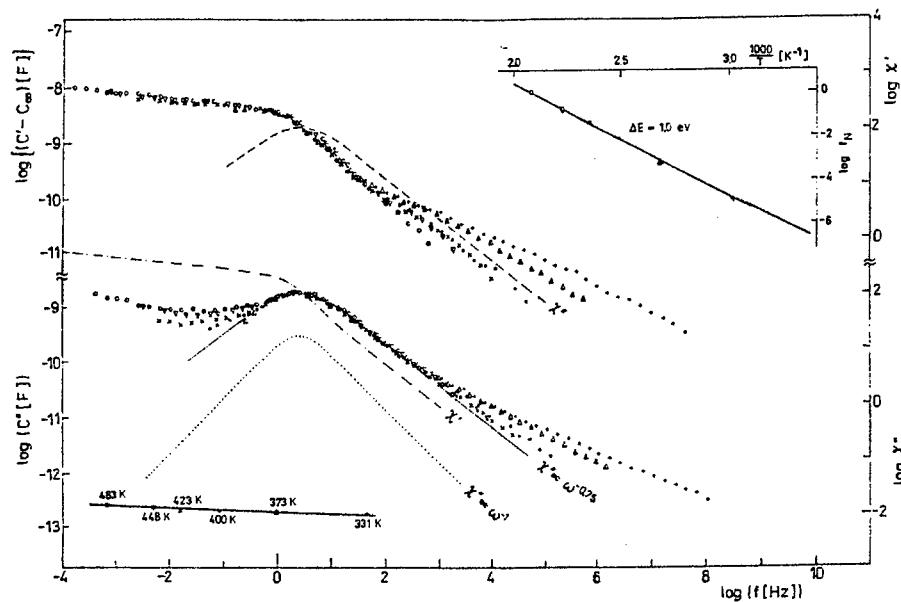

Fig.2 Frequency domain dielectric response of Al/Dy$_2$O$_3$/Al thin-film samples presented in the normalized scale.

6. Complex impedance diagnostics

On the basis of dielectric data in frequency domain complex impedance graphs were plotted for different temperatures, voltage and specimen thickness [4]. Analysis of these results [4] shows clearly existence of two regions corresponding to: volume of insulating films and M/I interfaces. Resistances of M/I regions are extremally high, typicaly about 1000 times greater than resistance of insulator.Resistance of the volume determined by this method was themally activated (E=1eV) and corresponds with thermal activation of traps in Dy_2O_3.

7. Thermally stimulated currents (TSD and TSP)

Al-Dy_2O_3-Al sandwiches were also examined with the method of thermally stimulated currents. The TSD and TSP measurements were carried out in the temperature region 300K-500K. The TSD and TSP thermograms are characterized only by a single peak located between 360K and 400K depending on the rate of heating. Estimation of the activation energy of defects responssible for the TSD and TSP peak give E=0.7eV as determined with the method of Garlick-Gibbson.In TSP curves measured at U>2.5V this peak disapeared due to high contribution of d.c. conductivity. Also high values of the polarization voltages (for U>6V) cause that the TSD peak was completly deformed. This behaviour corresponds with electrode-volume transition observed in the impedance studied. For high voltages barriers at M/I boundaries become more transparent for electrons and their resistance decrease at least 1000 times and $R_b < R_v$.

8. Conclusions

Presented results lead us to the conclusion that dielectric properties and charge transport in vacuum deposited Al/Dy_2O_3/Al thin film structures depend on the volume of insulator as well as on M/I interfaces. To explain properties of these sandwiches we propose the model in which despite of the insulating film there are two Schottky barries formed at each M/I boundary. At high temperatures these barriers can limit current transport at a constant electric field or can give main contribution to dielectric polarization. The activation energy for electrical conductivity can be connected with energy barrier at M/I boundary or with ionisation energy of coulombic centers in near-electrode region. For low temperatures barriers are transparent for carriers which can move from one electrode to the second by hopping near Fermi level. This lead to almoust temperature independent electrical conductivity and flat dielectric characteristics at high frequencies.

References

[1] M.Gasgnier, Phys.Stat.Sol.(a), vol.114, pp.11-71, 1989.

[2] T.Wiktorczyk,K.Nitsh, Z.Bober, Thin Solid Films,vol.157,pp.13-20, 1988.

[3] T.Wiktorczyk,Equilibrium structure and properties of surfaces and inter-faces, pp.341-346, ed. by A.Gonis and G.M.Stocks, Plenum Press, NY 1992.

[4] T.Wiktorczyk, Phys.Stat.Sol.(a), vol.139, pp.397-411, 1993.

MOLECULAR MODEL FOR ROTATIONAL VISCOSITY IN A NEMATIC LIQUID CRYSTAL NEAR A SOLID SURFACE

A. Zakharov

St.Petersburg Institute for Machine Sciences,Russian
Academy of Sciences,199178,St.Petersburg, Russia

The purpose of this note is to present a simple molecular
model based upon the random walk theory together with some
ideas of Zubarev's nonequilibrium statistical operator and
Rott's conditional distribution method allowing calculation
of the rotational viscosity coefficient (RVC) of a nematic
liquid crystal (NLC) near the interacting wall.The essence
of the former approach is that one considers not only auto-
correlations of the microscopic stress tensor [1-4], but
take into account the additional correlations stress tensor
with the director and fluxes the tensor of the order para-
meter(OP)[5].Results of the calculations of these correla-
tions in the bulk of the NLC show that they gives the
significant contributions to the viscosity coefficients [6]
because there are interactions between the hydrodinamical
flow of the fluid and the molecular orientations.The
general expression for the macroscopic stress tensor and
equations of motion for the director n and the tensor OP
D_{ij} for the uniaxial NLC's requires nonequilibrium
averaging (NEA) the local balance equations

$$\dot{\rho} = -\nabla_i P_i, \quad \dot{P}_i= \nabla_j \sigma_{ij}, \dot{h} =- \nabla_i J_i, \quad e_{ikl}\sigma_{lk}+ M_i =0, \quad (1)$$

where ρ, P and h are the densities of mass, momentum and
energy, σ_{ij} the stress tensor, M is the volume density of
moment and J_i is the flow energy.The microscopic tensor of
the OP can be expressed as [7]

$$\hat{D}_{ij}(r)=\sum_{\alpha,k} m^{\alpha k}[(r^{\alpha k}_i-r^\alpha_i)(r^{\alpha k}_j-r^\alpha_j) - \tfrac{1}{3}\delta_{ij}(r^{\alpha k}-r^\alpha)^2]\delta(r -r^\alpha),$$

$$(2)$$

where $r^{\alpha k},m^{\alpha k}$are the coordinate and mass of the kth
particle in the αth molecule and $r^\alpha$is the molecular centre
of mass.The equation of motion for $\hat{D}_{ij}$is of the form

$$\dot{\hat{D}}_{ij} = J^d_{ij} = 2(\hat{L}_{ij} - 3^{-1}\delta_{ij}\hat{L}_{kk}) + \hat{J}_{ij}, \qquad (3)$$

where

$$\hat{L}_{ij} = 2^{-1}(\hat{P}_{ij} + \hat{P}_{ji}), \quad \hat{P}_{ij} = \sum_{\alpha,k} \pi^{\alpha k}_i r^{\alpha k}_j \delta(r - r^\alpha),$$

$\pi^{\alpha k}$ is the momentum conjugated by $r^{\alpha k}$, and $\hat{j}_{ij}$ is the source density. The macroscopic OP $D_{ij} = \langle \hat{D}_{ij} \rangle$, where angular brackets mean of the NEA. The introduce a dynamic density of a small rotational angle(RA) $\hat{\theta}_i(r) = \sum \theta^\alpha \delta(r-r^\alpha_i)$, where θ^α is the RA of a molecule with a number α. After NEA the equation of motion for $\hat{\theta}_i$

$$\dot{\hat{\theta}}_i(r) = J^\theta_i = \sum_{\alpha=1}^{N} \omega^\alpha_i \delta(r-r^\alpha) - \nabla_k\left(\sum_{\alpha=1}^{N} m_k^{-1} p^\alpha_k \theta^\alpha_k \delta(r-r^\alpha) \right), (4)$$

reduces to the one for director evolution. Here ω^α_i is the angular velocity (AV) of a molecule, P^α_k is the molecule momentum m is the molecule mass. Averaging the microscopic tensor $\hat{\theta}_{ij}$ and Eqs.(3-4) yields the relations of statistical hydrodynamics of NLCs

$$\sigma_{ij} = -P\delta_{ij} + a_{ijkl}\varepsilon_{kl} + E_{ijkl}\nu_{kl} - \lambda_{ijk}M_k, \qquad (5)$$

$$\varepsilon_{ikl}n_k n_l = \omega_i + \lambda_{ikl}\varepsilon_{kl} - A_{ikl}\nu_{kl} + b_{ik}M_k. \qquad (6)$$

$$\dot{D}_{ij} = -F_{ijkl}\nu_{kl} + \theta^1(E_{ijkl}\varepsilon_{kl} + A_{ijk}M_k). \qquad (7)$$

here $\theta = kT$ is the temperature, $\varepsilon_{ij} = \nabla_j v_i - \omega_k\varepsilon_{ijk}, \omega_k$ is the average AV of molecular rotation, v_i is the average velocity of its centre mass, ε_{ijk} is the Levi-Civita symbol, $M_i = \varepsilon_{ijk}n_j h_k, h_k$ is the molecular field. In the Eqs.(5-6) the last three and in Eq.(7) the last two terms are dissipative contributions. So, the first among the last three terms in Eq.(5) is the traditional the autocorrelation contribution to the microscopic stress tensor (ST), the second and the third terms are the correlations ST with the flux tensor of of the OP and with the director one, accordingly. The similar contributions exist in the other Eqs.(6-7) and can be expressed in terms of $A_{ikl}, E_{ijkl}, \lambda_{ijk}$ and F_{ijkl}. Expressions for A_{ikl}, F_{ijkl} and b_{ij} in Eqs.(5-7) require the averaging with help of the distribution function which have been obtained by means of solving of the appropriate kinetic Fokker-Planck (FP) equation. The averaging of E_{ijkl}, λ_{ijk} and

a_{ijkl} require the distribution function (DF) which would obtained solving the hydrodynamics FP equation. One can obtain the hydrodynamics equations for nematic [1] and the expression for all six Leslie VCs in terms of the tensor components entering into Eqs.(5-7),which expressed by Green-Kubo-like formulas in the form of time integrals of time correlation functions (8-11).As result,the RVC can be written thus as a function of the temperature $\theta = kT/\varepsilon_o$, density $\rho = v^{-1} (\equiv N\sigma_o^3/V)$ and set of the NCL OPs [6,8]

$$\gamma_1 / \left[\frac{(\varepsilon_o I)^{1/2}}{\sigma_o^3} \right] = \frac{3(2\pi)^{1/2}}{\pi^3} \cdot \frac{\theta^{1/2}}{v} \cdot \frac{2 f(<P_2>)}{1 - \frac{5}{2} <P_2> + \frac{27}{8} <P_4> - \frac{65}{16} <P_6>} .$$

where

$$f(<P_2>) = \frac{(3.181 + 0.757 <P_2>) <P_2>^2}{2.881 + <P_2> + 12.36 <P_2>^2 + 4.69 <P_2>^3 - 0.743 <P_2>^4}$$

We estimate γ_1 for the PAA(Paraazoxyanisole) at T=390K with I=20×10^{-44}kg m^2, k=1.38×10^{-23} J/K, σ_o=5.01 Å, ε_o/k=520K. According to our calculations $\gamma_1 \approx 0.0536$ [ps].This value clouse enough experimental data $\gamma_1 \approx 0.067$ [ps][9].
When the NLC is placed in contact with a solid wall, all OPs becomes depends upon the distance from the wall and the molecules nearest to the surface may have a tendency to be located in a plane parallel to the surface.Due to more stronger interaction between solid wall and the molecules of the NLC than between the molecules consists of nematic one, the existence of this layer favours the formation of a second one, and so on. The question how long this effect propogate into the NLC a recent have been investigated [10]. For this purpose the intermolecular interaction it have been chose due to Berne and Pechukas [11]. The molecule – wall interaction have been chose due to (9-3)Lennard-Jones like potential with the potential energy and size parameters depend upon molecular orientations. The calculations were carried out with the values of the potential parameters of the corresponding values for PAA: σ_o= 5.01 Å, ε_o/ k= 520K, and surface parameter ε_{ow}= 5.0·ε_o. It found that the RVC

decrease with the growth of the distance from the wall and of the temperature Θ. The value of the γ_1 to vary rapidly (typically over two or three molecular cells) between the RVC $\gamma_1(1)$ and γ_b (γ_b is the bulk RVC). We can ascribe such behaviour of the RVC to a tendency of the molecules to be more ordered near the surface than in the bulk. The similar change in shear viscosity in the boundary layers of the isotropic liquids was attributed to phenomena related to orientation of the liquid molecules under the influence of the solid surface[12].

R e f e r e n c e s

[1] P.G.de Gennes, The Physics of Liquid Crystals (Clarendon Press, Oxford,1974)

[2] S.Hess ,Z.Naturforsch.,v.A30,p.1224,1975.

[3] M.Doi , J.Polimer Sci.,v.19,p.229,1981.

[4] M.A.Osipov and E.M.Terenjev,Phys.Lett.v.A134,p.301,1989

[5] V.B.Nemtsov,Mol.Cryst.Liq.Cryst.,v.192,p.137,1990;Theor. and Math.Phys.(In Russian) v.25,p.118,1975.

[6] V.B.Nemtsov and A.V.Zakharov, Euro Phys.Lett.,(1994)

[7] D.Forster et al., Phys.Rev.Lett.,v.26p.1016,1971.

[8] E.T.Brook-Levinson and A.V.Zakharov Euro.Phys.Lett., v.22,p.439,1993.

[9] H.Gasparoux and J.Prost, J.de Phys.,v.32,p.9539,1971

[10] B.J.Berne and P.Pechukas,J.Chem.Phys.,v.56,p.4213,1972

[11] A.V.Zakharov, Phys.Lett., A (1994)(In press)

[12] N.V.Churaev,V.B.Sobolev and Z.M.Zorin, In:Thin liquid films and boundary layers.London-N.Y.,AP,p.213,1971.

SLOW ELECTRICAL CURRENT DECAY IN CONCRETE SUBJECTED TO DIFFERENT ENVIRONMENTAL CONDITIONS.

A. Zieliński, J. Szyszka Faculty of Civil Engineering, Technical University of Rzeszow, Poland
A. Bąk, J. Michalski, Chair of Physics, Technical University of Rzeszow, Poland
W.L. Szymański, A.B. Szymański, Cracow Institute of Technology, Kraków, Poland

Abstract.

The migration of ionic species in concrete is important, for example, in corrosion problems. The time evolution of salinisation and desalinisation processes may be of interest for such field of concrete application to bridge and marine constructions. In our studies the concentration and migration of charged species in concrete have been studied by means of time-domain dielectric spectroscopy method. The apparatus used has been described elsewhere [1]. The concrete has the composition /gravimetrically/; 65,12% of the Portland cement 350 from Cement Mill Malogoszcz, 24,18 % of water and 10,70% of the sand. The samples were kept for two weeks before the tests. Samples used for experiments were flat concrete discs 46,3 mm in diameter, 11.2 mm thick, supplied with guard ring. The following electrodes have been used:

1/pressed metal electrodes,

2/electrodes consisted of gel material salt richly.

The concrete samples were predated before measurement. This treatment was aimed at changing the concentration of salt in the concrete. On pretreatment and environmental condition the electrical low frequency properties of concrete may change in broad range. This does suggest the possibility of monitoring of the state of concrete and determination of the kinetics of salinization\desalinization processes.

Bibliography:
[1].W.L.Szymanski, A.B.Szymanski, Abstracts of Th Conference "Dielectric and Related Phenomena" Zakopane, Poland, 12-16.09.1992.p.19

Dielectric Behaviour of Polyethylene

D.K. DAS - GUPTA
Bangor

ABSTRACT

The behaviour of the frequency dependent complex permittivity may provide useful information on the changes in the electronic band structure and the morphology of polyethylene and its aging with AC electrical stress in dry and humid environment. The present paper discusses the electron loss energy spectroscopy of polyethylene with respect to its valence band structure and a determination of its very high frequency dielectric constant. The Small Angle Light Scatterin Studies (SALS) provides information on morphological changes at very high fields and is useful method to investigate the changes in the sphelutic.

Dielectric Properties of Nematic Liquid Crystal 4'-pentyl-4-cyanobiphenyl in Porous Membranes

S.A.Różański[†], F.Kremer[‡]

†Maria Skłodowska-Curie High School
W.Pola 11, Pl-64920 Piła, Poland

‡Fakultat für Physik und Geowissenschaften
Universität Leipzig, Linnéstr. 5, D- 04103 Leipzig, Germany

Broadband dielectric spectroscopy (10^2 Hz - 10^9 Hz) is employed to study the molecular dynamics of the liquid crystal 4'-pentyl-4-cyanobiphenyl (5CB) in cylindrical channels of Anopore membranes having a diameter between 0.2 µm and 0.02 µm and thickness about 60 µm, chemically modified using aliphatic acid $C_9H_{19}COOH$ as a surface coupling agent. In the 5CB/Anopore system one single relaxation process is observed, the δ-relaxation, which is assigned to the hindered rotation of the molecules around its short axis. This process is strongly modified by the confining geometry with surface coupling agent. The relaxation rate in the isotropic phase is nearly uninfluenced by the presence of the inner surfaces, it is in the nematic phase by two orders of magnitude faster for the porous materials with modified surface as compared to the bulk. This phenomena is connected with changing of the orientation of the molecules from planar to homeotropic and activation of second process connected with precesion of the long axis of the molecules around the director. The dielectric strength of the δ-relaxation is considerebly weakened for the 5CB/Anopore system. A pronounced broadening of the relaxation time distribution is observed for the liquid crystal in the porous environment modified by aliphatic acid.

ASEA BROWN BOVERI in brief

The Asea Brown Boveri Group was formed in January 1988 as the result of merger – on a 50 / 50 base – of the electrical engineering activities of Asea and BBC Brown Boveri. Asea and BBC each have experience extending back some one hundred years in this business.

Ownership

ASEA AB, Stockholm (Sweden) and BBC Brown Boveri Ltd, Baden (Switzerland) own 50 percent each of the shares of ABB Asea Brown Boveri Ltd, Zurich (Switzerland).

ABB Asea Brown Boveri Ltd, Zurich is the Holding Company and Corporate Headquarters of the ABB Asea Brown Boveri Group, Comprising 1300 companies around the world.

While the shares of ABB Asea Brown Boveri Ltd are publicly traded, the shares of the two parent companies, ASEA AB and ABB Brown Boveri Ltd, are listed on various stock exchanges in Europe and the United States.

Scope of Business

The ABB Asea Brown Boveri Group is an electrical engineering company with global operations. Earnings after financial items were US$ 1,192 million, orders received US$ 29,406 million and revenues US$ 28,315 million in 1993. At year and 1993 the Group employed some 206,490 people. Net income in 1993 totaled US$ 68 million.

ABB develops, produces, sells, and services systems and products in a wide range of areas generally related to the production, distribution and application of electricity.

Its principal activities are in the fields of:

◦ power generation plants for primary energy – coal, gas, oil, water, nuclear;

◦ high-voltage transmission of electricity and systems with such products as switchgear, transformers, relays and cables;

◦ medium- and low-voltage distribution including installation.

These three Segments together contribute almost half of total sales.

Another area of activity is the production of high-speed trains, locomotives and urban transportation systems. Other areas of activity include installation

material, indoor climate, service, general contracting, oil and gas, robotics, superchargers and power lines.

The Financial Services Segment provides financing, leasing, treasury operations, insurance, trading, and portfolio managment for companies within the ABB Group and for third parties.

Asea Brown Boveri in Poland

ABB has been present to Poland since 1990 through 13 companies located in 6 major towns. The total investments is estimated at 150 MusD what gives ABB a place in among ten largest investors in the country. Polish ABB companies employ 7 000 people and in 1993 reported revenues of 220 MusD, 75% of which was directed to local market.

The largest ABB companies in Poland are: ABB Zamech in Elbląg, ABB Dolmel and Dolmel Drives in Wrocław, ABB Elta in Łódź, ABB Zwus Signal in Katowice.

Asea Brown Boveri Ltd	Telefon:	Fax:	Telex:
ul. Nowy Świat 19	48-39-120705,	48-39-120707,	813360
00-029 Warszawa, Polska	48-22-269233,	48-22-267289.	